

3-2023

**DESIGN AND ASSESSMENT OF A LEO GNSS
MINICONSTELLATION FOR POSITIONING, NAVIGATION, AND
TIMING (PNT)**

Mariya Abdulkhaleq Mohamad

Follow this and additional works at: https://scholarworks.uaeu.ac.ae/all_theses



Part of the [Astrophysics and Astronomy Commons](#), and the [Physics Commons](#)



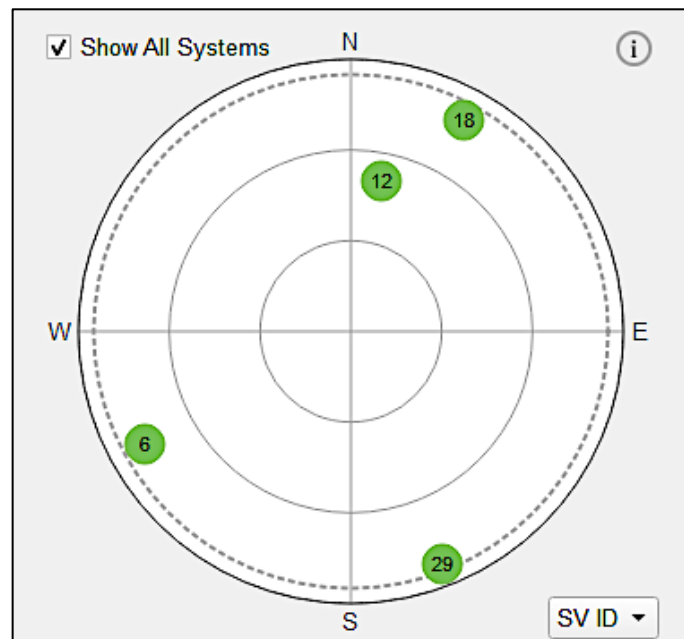
MASTER THESIS NO. 2023: 44

College of Science

Department of Physics

DESIGN AND ASSESSMENT OF A LEO GNSS MINI-CONSTELLATION FOR POSITIONING, NAVIGATION, AND TIMING (PNT)

Mariya Abdulkhaleq Abdullah Mohamad



March 2023

United Arab Emirates University

College of Science

Department of Physics

DESIGN AND ASSESSMENT OF A LEO GNSS MINI-
CONSTELLATION FOR POSITIONING, NAVIGATION, AND
TIMING (PNT)

Mariya Abdulkhaleq Abdullah Mohamad

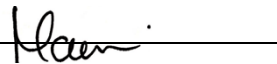
This thesis is submitted in partial fulfilment of the requirements for the degree of Master
of Science in Space Science

March 2023

Cover: Sky View Diagram of 4 LEO GNSS Satellites in the visibility of the receiver.
(Photo: Screenshot form Skydel Simulator generated by Mariya Abdulkhaleq Abdullah
Mohamad)

Declaration of Original Work

I, Mariya Abdulkhaleq Abdullah Mohamad, the undersigned, a graduate student at the United Arab Emirates University (UAEU), and the author of this thesis entitled “*Design and Assessment of a LEO GNSS Mini-Constellation for Positioning, Navigation and Timing (PNT)*”, hereby, solemnly declare that this is the original research work done by me under the supervision of Dr. Mohammad Abdel-Hafez, in the College of Engineering at UAEU. This work has not previously been presented or published or formed the basis for the award of any academic degree, diploma or similar title at this or any other university. Any materials borrowed from other sources (whether published or unpublished) and relied upon or included in my thesis have been properly cited and acknowledged in accordance with appropriate academic conventions. I further declare that there is no potential conflict of interest with respect to the research, data collection, authorship, presentation and/or publication of this thesis.

Student's Signature: 

Date: 1-2-2023

Advisory Committee

1) Advisor: Dr. Mohammad Abdel-Hafez

Title: Associate Professor

Department of Electrical and Communication Engineering

College of Engineering

2) Co-advisor: Dr. Alina Hasbi

Title: Research Associate

The National. Space Science and Technology Center

Approval of the Master Thesis

This Master Thesis is approved by the following Examining Committee Members:

- 1) Advisor (Committee Chair): Dr. Mohammed Abdel-Hafez
Title: Associate Professor
Department of Electrical and Communication Engineering
College of Engineering

Signature  Date 3-5-2023

- 2) Member: Dr. Alina Hasbi
Title: Research Associate
The National Space Science and Technology Center

Signature  Date 3-5-2023

- 3) Member (Internal Examiner): Prof. Dr. Mohamed Yagoub
Title: Professor
Department of Geography and Urban Sustainability
College of Humanities and Social Studies

Signature  Date 3-5-2023

- 4) Member (External Examiner): Dr. Nesreen Ziedan
Title: Professor
Department of Computer and Systems Engineering, Faculty of Engineering
Institution: Zagazig University, Egypt

Signature  Date 3-5-2023

This Master Thesis is accepted by:

Dean of the College of Science: Professor Maamar Benkraouda

Signature  _____

Date 6/7/2023

Dean of the College of Graduate Studies: Professor Ali Al-Marzouqi

Signature  _____

Date July 10, 2023

Abstract

Recently, there has been a resurgent demand in the United Arab Emirates for more accurate positioning, navigation, and timing signals, especially for some targeted applications such as autonomous vehicles and flying taxis. The existing Global Navigation Satellite Systems (GNSS) provide real-time positioning accuracy for up to several meters, while the targeted applications require fast convergence of centimeter-level positioning accuracy. Recent studies have shown that transmitting GNSS signals from a Low Earth Orbit (LEO) instead of a Medium Earth Orbit (MEO) would enhance positioning accuracy. The main objective of this thesis is to design and simulate an optimum scenario of a mini-LEO constellation transmitting GNSS signals in LEO and assess its performance using a GNSS simulator tool. The second objective is to evaluate the performance of a ground-based GNSS receiver receiving GNSS signals from LEO regarding the receiver's time to lock, locking period, continuity, Position Dilution of Precision (PDOP) and 3D positioning accuracy. The final objective is to compare the performance of the simulated mini-LEO GNSS constellation with the existing MEO GPS and Galileo. Skydel GNSS simulator tool, single frequency L1/E1 ublox receiver, Systems Tool Kit (STK), and u-center software were used to conduct this research. The best simulated LEO scenario had a design consisting of 35 satellites at 800 km altitude, distributed into 5 planes, with 7 satellites in each plane, the planes were 45° apart and the satellites were 30° in each plane. The results showed a range of PDOP values from 2.1 to 3.3, 3D positioning accuracy of 5.86 m, and the time the receiver took to lock was about 1 minute with a maximum locking period of 3 minutes and with no continuity. The results obtained from the simulated LEO constellation assessed using the ublox receiver were no better than those of the simulated MEO GPS and Galileo. The main reason behind the obtained results is that the current GNSS receivers are not designed to cope with the higher dynamics of the satellites in LEO.

Keywords: Low Earth orbit, Medium Earth Orbit, Global navigation Satellite System, Skydel, STK.

Title and Abstract (in Arabic)

تصميم وتقييم أداء كوكبة مصغرة من نظام الأقمار الصناعية للملاحة العالمية في المدار الأرضي المنخفض لتحديد المواقع والملاحة والتوقيت

الملخص

في الآونة الأخيرة ، هناك طلب متزايد في دولة الإمارات العربية المتحدة على إشارات أكثر دقة لتحديد المواقع والملاحة والتوقيت، خاصة بالنسبة لبعض التطبيقات المستهدفة مثل السيارات ذاتية القيادة و التاكسي الجوي ذاتي القيادة. توفر الأنظمة الحالية لتحديد المواقع (GNSS) دقة تصل إلى عدة أمتار باستخدام الوقت الفعلي لتحديد المواقع، بينما تتطلب التطبيقات المستهدفة دقة سريعة تصل إلى عدة سنتيمترات. لقد أظهرت دراسات حديثة أن إرسال إشارات نظام الملاحة العالمي من المدار المنخفض للأرض بدلاً من المدار المتوسط من شأنه أن يعزز دقة تحديد المواقع.

الهدف الرئيسي من هذه الأطروحة هو تصميم ومحاكاة أمثل سيناريو لكوكبة مصغرة من الأقمار الصناعية ترسل إشارات أنظمة الملاحة العالمية من المدار الأرضي المنخفض، وتقييم أدائها باستخدام جهاز محاكاة أنظمة الملاحة العالمية عبر الأقمار الصناعية. الهدف الثاني من هذه الأطروحة هو تقييم أداء المستقبل الأرضي (GNSS Receiver)، الذي يتلقى الإشارات المرسل من نظام الملاحة العالمية في المدار الأرضي المنخفض من حيث الوقت الذي يستغرقه المستقبل لتتبع أربعة أقمار صناعية، فترة التتبع، استمرارية التتبع، قوة الأبعاد الهندسية للأقمار الصناعية (PDOP)، ودقة الموقع ثلاثي الأبعاد. والهدف الأخير من هذه الأطروحة هو مقارنة أداء سيناريو محاكاة الكوكبة المصغرة من الأقمار الصناعية للملاحة العالمية في المدار الأرضي المنخفض مع الأنظمة الحالية للملاحة العالمية في المدار الأرضي المتوسط مثل نظام غاليليو التابع للاتحاد الأوروبي (Galileo) ونظام جي بي اس التابع للولايات المتحدة الأمريكية (GPS).

تم استخدام أداة محاكاة أنظمة الأقمار الصناعية للملاحة العالمية سكايدل (Skydel)، والمستقبل الأرضي أحادي التردد يوبلكس (ublox L1/E1)، وبرنامج محاكاة الأنظمة (STK)، وبرنامج يوسنتر (u-center) لإجراء هذا البحث. كان أمثل تصميم لمحاكاة الكوكبة المصغرة من الأقمار الصناعية للملاحة العالمية في المدار الأرضي المنخفض يتكون من 35 قمراً صناعياً على ارتفاع 800 كم، موزعة على خمس مدارات في كل مدار سبعة أقمار صناعية، وكانت المدارات متباعدة عن بعضها البعض 45° والأقمار الصناعية متباعدة عن بعضها البعض 30° . أظهرت نتائج تقييم أداء هذا التصميم قيمة 2.1 إلى 3.3 لقوة الأبعاد الهندسية للأقمار الصناعية، ودقة الموقع ثلاثي الأبعاد تصل إلى 5.86 متر، والوقت الذي استغرقه المستقبل الأرضي لتتبع أربعة أقمار صناعية كان حوالي دقيقة واحدة، مع أقصى فترة تتبع وصلت إلى ثلاثة دقائق، وبدون استمرارية. وكانت النتائج التي تم الحصول عليها من الكوكبة المصغرة للأقمار الصناعية في المدار الأرضي المنخفض أسوأ من التي تم الحصول عليها عند تقييم أداء الأنظمة الحالية للملاحة العالمية في المدار الأرضي المتوسط. السبب الرئيسي الذي يكمن خلف النتائج التي تم

الحصول عليها هو أن المستقبلات الأرضية الحالية ليست مصممة لاستقبال إشارات تحديد المواقع من المدار الأرضي المنخفض، وخصوصا عند الأخذ بعين الاعتبار الديناميكيات العالية للأقمار الصناعية في هذا المدار.

مفاهيم البحث الرئيسية: المدار الأرضي المنخفض، المدار الأرضي المتوسط ، أنظمة الملاحة العالمية عبر الأقمار الصناعية، سكايدل، STK.

Acknowledgments

My thanks go to Dr. Aquib Moin for his leadership and professional guidance throughout my time as a graduate student at UAEU. I truly appreciate you and your time preparing and empowering future space scientists and engineers for this nation. I'm also privileged to be your student in some courses, you have a very special and creative way of teaching, and I really enjoyed every minute of your lectures.

I'm highly thankful to my technical advisor Dr. Alina Hasbi, for providing me with an invaluable practical experience and knowledge in the field of LEO GNSS. Under your guidance and inspiration, I learned and accomplished more than I thought I could. Through obstacles and some difficult days, I went through, you have always maintained your patience and warm heart. My heart expresses gratitude for you, today and forever!

Special thanks go to my academic advisor Dr. Mohammed Abdel-Hafez for his guidance and advice. You told me to pay extra effort for this thesis research until ensuring an addition of valuable knowledge to the field of Space Science, which has motivated me to go above and beyond! Thank you truly and sincerely.

I also want to thank my mother, brothers and sisters, cousins, and friends for keeping up with me and supporting me during this journey. Thank you for believing in me and always knowing how to motivate and encourage me to move forward. I appreciate you all so much!

Dedication

*To my number one motivator
my beloved husband!*

Table of Contents

Title	i
Declaration of Original Work.....	iii
Advisory Committee	iv
Approval of the Master Thesis	v
Abstract	vii
Title and Abstract (in Arabic)	viii
Acknowledgments	x
Dedication	xi
Table of Contents	xii
List of Tables.....	xiv
List of Figures	xv
List of Abbreviations.....	xvii
Chapter 1: Introduction	1
1.1 Overview and Problem Statement	1
1.2 Research Objectives.....	1
1.3 Relevant Literature.....	2
1.3.1 Types and Operation Principles of the Global Navigation Satellite Systems (GNSS).....	2
1.3.2 Limitations of the Current MEO GNSS.....	5
1.3.3 Advantages of LEO GNSS	6
1.3.4 Issues with Tracking LEO Satellites.....	8
1.3.5 The Current LEO PNT Constellations	9
Chapter 2: Orbit Simulation Methodology	10
2.1 Skydel GNSS Simulator	10
2.1.1 Modifying the GPS Constellation from MEO to LEO using Skydel Software	14
2.1.2 Modifying Galileo and BeiDou Constellations from MEO to LEO using Skydel Software	15
2.1.3 Area Coverage of a MEO Satellite versus a LEO Satellite.....	16
2.2 Designing a Mini Constellation of a LEO-based GNSS using STK	17
2.2.1 Walker tool.....	17
2.2.2 Access Times	19
2.3 Importing the Orbital Parameters from STK to Skydel	19

2.4 Assessing the Performance of a GNSS Constellation using Skydel and U-center	20
Chapter 3: Results of the Orbital Simulation	26
3.1 Results of the Case Studies of the Mini-LEO Constellation Design using STK	26
3.1.1 Scenario 1	26
3.1.2 Scenario 2.....	28
3.1.3 Scenario 3.....	30
3.1.4 Scenario 4.....	31
3.1.5 Scenario 5.....	33
3.1.6 Scenario 6.....	34
3.1.7 Scenario 7.....	36
3.1.8 Scenario 8.....	37
3.1.9 Scenario 9.....	38
3.2 Importing the Orbital Parameters from STK to Skydel.....	40
3.3 Assessing the Performance of a LEO-based GNSS using Skydel.....	43
3.4 A Comparison Assessment between the Performance of LEO and MEO-based GNSS using Skydel.....	54
Chapter 4: Discussions	55
4.1 Discussion of the Performance of the Simulated LEO Constellation.....	55
4.2 Link Budget Analysis of GNSSaS.....	64
Chapter 5: Conclusion.....	66
5.1 Conclusions.....	66
5.2 Research Findings and Limitations.....	66
5.3 Recommendations and Way Forward.....	67
References	68
List of Publications.....	72
Appendices	73
Appendix A: Hardware and Software Specifications	73
Appendix B: Scenario 11	74
Appendix C: 3D & 2D Graphics for the Tested Scenarios in STK	77

List of Tables

Table 1: Comparison between 6 GNSS constellations.....	3
Table 2: Comparison between MEO and LEO GNSS	8
Table 3: The current known LEO PNT constellations.....	9
Table 4: List of the hardware used in this research	13
Table 5: RAAN & true anomaly of scenario 1.....	26
Table 6: RAAN & true anomaly of scenario 2.....	29
Table 7: RAAN & true anomaly of scenario 3.....	30
Table 8: RAAN & true anomaly of scenario 4.....	32
Table 9: RAAN & true anomaly of scenario 5.....	33
Table 10: RAAN & true anomaly of scenario 6.....	35
Table 11: RAAN & true anomaly of scenario 7.....	36
Table 12: RAAN & true anomaly of scenario 8.....	37
Table 13: RAAN & true anomaly of scenario 9.....	39
Table 14: Summary of the 9 scenarios	40
Table 15: Orbital parameters of scenario 9 in Skydel.....	41
Table 16: RAAN & true anomaly for each satellite in scenario 9	41
Table 17: Figures of merit of scenario 9	44
Table 18: Orbital parameters of scenario 10 in Skydel.....	45
Table 19: RAAN & true anomaly for each satellite in scenario 10	45
Table 20: Figures of merit of scenario 10	46
Table 21: Orbital parameters of scenario 12 in Skydel.....	47
Table 22: RAAN & true anomaly for each satellite in scenario 12	48
Table 23: Figures of merit of scenario 12	50
Table 24: Orbital parameters of scenario 13 in Skydel.....	51
Table 25: RAAN & true anomaly for each satellite in scenario 13	52
Table 26: Figures of merit of scenario 13	53
Table 27: Performance comparison between LEO and MEO constellations.....	54
Table 28: Link budget of a LEO GNSS spacecraft.....	65

List of Figures

Figure 1: GNSS three segments	3
Figure 2: The concept of trilateration.....	4
Figure 3: Trilateration with four satellites.....	5
Figure 4: Poor PDOP and good visibility.....	8
Figure 5: Good PDOP and good visibility	8
Figure 6: Diagram showing propagation of the real GNSS signals from the satellite to the GNSS receiver	10
Figure 7: Orolia Skydel GNSS Simulator Hardware Setup	11
Figure 8: Diagram of the hardware components that compose Skydel simulator.....	12
Figure 9: A screenshot from Skydel showing the orbits of GPS space vehicles.....	14
Figure 10: A screenshot showing that the desired LEO altitude is out of range for GPS constellation	15
Figure 11: Modification of GPS altitude in .sdx configuration file	15
Figure 12: Area coverage of a LEO satellite versus a MEO satellite.....	16
Figure 13: Different colour planes (STK)	18
Figure 14: Access times graph in STK.....	19
Figure 15: The input orbital parameters in Skydel.....	20
Figure 16: Inserting vehicle position in Skydel.....	21
Figure 17: Sky plot, DOP values, and signal power in Skydel	21
Figure 18: Map view in Skydel	22
Figure 19: Deviation graph in Skydel	22
Figure 20: Enabling the desired constellations in u-center	23
Figure 21: Selecting the dynamic model in u-center.....	24
Figure 22: Logging the desired parameters in u-center software.....	24
Figure 23: The tracked satellites by the receiver in u-center software.....	25
Figure 25: 2D graphic (scenario 1).....	27
Figure 24: 3D graphic (scenario 1).....	27
Figure 26: Access times (scenario 1)	28
Figure 27: Access times (scenario 1) zoomed in.....	28
Figure 28: Access times (scenario 2)	29
Figure 29: Access times (scenario 3)	31
Figure 30: Access times (scenario 4)	32
Figure 31: Access times (scenario 5)	34
Figure 32: Access times (scenario 6)	35
Figure 33: Access times (scenario 7)	36
Figure 34: Access times (scenario 8)	38
Figure 35: Access times (scenario 9)	40
Figure 36: Scenario 9 at 08:25 am in Skydel	42
Figure 37: Scenario 9 at 10:15 in Skydel	42

Figure 38: Simulator position in Skydel.....	43
Figure 39: The deviation graph of scenario 9 in Skydel	44
Figure 40: Satellite spatial density in scenario 10	46
Figure 41: Receiver’s locking period for scenario 12	49
Figure 42: Deviation graph of scenario 12	50
Figure 43: Sky view of scenario 13 in Skydel.....	53
Figure 44: Doppler frequency vs. elapsed time of a LEO satellite at 800 km	56
Figure 45: Doppler frequency vs. elapsed time of a MEO Galileo satellite at 23,229 km	56
Figure 46: Doppler slope vs. elapsed time of a LEO satellite at 800 km.....	57
Figure 47: Doppler slope vs. elapsed time of a MEO Galileo satellite at 23,229 km	57
Figure 48: Radial velocity vs. elapsed time of a LEO satellite at 800 km	58
Figure 49: Radial acceleration vs. elapsed time of a LEO satellite at 800 km.....	59
Figure 50: Radial velocity vs. elapsed time of a MEO satellite at 23,229 km.....	59
Figure 51: Radial acceleration vs. elapsed time of a MEO satellite at 23,229 km	60
Figure 52: Example of the measured C/N0 of the tracked satellites by ublox receiver.....	62

List of Abbreviations

C/N0	Carrier to Noise Ratio
CFG	Configuration
COTS	Commercial Off-The-Shelf
DC	Direct Current
DOP	Dilution of Precision
EIRP	Equivalent Isotropic Radiated Power
FAA	Federal Aviation Administration
FSPL	Free Space Path Loss
GNSS	Global Navigation Satellite System
GNSSaS	Global Navigation Satellite Systems Augmentation Signaling
GPS	Global Positioning System
IRNSS	Independent Regional Navigation Satellite System
LEO	Low Earth Orbit
LNA	Low Noise Amplifier
LOS	Line of Sight
MEO	Medium Earth Orbit
NAV	Navigation
NSSTC	National Space Science and Technology Center
PACC	Positioning Accuracy
PC	Personal Computer
PDOP	Position Dilution of Precision
PNT	Positioning, Navigation and Timing
PPP	Precise Point Positioning
QZSS	Quasi-Zenith Satellite System
RAAN	Right Ascension of Ascending Node

RF	Radio Frequency
RTK	Real-Time Kinematic
RXM	Receiver Manager
SDR	Software-Defined Radio
SDX	Software-Defined Simulator
STK	Systems Tool Kit
SV	Space Vehicle
TBD	To be Determined
UAE	United Arab Emirates
UAEU	United Arab Emirates University
UAV	Unmanned Aerial Vehicle
UBX	Ublox Receiver
US	United State
USB	Universal Serial Bus
USRP	Universal Software Radio Peripheral

Chapter 1: Introduction

1.1 Overview and Problem Statement

Recently, there has been a resurgent need for alternative navigation solutions to provide high precision and accuracy in positioning, navigation, and timing signals, particularly for some targeted applications such as autonomous vehicles and flying taxis. The current Global Navigation Satellite Systems such as GPS, BeiDou, Galileo and GLONASS can only provide positioning accuracy for up to meter-level in open civilian services. According to the Federal Aviation Administration website (FAA, 2023), the basic GPS service provides an accuracy level of up to 7 meters for civilians. This accuracy would not be sufficient for targeted critical applications in the UAE, such as autonomous vehicles and flying taxis, which would require a high precision centimeter-level accuracy and fast convergence of positioning accuracy.

Low Earth Orbit-based navigation satellites have advantages in terms of fast-changing geometry, and low free space signal loss, which can serve as a complementary or extension of the current Medium Earth Orbit-based Global navigation Satellite System. Therefore, LEO-based navigation augmentation is considered as one of the key technologies of next-generation positioning, navigation, and timing systems. Studies have shown that broadcasting navigational signals from a LEO satellite could improve the positioning accuracy on the ground compared to MEO GNSS due to its faster orbital movement and improved signal quality in multi-path environments (Su et al., 2019). LEO-augmented GNSS signals could also significantly reduce the acquisition time for a position determination as compared to conventionally used positioning methods such as Real Time Kinematic (RTK) and Precise Point Positioning (PPP) using GNSS MEO satellites.

1.2 Research Objectives

- I. To design and simulate an optimum orbital scenario of a mini-LEO constellation transmitting GNSS signals at 800 km altitude and 40 degrees inclination angle and having at least 4 satellites in the sky view.

- II. To test the orbital scenario using a GNSS simulator and assess the receiver's performance regarding the receiver's time to lock, locking period, continuity, PDOP and the 3D positioning accuracy.
- III. To compare the performance of the simulated mini-LEO GNSS constellation with the existing MEO GPS and Galileo.

1.3 Relevant Literature

Nowadays, millions of smartphones and devices make use of GNSS. The Global Navigation Satellite System (GNSS) is a constellation of satellites providing Positioning, Navigation, and Timing (PNT) services. A satellite navigation system called Parus expanded into Glonass was first developed by the Soviet Union back in 1974 (Mcduffie, 2017). Parus was primarily developed for use by the Russian military and similarly the GPS for the US military. In 1983, a Korean passenger aircraft experienced a navigation error and entered the Soviet-prohibited airspace. The aircraft got shot down killing all the passengers. After realizing that a worldwide GPS could have prevented such an accident, the US President Ronald Reagan opened the system to be used by the public in September 1983 (Mcduffie, 2017).

1.3.1 Types and Operation Principles of the Global Navigation Satellite Systems (GNSS)

Currently, there are four global GNSS constellations and two regional GNSS constellations. The six constellations are mainly located in the Medium Earth Orbit and are illustrated in Table 1 (NovAtel, 2023).

Table 1: Comparison between 6 GNSS constellations

	Name	Operator	Altitude (km)	Number of Satellites	Frequency (MHz)
Global	Glonass	Russia	19,130	24	L1 (1598.0625-1605.375), L2 (1242.9375-1248.625), L3 (1202.025)
	GPS	US	20,180	31	L1 (1575.42), L2 (1227.60), L5 (1176.45)
	Gallio	Europe	23,222	26	Along L-band spectrum: E1 (1575.42), E5 (1191.795), E5a (1176.45), E5b (1207.14), E6 (1278.75)
	BeiDou	China	21,528 35,786	48	B1I (1561.098), B1C (1575.42), B2a (1175.42), B2I and B2b (1207.14), B3I (1268.52)
Regional	QZSS	Japan	32,000 40,000	4	L1 (1575.42), L2 (1227.60), L5 (1176.45), L6 (1278.75)
	IRNSS/NavIC	India	36,000	8	L5 frequency (1176.45), S-Band (2492.028)

The basic principles of GNSS should first be understood to understand how the satellites orbiting the Earth could tell a person’s location. GNSS has three segments: the space segment, control segment, and user segment, as shown in Figure 1.

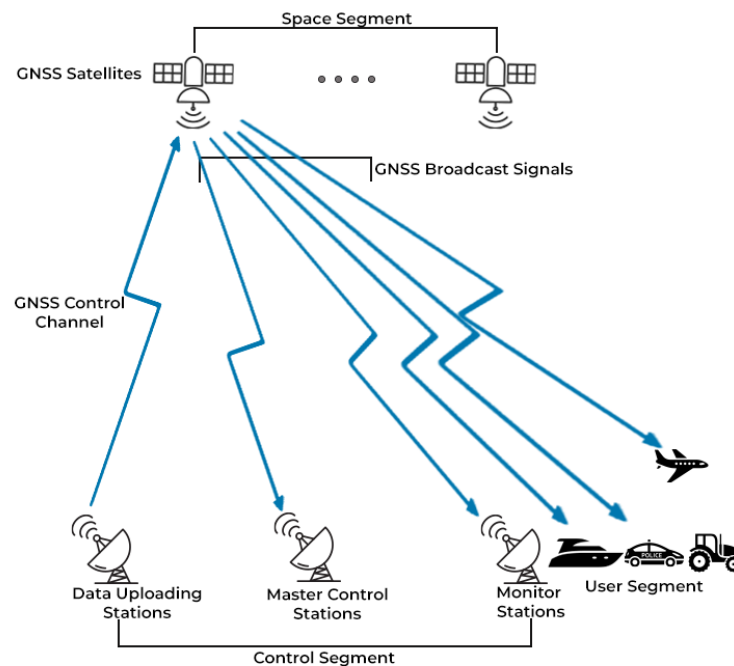


Figure 16: GNSS three segments (BasuMalick, 2022)

The space segment is represented by a constellation of satellites distributed into planes in an arrangement that ensures at least a visibility of four satellites by a receiver. Onboard these satellites, atomic clocks that are used to transmit signals from the satellite to the receiver at precise times. Secondly, the control segments are used to control, monitor, track, and communicate with the satellites ensuring the synchronization of the satellites' clocks and transmitting back the information on the satellite's orbit (BasuMalick, 2022). Thirdly, the user segment could be any device with a GNSS receiver, such as our cars and/or mobile phones. The GNSS receiver uses the trilateration technique, which positions an object from three distances to determine the user's position, speed, and elevation (BasuMalick, 2022). The GNSS receiver receives the radio frequency signal from the satellite via the receiving antenna. The received radio signals have a navigation message that contains information that aids in computing the navigation solution and calculating the difference between the broadcast time and the time of receiving the signal by taking into consideration the time delays caused by a signal traveling from a satellite to a receiver. Then, the receiver uses the speed of light to measure the distance traveled by the RF signals from all three satellites (BasuMalick, 2022). Finally, using the satellite position at the transmit time, the receiver can derive its location. Furthermore, adding another satellite to the visibility of the receiver would provide the receiver's clock bias that would eliminate the need for atomic clocks at the receiver end. The receiver would then use these four satellites to calculate latitude, longitude, altitude, and time. The basic concept of trilateration is represented in Figure 2.

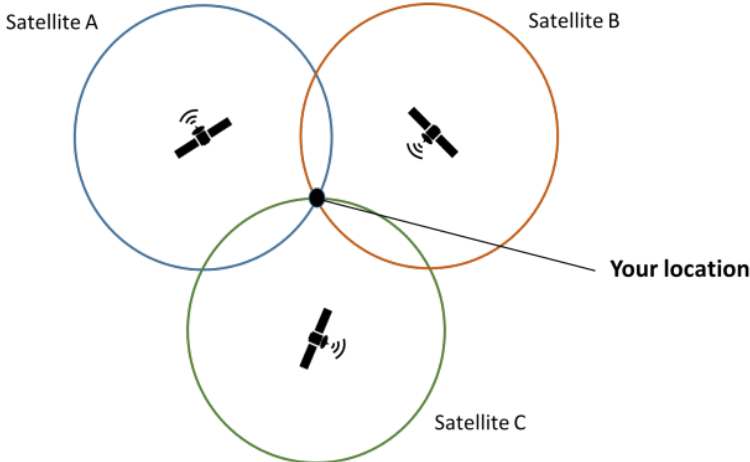


Figure 17: The concept of trilateration (Ong, 2016)

Data from the first satellite or satellite A provides a general user location within a large circle. Then, data from satellite B adds another circle that overlaps with the first circular area provided by satellite A. One of the two points of overlap now could be the correct user location. Adding the third satellite, or satellite C, gives the user location position on the Earth surface. As stated by (Zahradnik, 2021), data from a fourth satellite or more would further enhance the accuracy of the user’s location and enables calculating factors like elevation or altitude in the case of aircraft. Figure 3 illustrates the concept of trilateration using four satellites in view of the user receiver. Trilateration concept is well explained in (Misra & Enge, 2011). In a nutshell, if the transmit time of the signal and the speed of the signal propagation are already known, the distance from the satellite to the receiver could be calculated by multiplying the speed of light by the travel time of the RF signal from the satellite to the receiver (FAA, 2023). Since the GNSS satellite’s clock and the GNSS receiver’s clock are not always perfectly synchronized, the time offset between the clocks should be accurately determined to accurately measure the distance.

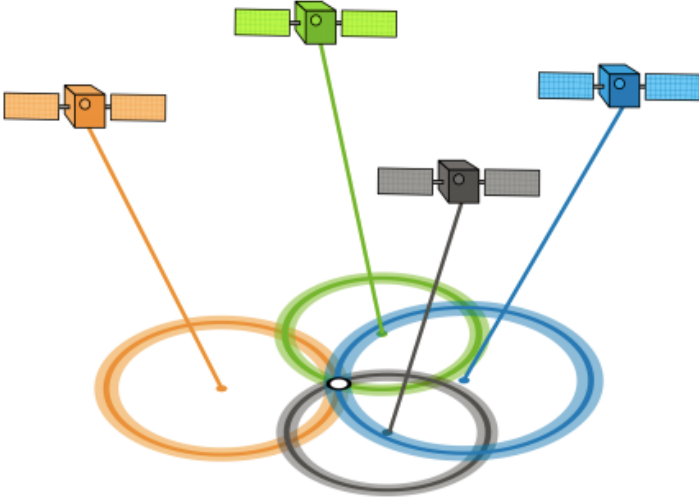


Figure 18: Trilateration with four satellites (GISGeography, 2022)

1.3.2 Limitations of the Current MEO GNSS

One of the most used smartphone applications nowadays is Google Maps, which uses GPS constellation at an approximate altitude of 20,000 km to determine our locations. Even though it works well to navigate us from one location to another, its

signals are considered very weak. Therefore, they become unreliable in urban canyons such as cities and mountain valleys. Furthermore, according to Lawrence et al., (2017), GPS is considerably limited when used in deep attenuation environments, as it was primarily developed to be used in open-sky environments. In addition, it is susceptible to jamming, in which a 20-watt GNSS jammer could deny the service above a city block (Lawrence et al., 2017).

Furthermore, the accuracy level of GPS and the other GNSS constellations can only reach meter-level using the normal point positioning technique, however, the current market demands for centimeter-level accuracy, especially in critical applications such as flying taxis and unmanned vehicles. For example, the mean accuracy for GPS using smartphones in open-sky environments is 4.9 meters (Diggelen & Enge, 2015). When indoors, the accuracy level becomes 10 meters (Puzzo, 2021). This level of accuracy could be acceptable for most people to know their locations and calculate their routes from one place to another. However, for many applications such as UAVs and autonomous vehicles, a very quick and accurate positioning anywhere and anytime is required.

Recently, there has been a resurgent interest in developing LEO GNSS navigation constellations, and some theoretical studies have been conducted to assess the benefits of LEO-based navigation systems.

1.3.3 Advantages of LEO GNSS

According to Su et al., (2019), the rapid orbital movement of LEO satellites provides faster geometric change and faster integer ambiguity resolution. In a study that was conducted by Su et al., (2019), a simulation was used to augment the BeiDou-3 constellation with 120 LEO GNSS satellites. Using the Precise Point Positioning (PPP) technique, the simulation demonstrated a reduction of the convergence time from about 30 minutes to just 1 minute, which provides great importance for real-time PPP applications. The PPP technique works on the principle of removing system errors such as ionospheric errors. It uses global and/or regional reference stations to estimate real-time satellite orbit/clock errors and directly send the corrections to the end user via a

satellite or over the Internet (Chen, 2022). The disadvantage of this technique is that it requires an average convergence time of 20 to 40 minutes to give a cm-level positioning accuracy. This is unacceptable for automotive industries such as self-driving cars, which require very fast convergence of positioning determination. With the rapid orbital movement of LEO satellites, the convergence time could be reduced to only 1 minute to give less than 10 cm positioning accuracy (Long, 2019).

In addition, in the same study conducted by Su et al., (2019), the satellite Position Dilution of Precession (PDOP) has also been assessed, and the results showed considerable enhancement. DOP values describe the strength of the current satellite geometry, or configuration, on the data accuracy received by a GNSS receiver, and PDOP is considered the mean of DOP or the 3D positioning (Matt, 2017). A good PDOP value can be achieved by increasing the number of signals received by a GNSS receiver, and the more well spread the signals are from each other, the better the PDOP value would be (refer to Figures 4 & 5). As stated by Mapasyst, (2019), the smaller the PDOP value, the better the positioning accuracy. Values as small as 3 are considered good, and values greater than 7 are considered poor and should not be relied upon. Augmenting the BeiDou-3 constellation with 120 LEO GNSS satellites has reduced the average of the PDOP value from 1.63 to 1.22 (Su et al., 2019). Furthermore, the satellite visibility increased significantly in the simulation after augmenting the BeiDou-3 constellation with 120 LEO GNSS satellites, and the average number of the tracked satellites by a GNSS receiver got raised from approximately 10 satellites to 16 satellites, which would further enhance the positioning accuracy. Table 2 illustrates a comparison between MEO and LEO GNSS characteristics.

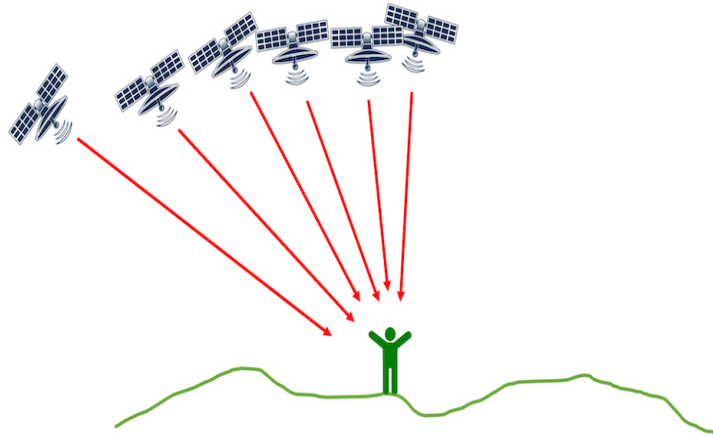


Figure 19: Poor PDOP and good visibility (Matt, 2017)

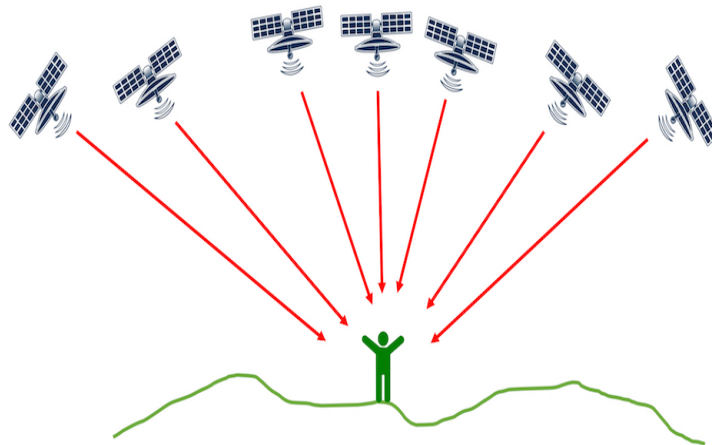


Figure 20: Good PDOP and good visibility (Matt, 2017)

Table 2: Comparison between MEO and LEO GNSS

Characteristic	MEO	LEO
Altitude (Roberts, 2022)	~24,000 km	160 to 2000 km
Orbital Period (Roberts, 2022)	~12 hours	90 minutes to 2 hours
Footprint in Diameter (Reid, 2016)	~12,000 km	3000 km (780 km)
Required Number of Satellites (Reid, 2016)	10s to 30s	100s to 1000s
Minimum Signal Strength on Ground (ISRO, 2017)	~ -160 dBW (-130 dBm)	~ -160 dBW (-130 dBm)

1.3.4 Issues with tracking LEO Satellites

Despite the promising advantages of LEO GNSS, there are several issues with tracking LEO satellites for positioning and navigation. Compared to MEO GNSS satellites, LEO satellites move at a much higher speed, which potentially causes high dynamic problems in the Line-of- Sight (LOS) direction subsequently leading to

instability in the receiver signal tracking loop (Liu & Wang, 2022). Due to its closeness to earth, LEO navigation signals have distinguished characteristics of large signal strength variation, large Doppler variation, and large acceleration variation than MEO navigation signals (Wang et al., 2019). An analysis performed by Wang et al., (2019) for Loujia-1A satellite showed that signal strength variation at 650 km altitude is more than 6 times the signal strength variation of a GPS signal during a satellite pass. They concluded that the large dynamics in signal strength causes inhomogeneity in receiver noise thus affecting the tracking performance of the receiver and pseudorange precision. This effect would require some changes in current receiver’s radio frequency front end (Wang et al., 2019). Doppler variation due to fast geometry change of a LEO satellite causes the receiver’s Doppler search time to be increased dramatically hence affecting the signal acquisition efficiency. Large acceleration variation of a LEO signal would increase the GNSS receiver complexity to be able to cope with high dynamic scenarios (Wang et al., 2019).

1.3.5 The Current LEO PNT Constellations

Several technology demonstrator satellites were recently launched in LEO, such as CentiSpace in 2018, Xona Pulsar, and GeeSat in 2022. Furthermore, a technology demonstrator satellite called GNSSaS from the UAE is planned to be launched. Table 3 lists the current and planned LEO GNSS constellations.

Table 3: The current known LEO PNT constellations

Name	Company	Country	Altitude	Date of Full Operational Capability
CentiSpace-1	Future Navigation	China	700 km	2028
Xona Pulsar	Xona space Systems	USA	525 km	2027
GeeSat-1	Geespace	China	621.5 km	2028
GNSSaS Technology Demonstrator	NSSTC	UAE	TBD	TBD

Chapter 2: Orbit Simulation Methodology

2.1 Skydel GNSS Simulator

A software-defined GNSS simulator has been used to create an orbital test scenario of a LEO GNSS constellation design and assess its performance. The GNSS simulator consists of a USRP as an RF front end, and a Skydel GNSS simulator software as the back end. Skydel software, owned by Orolia, allows the user to create highly complicated test scenarios for multiple GNSS constellations such as GPS, GLONASS, Galileo, and BeiDou.

To acquire and track the GNSS signals for positioning determination, the GNSS receiver must be outdoors in an open sky area to obtain positioning determination. Figure 6 illustrates the typical GNSS signal power when the signal propagates from an existing MEO GNSS satellite to the receiver. As shown in Figure 6, the transmitted power of the GNSS satellite is 52 dBm. After considering the Free Space Path Loss (FSPL) in MEO with an altitude of around 20,000 km, the minimum received power signal on the ground received by an omnidirectional antenna with 0 dBi gain as per GNSS standards is -130 dBm. In addition, the GNSS antenna normally has a Low Noise Amplifier (LNA), which amplifies the received signal to the level that can be detected by the receiver, usually 20 dB of gain. Finally, the typical GNSS receiver receives the signal at -110 dBm.

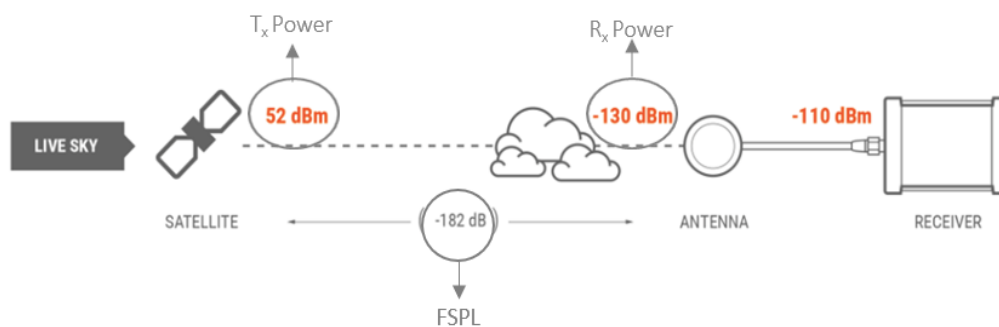


Figure 21: Diagram showing propagation of the real GNSS signals from the satellite to the GNSS receiver (Orolia Skydel User Manual, 2020)

A GNSS simulator that emulates the real GNSS signals is used to test the performance of a GNSS receiver in a controlled environment. Figure 7 illustrates the

hardware setup of the Orolia Skydel GNSS simulator used to conduct this research. Both the hardware and software used in this research have been chosen based on the resources available at the National Space Science and Technology Center (NSSTC) in UAE.

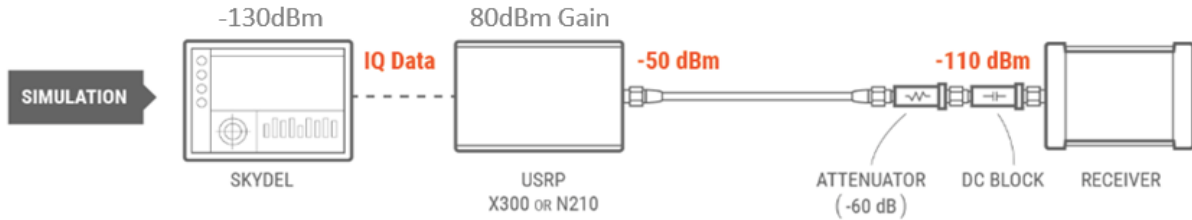


Figure 22: Orolia Skydel GNSS Simulator Hardware Setup (Orolia Skydel User Manual, 2020)

The following steps briefly detail the procedure of how the GNSS simulator mimics the real GNSS signals adapted from Orolia Skydel User Manual, 2020:

- Through a PC set up, the Skydel software generates I/Q samples representing the GNSS signals.
- The I/Q samples travel from the PC to the Software Defined Radio (X300 USRP) through a transport link such as a USB.
- The X300 USRP pulls the I/Q samples gradually and converts them to RF signals at a minimum of -50 dBm (80 dBm default gain).
- RF attenuators of -60 dB are connected between the USRP and the receiver, which converts the signal power to the typical value of -110 dBm power level. A DC block is connected between the attenuators and the receiver to prevent the DC voltage from traveling back from the GNSS receiver to the USRP.

The system setup and hardware components used for creating the test scenario are illustrated in Figure 8 (Orolia Skydel User Manual, 2020). Table 4 lists the hardware used in this research work.

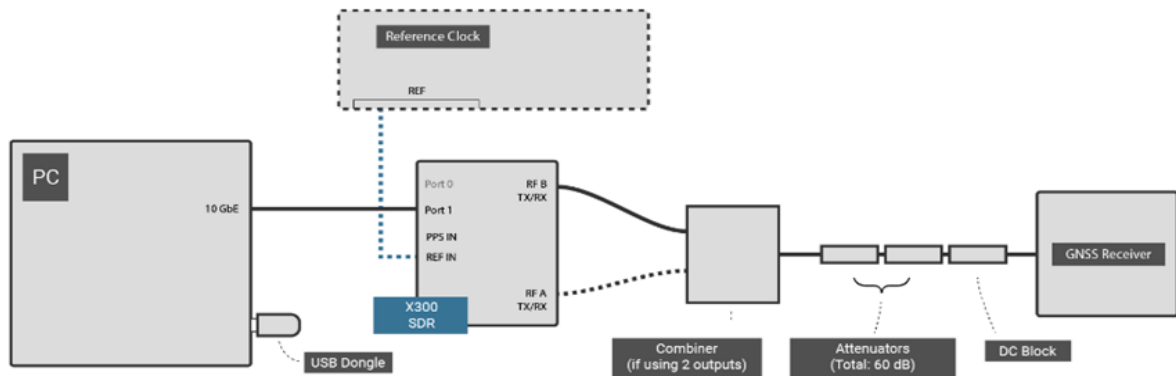







Figure 23: Diagram of the hardware components that compose Skydel simulator (Orolia Skydel User Manual, 2020)

Skydel software version 22.7.1, released on 23rd of September 2022, was used in this research. The main purpose of using Skydel software is to create a test scenario of a LEO GNSS and assess its performance. Using this software, attempts have been carried out to modify the altitude of the current GNSS constellations to an altitude of 800 km in LEO.

Table 4: List of the hardware used in this research

Hardware	Photo/Part No.
High-performance PC (minimal computer requirements is in Appendix A-i)	
Reference Clock (10 MHz)	<p>CDA 200</p> 
Software Defined Radio (SDR)	<p>USRP X300</p> 
GNSS receiver (Specifications in Appendix A-ii)	<p>ublox EVK-M8T single frequency receiver</p> 
2 Attenuators: 30 dB each	
DC Block	<p>BLK-18-S+</p> 

2.1.1 Modifying the GPS Constellation from MEO to LEO using Skydel Software

Using Skydel software, an attempt has been carried out to modify the altitude of the existing GPS constellation to a Low Earth Orbit at an altitude of 800 km using the following steps:

- a) After the desired constellation from Skydel setting was chosen, GPS in this case, the orbits feature, was selected.

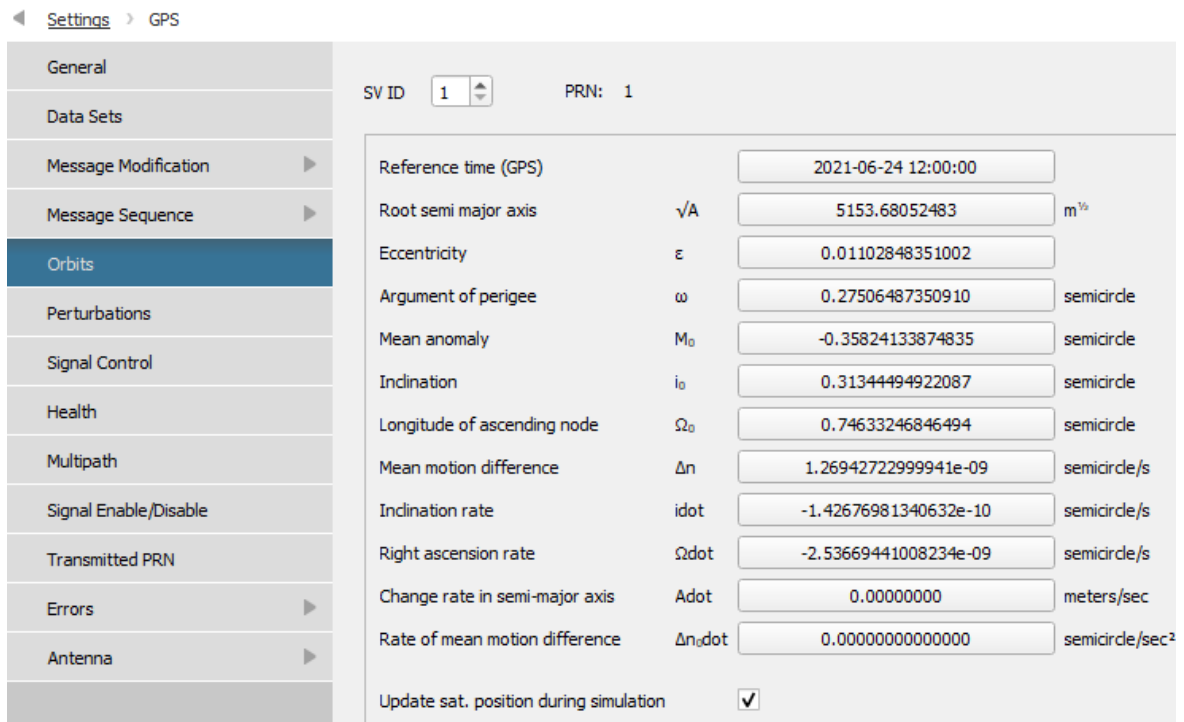


Figure 24: A screenshot from Skydel showing the orbits of GPS space vehicles

- b) By default, space vehicle ID 1 will always appear first with its specific orbital parameters. For example, GPS SV ID 1 is currently 20,189 km above the Earth's surface.
- c) To modify the satellite's altitude from MEO to LEO, the root semi major axis in the unit of $m^{1/2}$ was modified to the desired altitude, in this case 800 km would correspond to a semi major axis of 2677.87 $m^{1/2}$. However, the software did not accept the input of the new root semi major axis value. It indicated that the minimum root semi major axis for GPS is 5147.25 $m^{1/2}$, this is 20,122.87 km above Earth surface, which means the satellite will still be in a Medium Earth Orbit (refer to Figure 10).

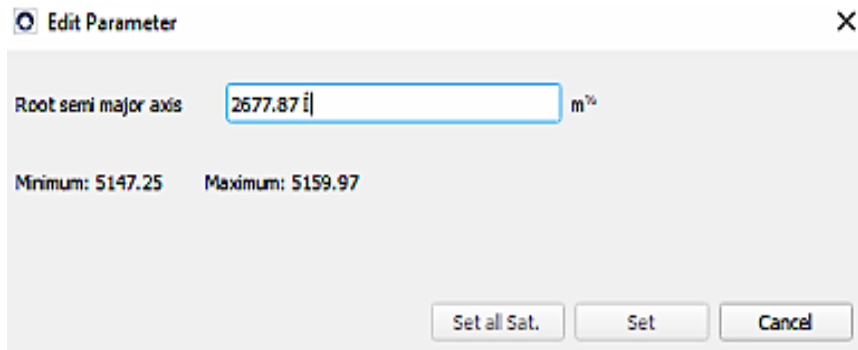


Figure 25: A screenshot showing that the desired LEO altitude is out of range for GPS constellation

To enable the modification of the GPS altitude to the desired LEO altitude, the .sdx configuration file was modified using the following method:

- Save the configuration file of step a)
- Edit the .sdx file and modify the SqrtA for each GPS SVID to the desired altitude in the <Ephemerides> section (refer to Figure 11).

2.1.2 Modifying Galileo and BeiDou Constellations from MEO to LEO using Skydel Software

```

<Ephemerides>
  <DeltaUtc A0="4.656612873100e-09" A1="1.332267630000e-14" RefSec="589824" RefWeek="2163"/>
  <LeapSeconds>18</LeapSeconds>
  <GPSEphemeris SVID="1">
    <Toc Rollover="2" Week="184" Sec="115200" LeapSeconds="0"/>
    <Toe Sec="115200" Week="2232"/>
    <Clock Bias="6.486773490906e-04" Drift="-1.170974428533e-11" DriftRate="0.000000000000e+00"/>
    <Perturbations Crs="-1.421562500000e+02" Cuc="-7.430091500282e-06" Cus="4.675239324570e-06" Cic="2.10
    <Orbit DeltaN="3.988023260033e-09" M0="1.396123775255e+00" e="0.000000000000e+00" SqrtA="2.67787e+03"
    <TransmissionTime>381618</TransmissionTime>
    <IssueOfData>105</IssueOfData>
    <Geo IsGeo="False" GeoLon="0.000000"/>
    <IssueOfDataClock>105</IssueOfDataClock>
    <CNavOrbit/>
  
```

Figure 26: Modification of GPS altitude in .sdx configuration file

The other GNSS constellations in Skydel software have been checked for the ability to be modified to a Low Earth Orbit. Skydel software allows modification of two GNSS constellations easier than GPS: Galileo and BeiDou. Both constellations had a minimum root semi-major axis of 2524 m^{1/2}. The root-semi major axis of Galileo SVID 3 has been modified from 5440.6 m^{1/2} (23,229 km) to 2677.87 m^{1/2} (800 km) above the Earth surface. However, not all Galileo SV IDs enable the modification of their orbital

parameters. Only 22 out of 36 Galileo satellites enabled the modification to LEO; those are SV IDs 1 to 36 except for; 6, 10, 14, 16, 17, 18, 20,22, 23, 28, 29, 32,34, and 35.

2.1.3 Area Coverage of a MEO Satellite versus a LEO Satellite

The current GNSS constellations orbit the Earth in MEO. For example, the Galileo constellation, consisting of 27 satellites, is orbiting the Earth at an altitude of 23,220 km above the Earth surface (Bury et al., 2021). 27 satellites are adequate to provide global coverage at this altitude but would not be sufficient at an altitude of 800 km. The closer the satellite is to the Earth’s surface, the less coverage area it would provide. Figure 12 illustrates the remarkable difference in the footprints of a LEO satellite compared to MEO (Guan et al., 2020).

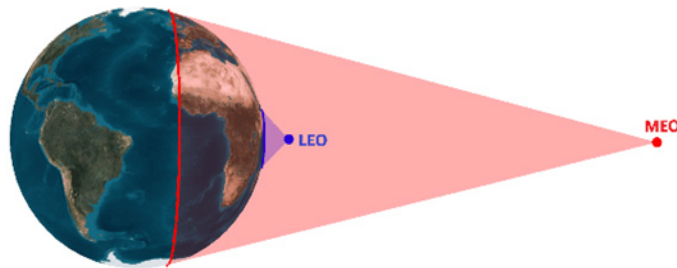


Figure 27: Area coverage of a LEO satellite versus a MEO satellite (Guan et al., 2020)

The coverage circle area of the satellite at Nadir is calculated using the formula $A=2\pi R^2h / (R + h)$; in which R is Earth’s radius (6371 km), and h is the satellite’s height above Earth’s surface (Guan et al., 2020). Modifying the altitude of the Galileo constellation from 23,220 km to 800 km corresponds to a reduction of the coverage area by 7.03. This means that for a LEO constellation to have global coverage as in MEO, a large number of satellites would be required. Thus, modifying the 22 Galileo SVIDs to LEO in Skydel software to an altitude of 800 km, will not provide global coverage. As a result, it would be more convenient to simulate a mini-LEO GNSS constellation in Skydel software.

The following sections describe the concept design of the mini constellation, which was first simulated in STK, and then the orbital parameters of the designed

constellation were finally imported to Skydel for the performance assessment of the LEO constellation.

2.2 Designing a Mini Constellation of a LEO-based GNSS using STK

A design of a mini constellation of 16-22 satellites was first simulated in this research using the Systems Tool Kit (STK) software (AGI, 2023). The altitude of 800 km was chosen in this research work due to a previous feasibility study conducted as the optimum altitude for the UAE's GNSSaS constellation network that meets the design requirements (NSSTC, 2019). The satellites in the constellation have the following orbital parameters:

- Inclination angle = 40°
- Altitude = 800 km above Earth's surface
- Argument of perigee = 0
- Coverage = $\pm 40^\circ$ latitude
- Eccentricity = 0

2.2.1 Walker Tool

Instead of inserting a satellite by satellite to create a constellation, the walker tool in STK enables the quick building of a satellite constellation. The user should first insert the original satellite, or the seed satellite, with the sub-objects required. The sub-objects, such as an antenna inserted in the seed satellite, will be copied to the child satellites when generating the constellation. There are three types of constellation configurations in STK:

1. Delta: The planes will be evenly distributed over 360° span,
2. Star: The planes will be evenly distributed over 180° span,
3. Custom: The user can specify the spaces between the planes and the inter-plane phasing.

Due to the limited number of GNSS satellites that can be simulated in Skydel software, the custom configuration would be the most convenient walker configuration to work with. The two critical inputs to design a custom constellation are the Right Ascension of Ascending Node or the RAAN increment and the True Anomaly. The

spaces between the orbital planes are identified by the RAAN increment entered in degrees. While the spaces between the satellites in one plane and/or adjacent planes, are identified by the True Anomaly, also entered in degrees.

After generating the constellation, the software will automatically give each plane a different color to easily track the satellites. Furthermore, it will also give a unique name for each satellite and its sub-objects, depending on the plane the satellite is assigned to and the number of the satellite inter-plane. For instance, satellite 31 in Figure 13 means that this is satellite number 1 in the third plane in the constellation.

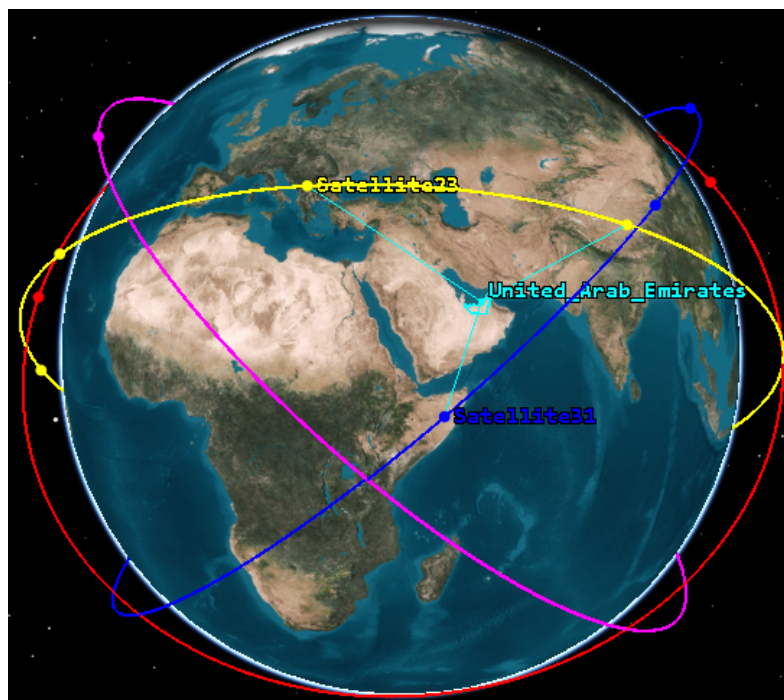


Figure 28: Different colour planes (STK)

2.2.2 Access Times

To calculate the access times between a sensor on the ground and a satellite, a user should first click the access tool icon (📡). After that, the object on the ground, or the access-for object, should be selected. In this study, the area target (UAE) has been selected. Then, the object a user wants to compute the access-to should be selected. In this research, satellite antennas have been selected. Finally, the access times graph is plotted as shown in Figure 14.

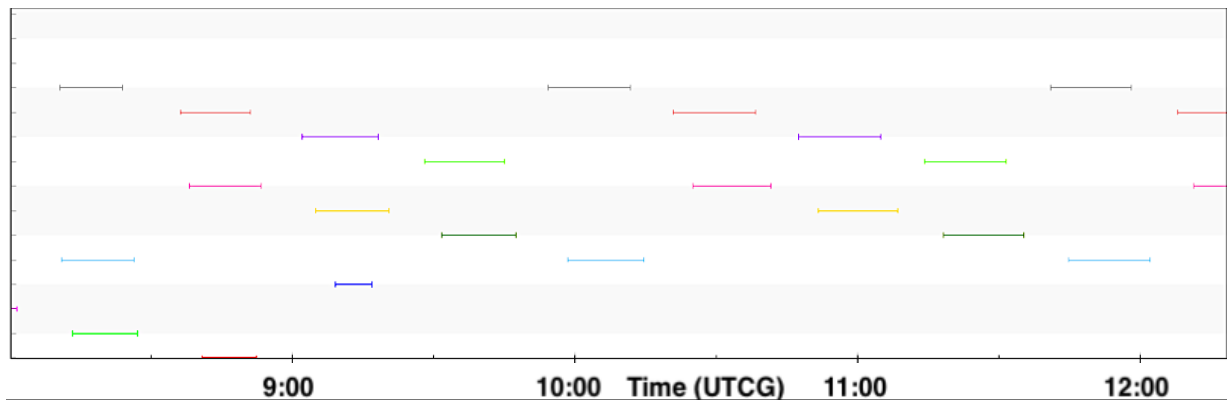


Figure 29: Access times graph in STK

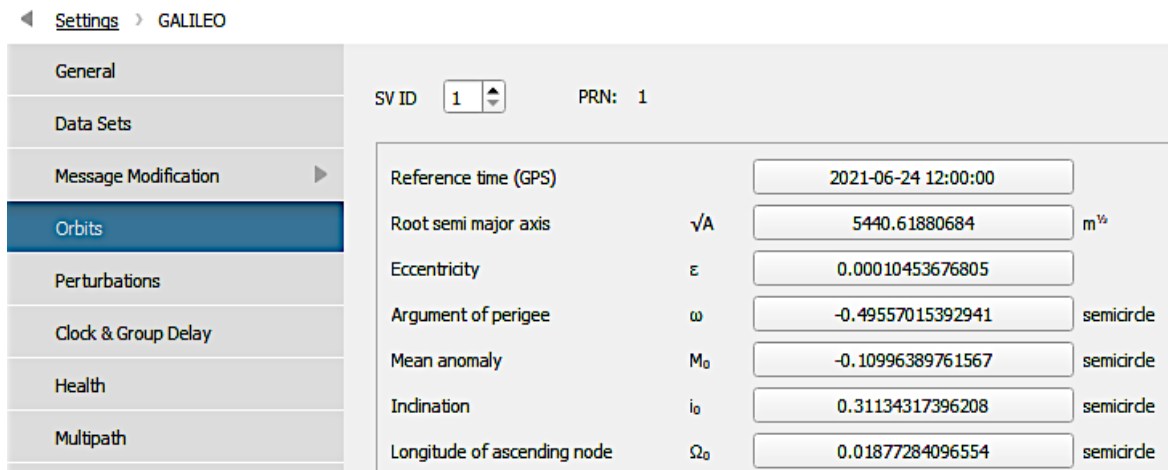
Several case studies have been performed using STK to find the best configuration of the satellites. The requirement is to have at least 4 satellites in view of the user receiver anywhere in the UAE. The contact time with the receiver should be adequate for the receiver to calculate its position of at least 8 to 10 minutes (Meg, 2022).

2.3 Importing the Orbital Parameters from STK to Skydel

To modify the orbital parameters of a satellite or a constellation in Skydel software, the following steps were followed.

- a) From the settings, the desired constellation was chosen. Galileo for example.
- b) The orbits feature was selected, followed by the SVID number to be modified.

c) The orbital parameters of the constellation design in STK were entered. As the angles units in STK are different from those in Skydel, each angle was converted from degrees to semicircle (refer to Figure 15). The exact reference time should also be imported.



Parameter	Symbol	Value	Unit
SV ID		1	
PRN		1	
Reference time (GPS)		2021-06-24 12:00:00	
Root semi major axis	\sqrt{A}	5440.61880684	m/s
Eccentricity	ϵ	0.00010453676805	
Argument of perigee	ω	-0.49557015392941	semicircle
Mean anomaly	M_0	-0.10996389761567	semicircle
Inclination	i_0	0.31134317396208	semicircle
Longitude of ascending node	Ω_0	0.01877284096554	semicircle

Figure 30: The input orbital parameters in Skydel

2.4 Assessing the Performance of a GNSS Constellation using Skydel and U-center

Using the test setup in Figure 8, the following steps were followed to test the performance of the GNSS receiver using the LEO GNSS constellation simulated in Skydel.

In Skydel software:

1. X300 was added as the output type.
2. The desired GNSS constellation and signal were selected. Galileo E1, for example.
3. In settings, the Vehicle was selected, followed by the input of the desired latitude, longitude, and altitude (refer to Figure 16).
 - The desired elevation angle of 5° was entered here.

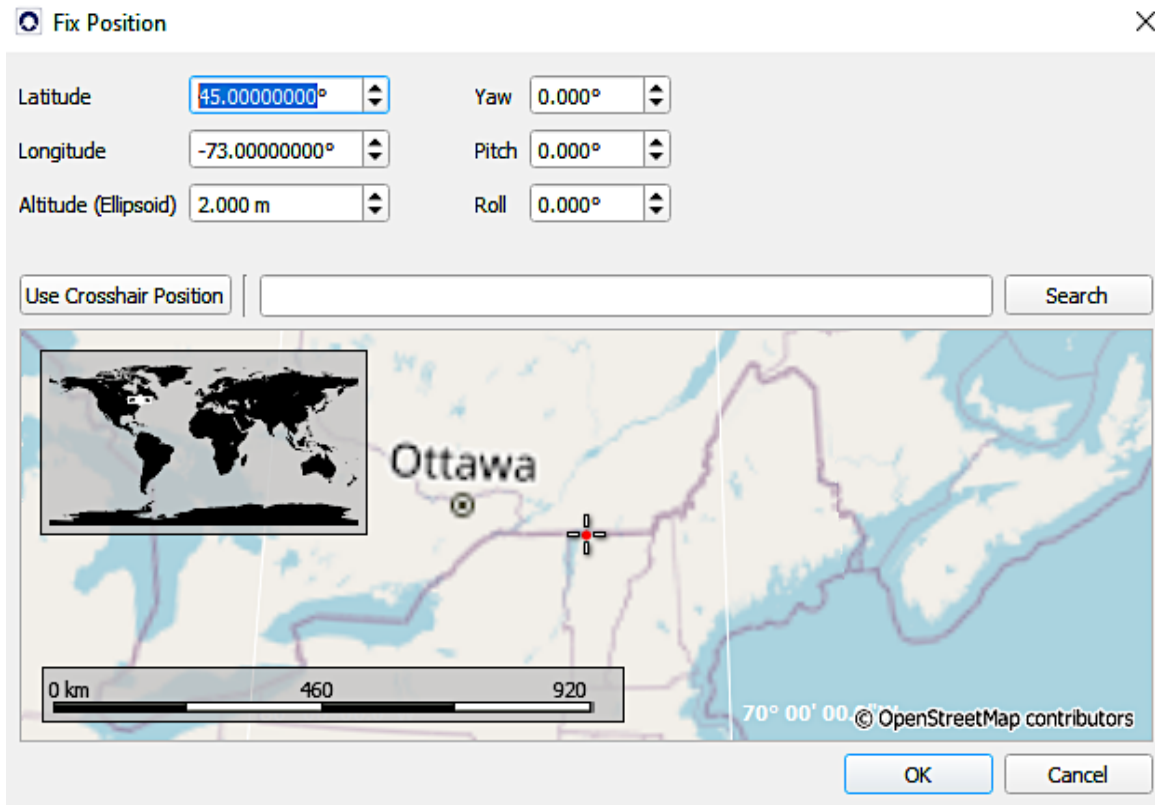


Figure 31: Inserting vehicle position in Skydel

4. Once the simulation is started, the following were observed (refer to Figure 17):
 - The number of tracked satellites in the Sky Plot
 - The transmitted signal power of each satellite
 - The Dilution of Precision (DOP) values

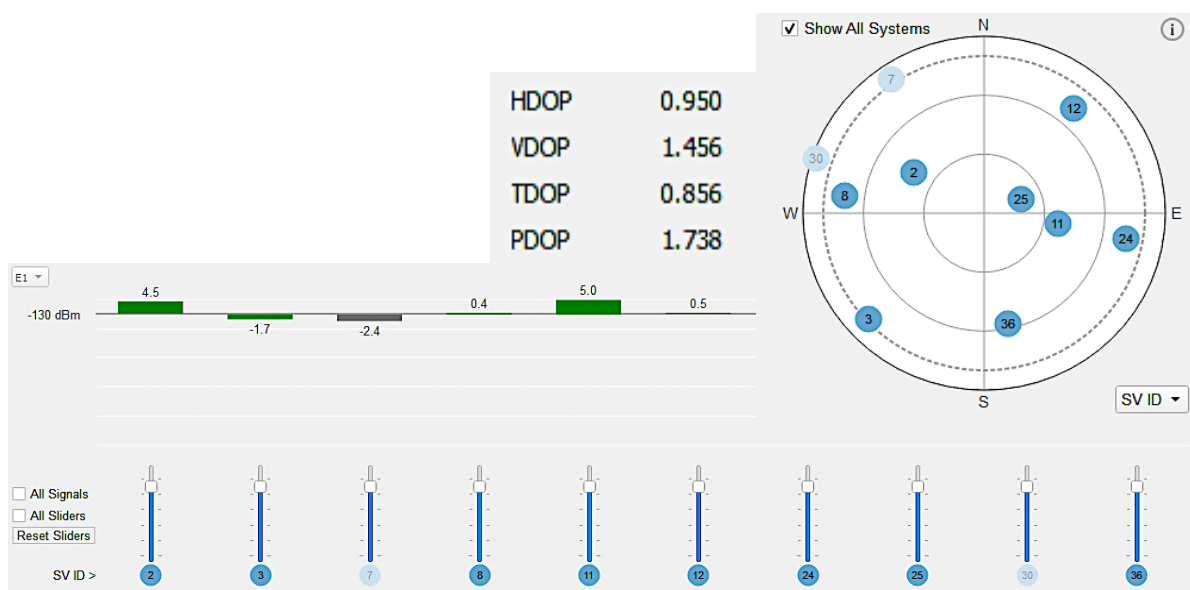


Figure 32: Sky plot, DOP values, and signal power in Skydel

5. The Map feature in settings was used to view the simulator position versus the receiver (refer to Figure 18).

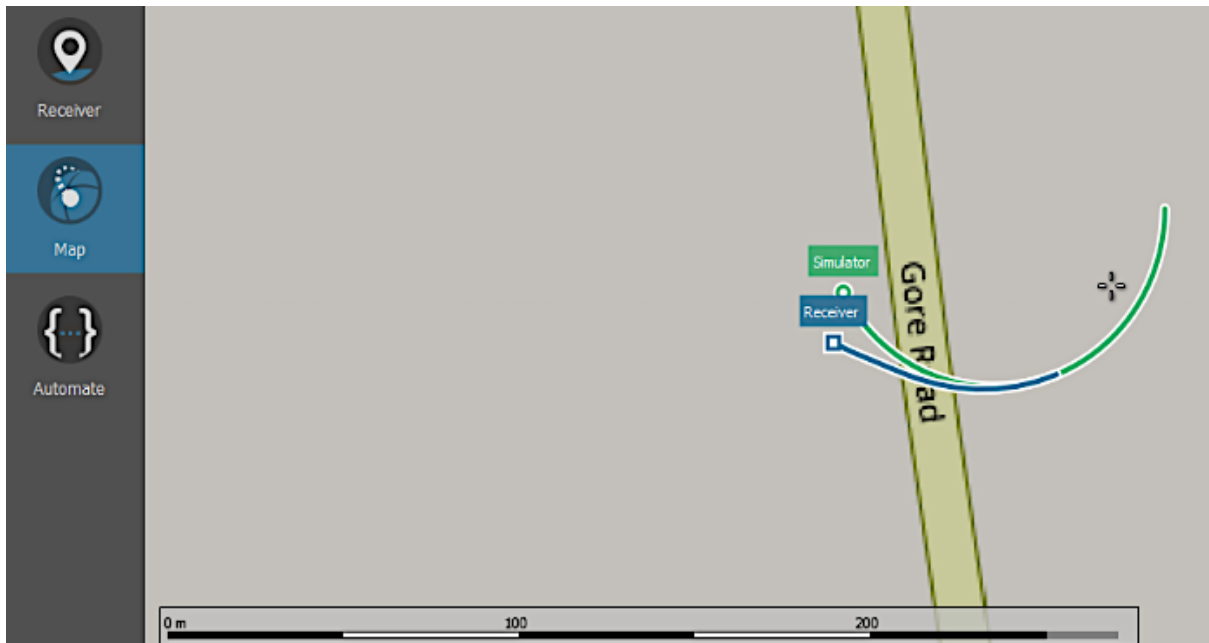


Figure 33: Map view in Skydel

6. The deviation tab was used to assess the deviation graph, illustrating the latitude, longitude, and altitude deviations (refer to Figure 19).

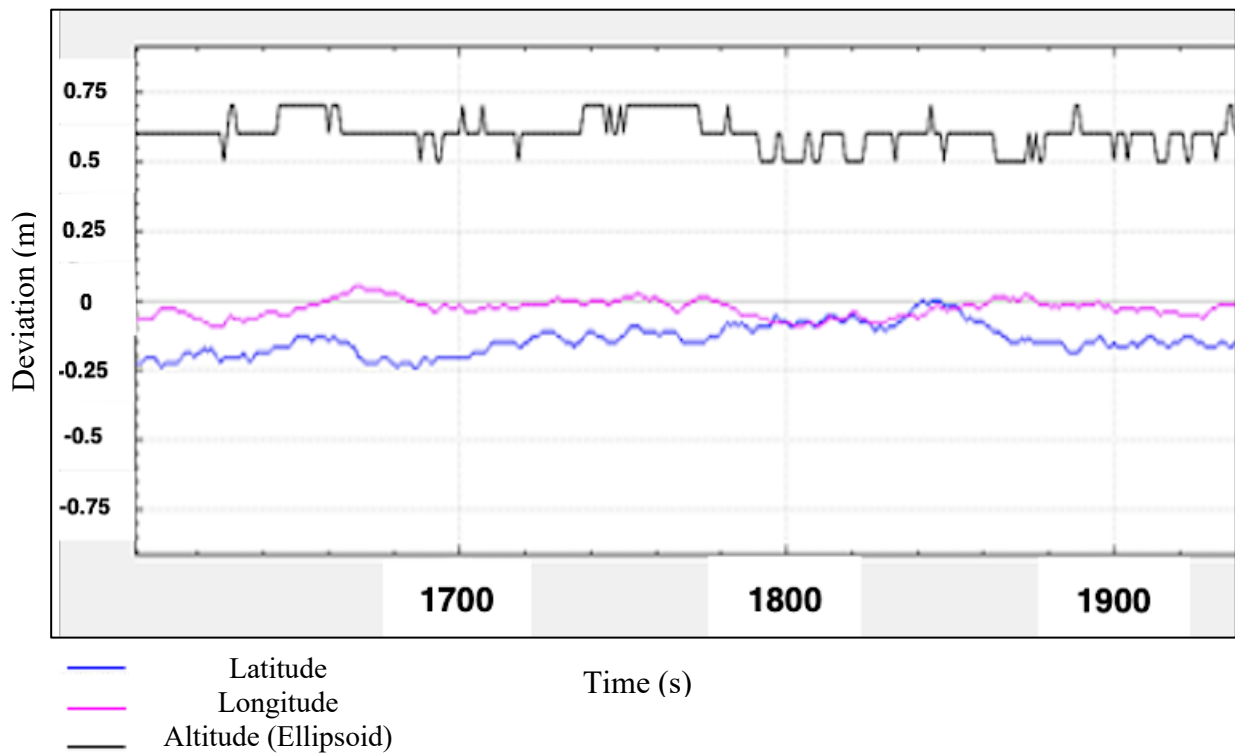


Figure 34: Deviation graph in Skydel

In addition to Skydel software, u-center software was used for logging more detailed parameters, such as the 3D positioning accuracy, while simulating in Skydel. After starting the simulation in Skydel, the following steps were followed.

1. The GNSS receiver was disconnected from Skydel and connected to u-center software.
2. The message view window was viewed using F9.
3. UBX, CFG (Config), and GNSS (GNSS Config), were selected, respectively, and the desired constellations were enabled (refer to Figure 20).

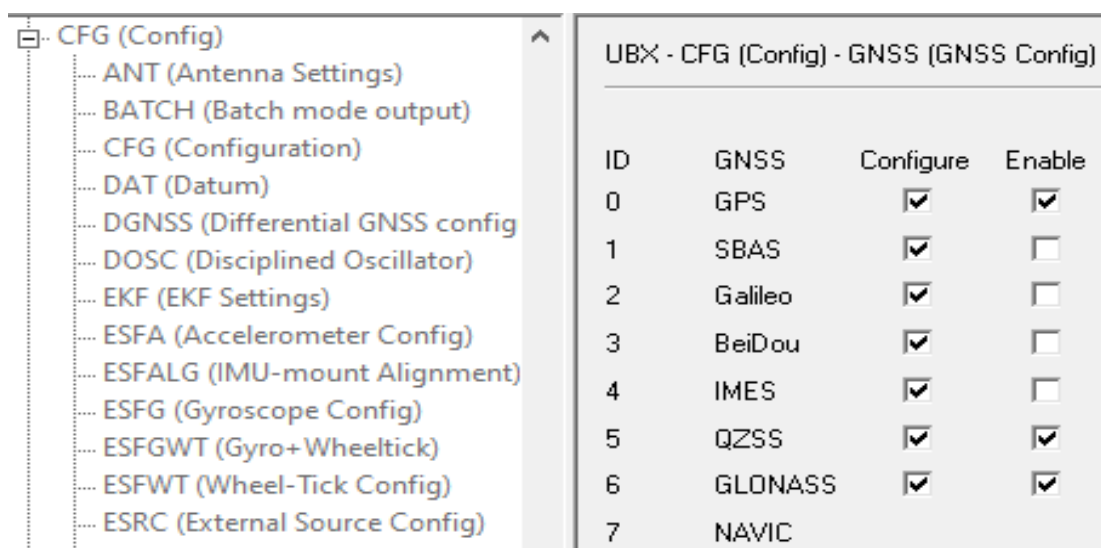


Figure 35: Enabling the desired constellations in u-center

4. NAV 5 (Navigation 5) and Airborne < 4g were selected as the Dynamic Model (refer to Figure 21).

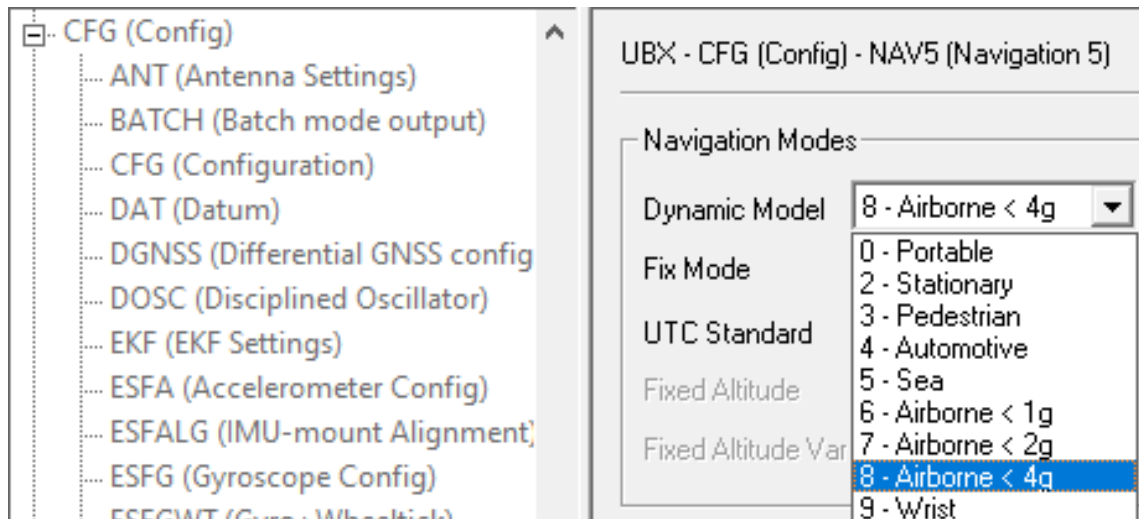


Figure 36: Selecting the dynamic model in u-center

5. Child Messages of NAV (Navigation) were Enabled.
6. Child Messages of the RXM (Receiver Manager) were Enabled.
7. The table View window was interfered with using F11.
8. The desired parameters to be logged, such as the carrier-to-noise ratio and the positioning accuracy, were added to the table view window (refer to Figure 22).

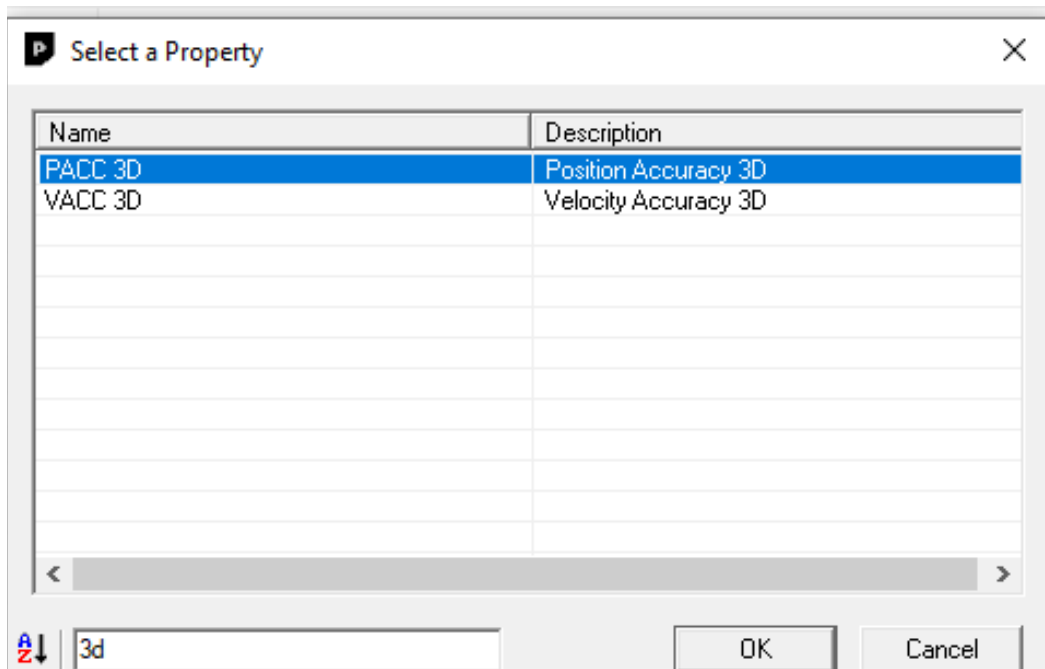


Figure 37: Logging the desired parameters in u-center software

Once the receiver locks with four satellites or more, it will give a 3D position fix. The receiver tracks only the satellites in green color. Figure 23 illustrates the tracked satellites as shown in u-center software. The x-axis represents the space vehicle ID in the constellation and the y-axis represents the carrier-to-noise ratio in dBHz unit.

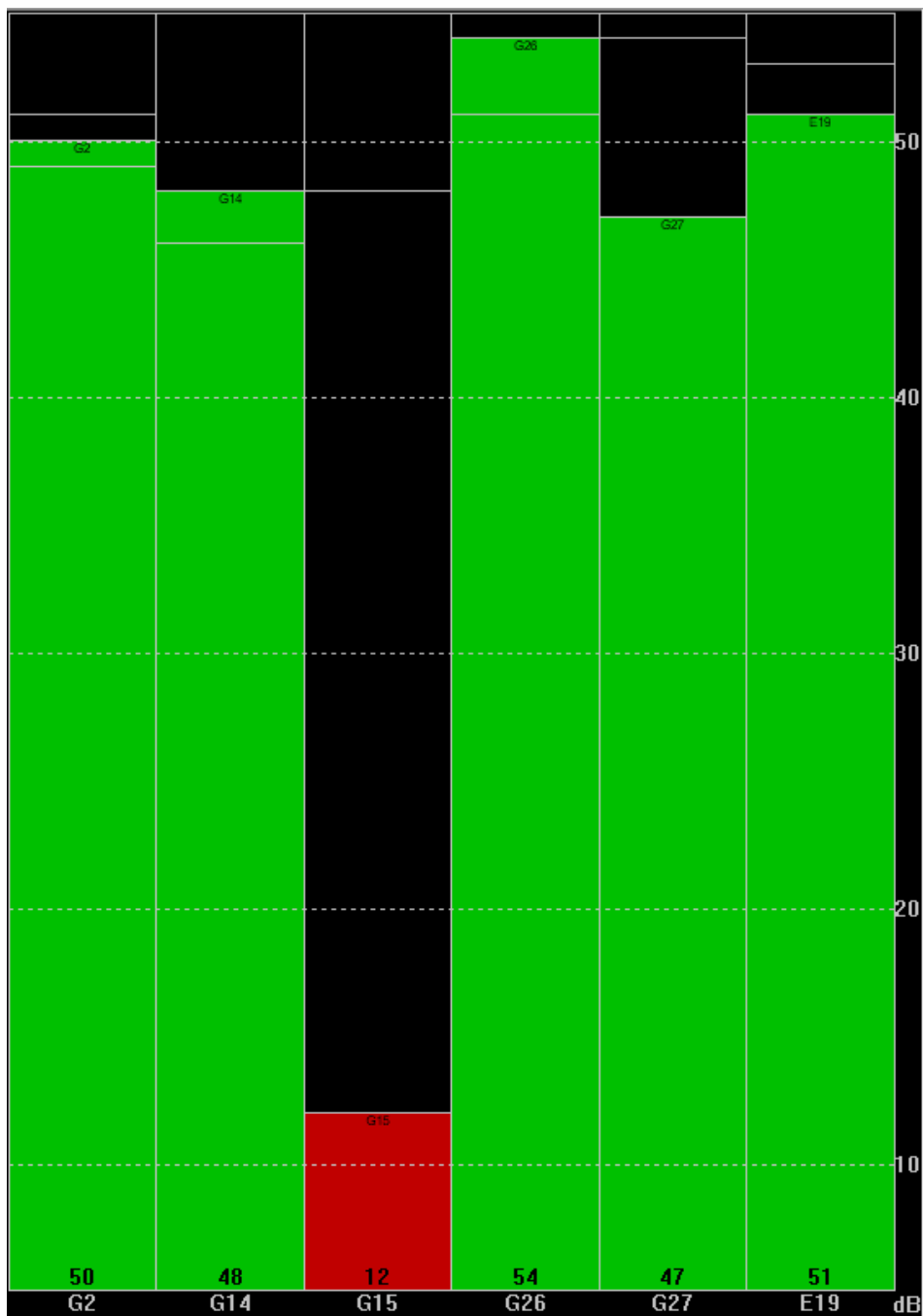


Figure 38: The tracked satellites by the receiver in u-center software

Chapter 3: Results of the Orbital Simulation

This chapter presents the results of the case studies conducted for different configurations of the mini-LEO constellation designs simulated using STK and Skydel. The figure of merit of each mini-LEO constellation design was assessed. Finally, the orbital parameters of the best configuration will be imported and tested using Skydel.

3.1 Results of the Case Studies of the Mini-LEO Constellation Design using STK

As explained in section 2.2, the walker tool in STK was used to design the mini GNSS constellation in LEO. Different configurations were created using 16 satellites distributed into 4 planes, with 4 satellites in each plane. Then, the configurations were assessed to determine whether they meet the desired requirement of having at least four satellites in the visibility of a receiver in the UAE for a minimum contact time of 8 to 10 minutes.

3.1.1 Scenario 1

A constellation of 16 satellites consisting of 4 planes, with 4 satellites in each plane. The planes are 90° apart, the satellites are 90° apart inter-plane, and the in-track spacing between the satellites in adjacent planes is 22.5°. Table 5 presents the degrees of the RAAN and the True Anomaly for this configuration. Figures 24 & 25 illustrate the 3D and 2D graphics, respectively, for this design in STK.

Table 5: RAAN & true anomaly of scenario 1

	Satellite Name	RAAN	True Anomaly
Plane 1	Sat 11	0°	0°
	Sat 12	0°	90°
	Sat 13	0°	180°
	Sat 14	0°	270°
Plane 2	Sat 21	90°	22.5°
	Sat 22	90°	112.5°
	Sat 23	90°	202.5°
	Sat 24	90°	292.5°
Plane 3	Sat 31	180°	45°
	Sat 32	180°	135°
	Sat 33	180°	225°
	Sat 34	180°	315°
Plane 4	Sat 41	270°	67.5°
	Sat 42	270°	157.5°
	Sat 43	270°	247.5°
	Sat 44	270°	337.5°

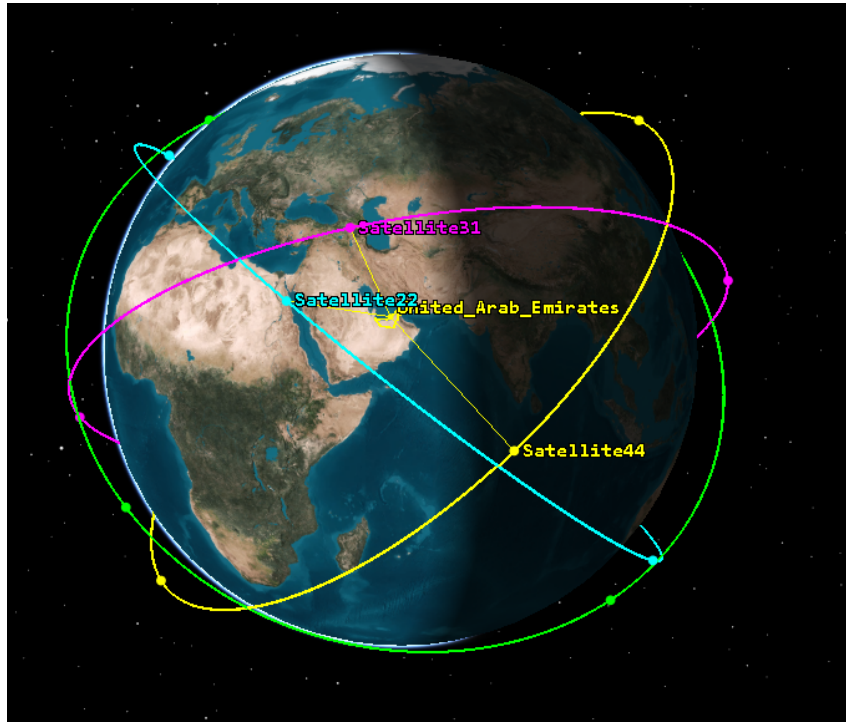


Figure 40: 3D graphic (scenario 1)

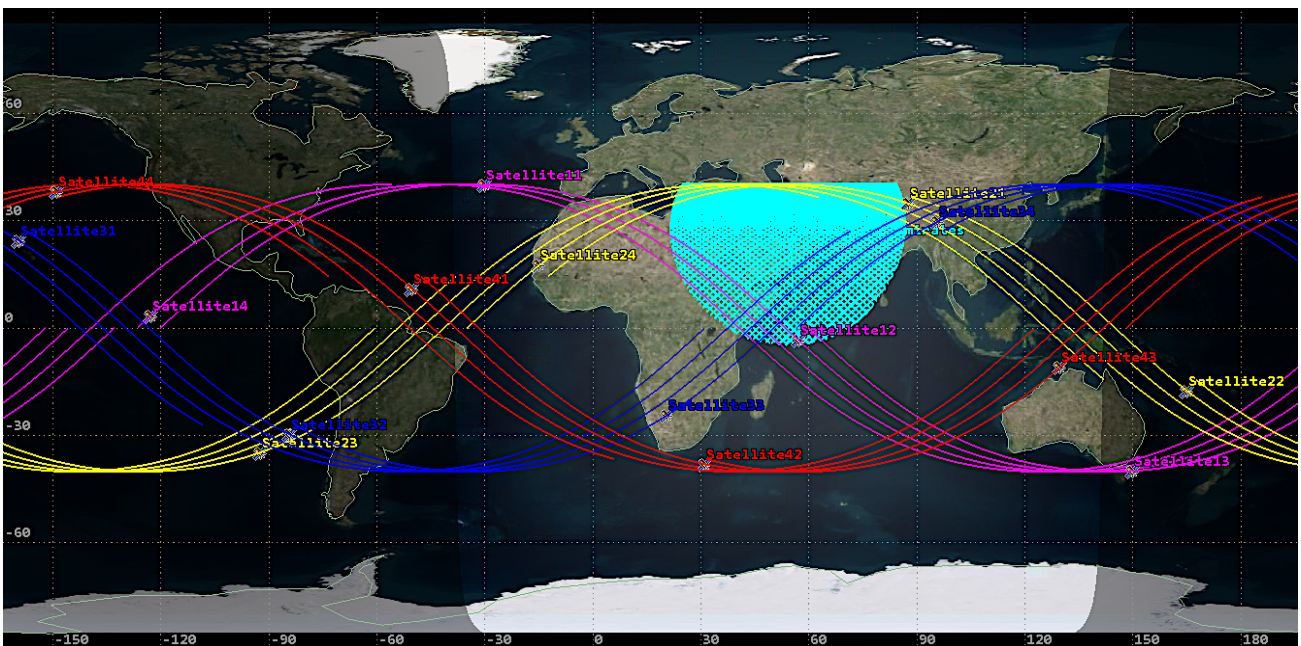


Figure 39: 2D graphic (scenario 1)

In this scenario, there were no more than three satellites visible to a receiver in the UAE simultaneously. As shown in Figure 24, the yellow lines that connect satellite 31, satellite 22, and satellite 44 to the area target (UAE), indicate a connection between the receiver and the satellites. The access times graph, as shown in Figure 26, was plotted to

analyse the access times over the receiver for all the 16 satellites of the constellation (refer to Chapter 2.2.2 for methodology). The access times graph for a period of 24 hours for this configuration as shown Figures 26 & 27 showed that this scenario is limited to the intersections of three satellites only, for an average time of 8 minutes, with the longest intersection time of 12 minutes. As the design requirement is to have a minimum visibility of four satellites from the receiver’s view, this configuration would not be assessed in Skydel.

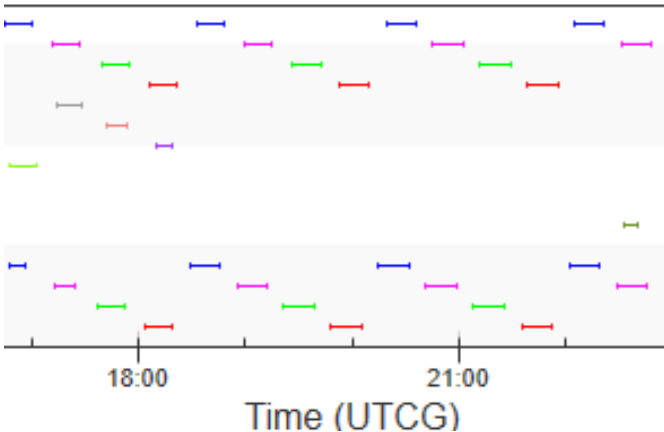


Figure 41: Access times (scenario 1)

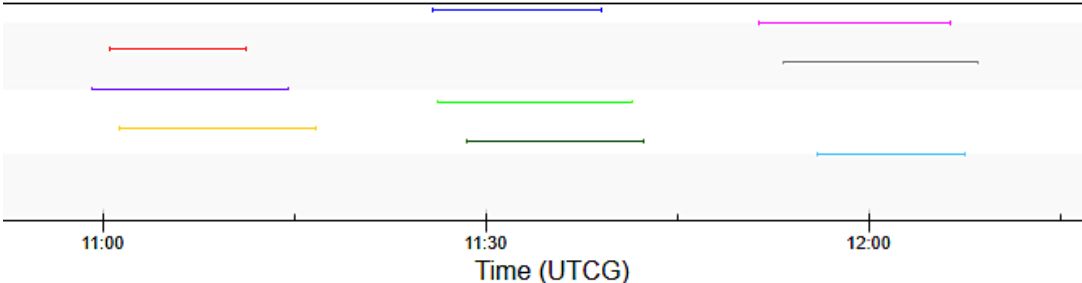


Figure 42: Access times (scenario 1) zoomed in

3.1.2 Scenario 2

A constellation of 16 satellites constating of 4 planes, with 4 satellites in each plane. The planes are 90° apart, the satellites are 45° apart inter-plane, and the in-track spacing between the satellites in adjacent planes is 22.5°. Table 6 specifies the degrees of the RAAN and the True Anomaly for this configuration. The 3D and 2D graphics for this design are illustrated in Appendix C-i.

Table 6: RAAN & true anomaly of scenario 2

	Satellite Name	RAAN	True Anomaly
Plane 1	Sat 11	0°	0°
	Sat 12	0°	45°
	Sat 13	0°	90°
	Sat 14	0°	135°
Plane 2	Sat 21	90°	22.5°
	Sat 22	90°	67.5°
	Sat 23	90°	112.5°
	Sat 24	90°	157.5°
Plane 3	Sat 31	180°	45°
	Sat 32	180°	90°
	Sat 33	180°	135°
	Sat 34	180°	180°
Plane 4	Sat 41	270°	67.5°
	Sat 42	270°	112.5°
	Sat 43	270°	157.5°
	Sat 44	270°	202.5°

As shown in Figure 28, 4 satellites were visible to the receiver, but only for an average period of 100 milliseconds in this scenario. The longest intersection time of the four satellites was 187 milliseconds. As a result, this configuration also does not meet the design requirement of the minimum contact time with the receiver.

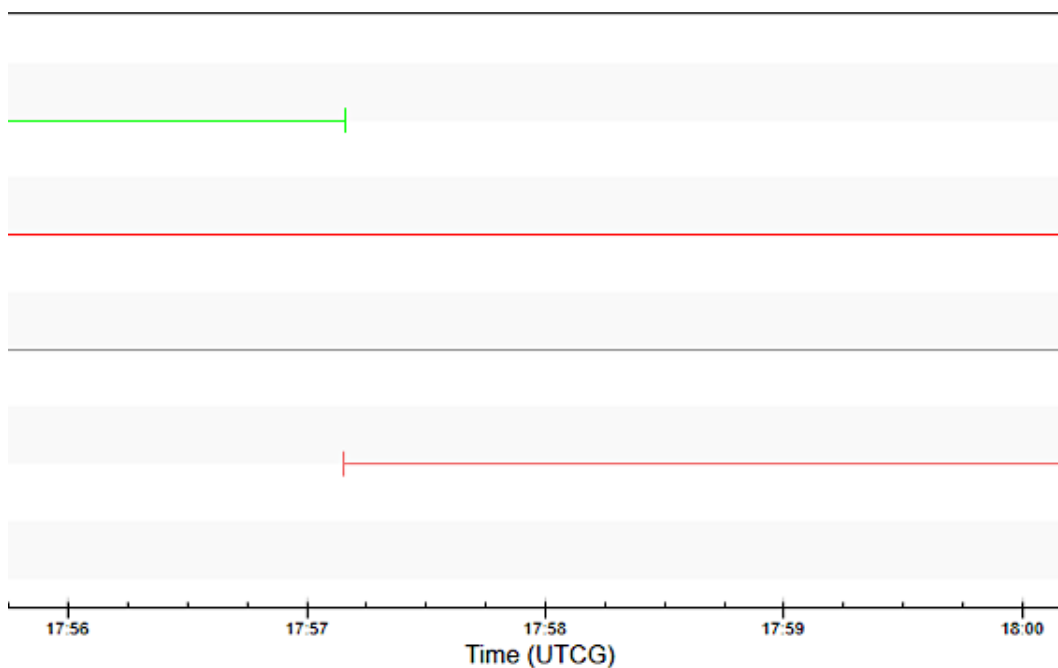


Figure 43: Access times (scenario 2)

3.1.3 Scenario 3

A constellation of 16 satellites consisting of 4 planes, with 4 satellites in each plane. The planes are 30° apart, the satellites are 90° apart inter-plane, and the in-track spacing between the satellites in adjacent planes is 22.5°. Table 7 specifies the degrees of the RAAN and the True Anomaly for this configuration. The 3D and 2D graphics for this design are illustrated in Appendix C-ii.

Table 7: RAAN & true anomaly of scenario 3

	Satellite Name	RAAN	True Anomaly
Plane 1	Sat 11	0°	0°
	Sat 12	0°	90°
	Sat 13	0°	180°
	Sat 14	0°	270°
Plane 2	Sat 21	30°	22.5°
	Sat 22	30°	122.5°
	Sat 23	30°	202.5°
	Sat 24	30°	292.5°
Plane 3	Sat 31	60°	45°
	Sat 32	60°	135°
	Sat 33	60°	225°
	Sat 34	60°	315°
Plane 4	Sat 41	90°	67.5°
	Sat 42	90°	157.5°
	Sat 43	90°	247.5°
	Sat 44	90°	337.5°

This scenario gives an access of 13 times per day over the UAE, with a visibility of 4 satellites over a receiver. The average access time with the receiver was about 1.5 minutes. As illustrated in Figure 29, the longest intersection time of 4 satellites was 2 minutes and 53 seconds. As a result, this configuration does not meet the requirement of the minimum contact time with the receiver and will not be considered.

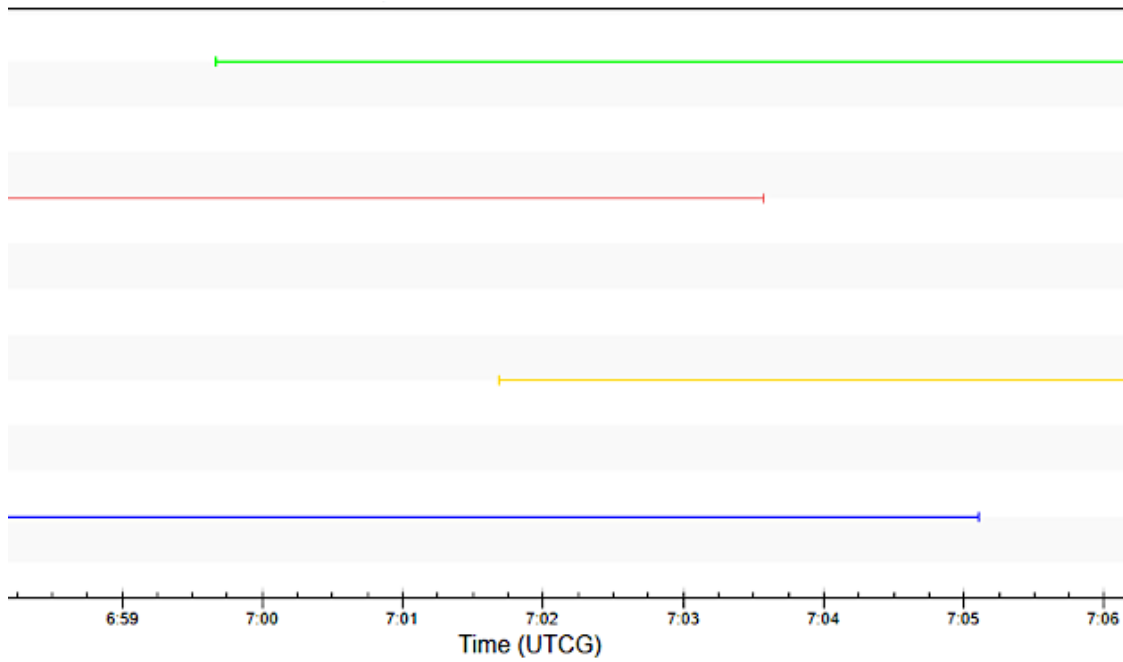


Figure 44: Access times (scenario 3)

3.1.4 Scenario 4

A constellation of 16 satellites consisting of 4 planes, with 4 satellites in each plane. The planes are 30° apart, the satellites are 45° apart inter-plane, and the in-track spacing between the satellites in adjacent planes is 22.5° . Table 8 specifies the degrees of the RAAN and the True Anomaly for this configuration. The 3D and 2D graphics for this design are illustrated in Appendix C-iii.

Table 8: RAAN & true anomaly of scenario 4

	Satellite Name	RAAN	True Anomaly
Plane 1	Sat 11	0°	0°
	Sat 12	0°	45°
	Sat 13	0°	90°
	Sat 14	0°	135°
Plane 2	Sat 21	30°	22.5°
	Sat 22	30°	67.5°
	Sat 23	30°	112.5°
	Sat 24	30°	157.5°
Plane 3	Sat 31	60°	45°
	Sat 32	60°	90°
	Sat 33	60°	135°
	Sat 34	60°	180°
Plane 4	Sat 41	90°	67.5°
	Sat 42	90°	112.5°
	Sat 43	90°	157.5°
	Sat 44	90°	202.5°

In this scenario, there were many intersections of 4 satellites for an average period of 2.5 minutes. Also, 15 times per day 5 satellites were visible over a receiver in the UAE simultaneously, with an average contact time of 1.5 minutes. As illustrated in Figure 30, there was also an intersection of 6 satellites over the receiver for a period of 114 milliseconds. Although this scenario met the minimum satellites' minimum visibility criteria, it did not meet the requirement of the minimum contact time with the receiver.

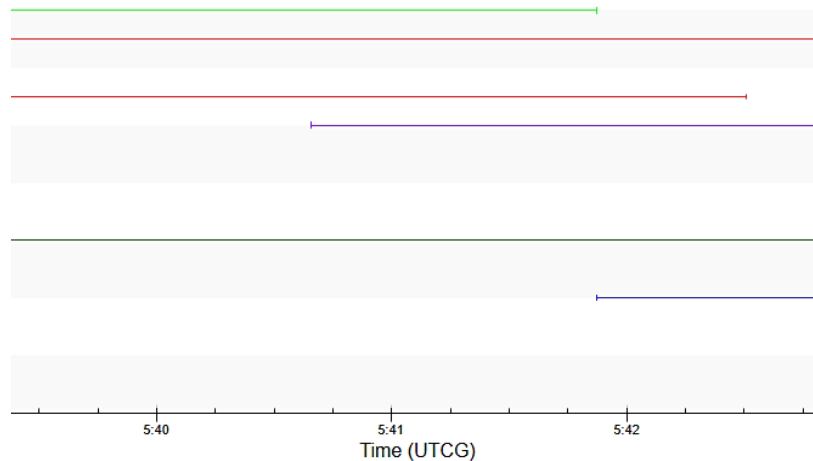


Figure 45: Access times (scenario 4)

3.1.5 Scenario 5

A constellation of 16 satellites consisting of 4 planes, with 4 satellites in each plane. The planes are 30° apart, the satellites are 30° apart inter-plane, and the in-track spacing between the satellites in adjacent planes is 0°; this means that the satellites will be next to each other in adjacent planes. Table 9 specifies the degrees of the RAAN and the True Anomaly for this configuration. The 3D and 2D graphics for this design are illustrated in Appendix C-iv.

Table 9: RAAN & true anomaly of scenario 5

	Satellite Name	RAAN	True Anomaly
Plane 1	Sat 11	0°	0°
	Sat 12	0°	30°
	Sat 13	0°	60°
	Sat 14	0°	90°
Plane 2	Sat 21	30°	0°
	Sat 22	30°	30°
	Sat 23	30°	60°
	Sat 24	30°	90°
Plane 3	Sat 31	60°	0°
	Sat 32	60°	30°
	Sat 33	60°	60°
	Sat 34	60°	90°
Plane 4	Sat 41	90°	0°
	Sat 42	90°	30°
	Sat 43	90°	60°
	Sat 44	90°	90°

Approximately 50 intersections of 4 satellites were spotted over a period of 24 hours in this scenario. This scenario showed an increase in the average contact time over a receiver to 7 minutes compared to the previous scenarios. Among the 50 intersections, 12-14 minutes of contact time was also observed (refer to Figure 31). There is a gap of 1 hour between every revisit of the satellites over the receiver and a long gap of 3.5 hours in which no satellite will be reaching the receiver. In conclusion, Scenario 5 did meet the requirement of having at least 8-10 minutes of contact time of 4 satellites over the receiver.

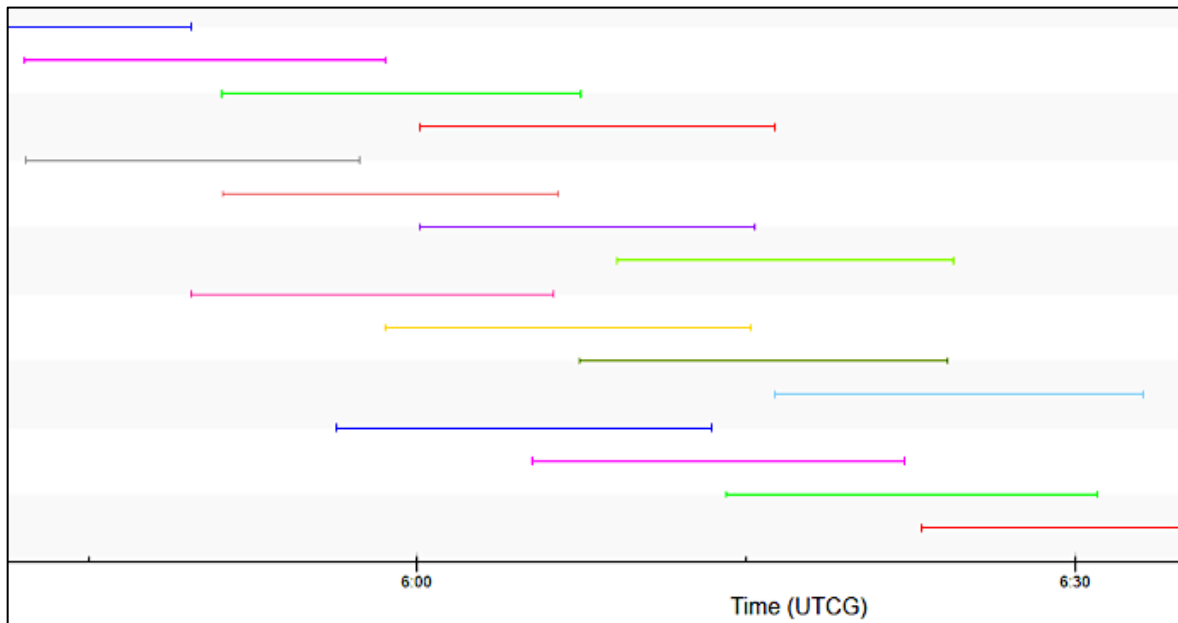


Figure 46: Access times (scenario 5)

The following scenarios have been tested with different configurations to obtain an optimum number of intersections of the satellites over the receiver for an adequate amount of time (8-10 minutes).

3.1.6 Scenario 6

A constellation of 16 satellites consisting of 4 planes, with 4 satellites in each plane. The planes are 30° apart, the satellites are 20° apart inter-plane, and the in-track spacing between the satellites in adjacent planes is 0° . Table 10 specifies the degrees of the RAAN and the True Anomaly for this configuration. The 3D and 2D graphics for this design are illustrated in Appendix C-v.

Table 10: RAAN & true anomaly of scenario 6

Scenario6	Satellite	RAAN	True Anomaly
Plane 1	Sat 11	0°	0°
	Sat 12	0°	20°
	Sat 13	0°	40°
	Sat 14	0°	60°
Plane 2	Sat 21	30°	0°
	Sat 22	30°	20°
	Sat 23	30°	40°
	Sat 24	30°	60°
Plane 3	Sat 31	60°	0°
	Sat 32	60°	20°
	Sat 33	60°	40°
	Sat 34	60°	60°
Plane 4	Sat 41	90°	0°
	Sat 42	90°	20°
	Sat 43	90°	40°
	Sat 44	90°	60°

The results in this scenario were approximately close to scenario 5, but with an increased average contact time with the receiver. Placing the satellites 10 degrees closer to each other in each plane has increased the average contact time of 4 satellites in view from 7 to 10 minutes. Figure 32 illustrates 10 minutes of contact time between 4 satellites with the receiver.

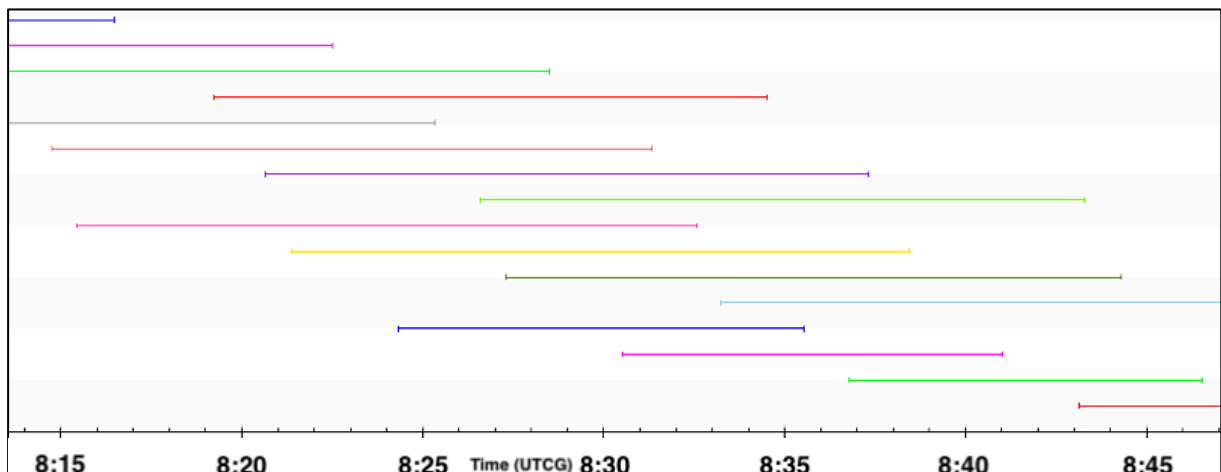


Figure 47: Access times (scenario 6)

3.1.7 Scenario 7

A constellation of 16 satellites consisting of 4 planes, with 4 satellites in each plane. The planes are 20° apart, the satellites are 20° apart inter-plane, and the in-track spacing between the satellites in adjacent planes is 0°. Table 11 specifies the degrees of the RAAN and the True Anomaly for this configuration. The 3D and 2D graphics for this design are illustrated in Appendix C-vi.

Table 11: RAAN & true anomaly of scenario 7

Scenario7	Satellite	RAAN	True Anomaly
Plane 1	Sat 11	0°	0°
	Sat 12	0°	20°
	Sat 13	0°	40°
	Sat 14	0°	60°
Plane 2	Sat 21	20°	0°
	Sat 22	20°	20°
	Sat 23	20°	40°
	Sat 24	20°	60°
Plane 3	Sat 31	40°	0°
	Sat 32	40°	20°
	Sat 33	40°	40°
	Sat 34	40°	60°
Plane 4	Sat 41	60°	0°
	Sat 42	60°	20°
	Sat 43	60°	40°
	Sat 44	60°	60°

In this scenario, there was an average contact time of 12 minutes with 4 satellites in view. Furthermore, there was an average contact time of 7 minutes with 5 satellites in view (refer to Figure 33).

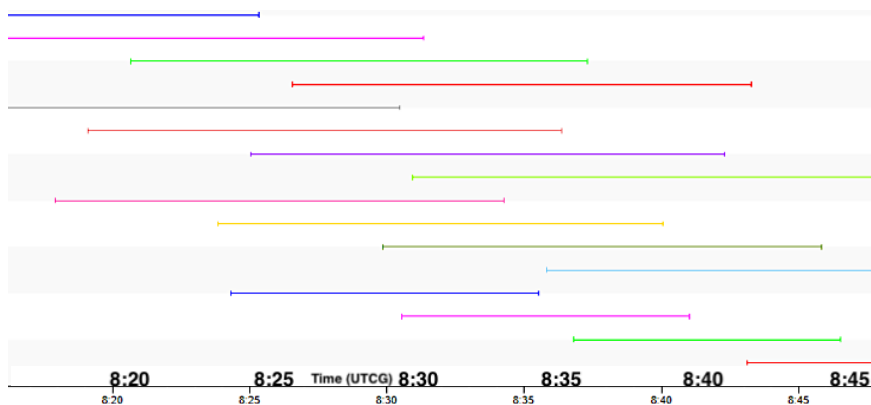


Figure 48: Access times (scenario 7)

3.1.8 Scenario 8

A constellation of 16 satellites consisting of 4 planes, with 4 satellites in each plane. The planes are 10° apart, the satellites are 20° apart inter-plane, and the in-track spacing between the satellites in adjacent planes is 0°. Table 12 specifies the degrees of the RAAN and the True Anomaly for this configuration. The 3D and 2D graphics for this design are illustrated in Appendix C-vii.

Table 12: RAAN & true anomaly of scenario 8

Scenario8	Satellite	RAAN	True Anomaly
Plane 1	Sat 11	60°	0°
	Sat 12	60°	20°
	Sat 13	60°	40°
	Sat 14	60°	60°
Plane 2	Sat 21	70°	0°
	Sat 22	70°	20°
	Sat 23	70°	40°
	Sat 24	70°	60°
Plane 3	Sat 31	80°	0°
	Sat 32	80°	20°
	Sat 33	80°	40°
	Sat 34	80°	60°
Plane 4	Sat 41	90°	0°
	Sat 42	90°	20°
	Sat 43	90°	40°
	Sat 44	90°	60°

This scenario showed an increase in the contact time of 5 visible satellites from 7 to 11 minutes compared to the previous scenario, with an access time of around 10 times a day (refer to Figure 34).

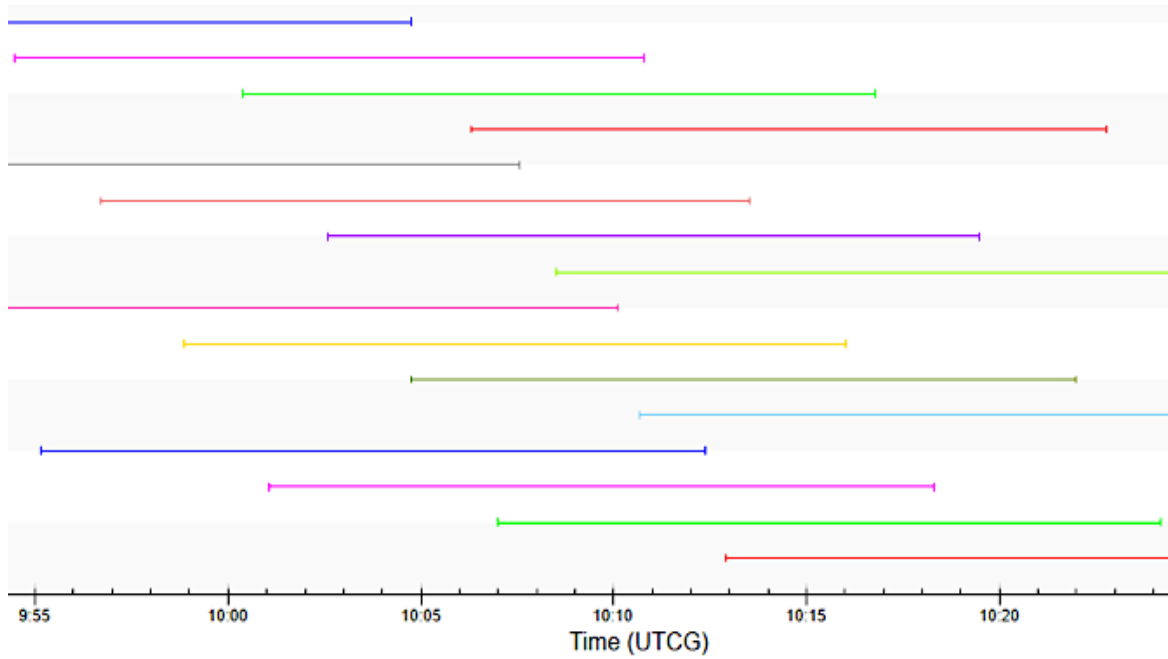


Figure 49: Access times (scenario 8)

3.1.9 Scenario 9

A constellation of 16 satellites consisting of 4 planes, with 4 satellites in each plane. The planes are 10° apart, the satellites are 10° apart inter-plane, and the in-track spacing between the satellites in adjacent planes is 0° . Table 13 specifies the degrees of the RAAN and the True Anomaly for this configuration. The 3D and 2D graphics for this design are illustrated in Appendix C-viii.

Table 13: RAAN & true anomaly of scenario 9

Scenario9	Satellite	RAAN	True Anomaly
Plane 1	Sat 11	60°	0°
	Sat 12	60°	10°
	Sat 13	60°	20°
	Sat 14	60°	30°
Plane 2	Sat 21	70°	0°
	Sat 22	70°	10°
	Sat 23	70°	20°
	Sat 24	70°	30°
Plane 3	Sat 31	80°	0°
	Sat 32	80°	10°
	Sat 33	80°	20°
	Sat 34	80°	30°
Plane 4	Sat 41	90°	0°
	Sat 42	90°	10°
	Sat 43	90°	20°
	Sat 44	90°	30°

In this scenario, all 16 satellites were visible over the receiver at the same time (refer to Figure 35). This scenario had the maximum satellite visibility for adequate contact time with the receiver. If a performance assessment comparison is carried out between a MEO and a LEO GNSS, the conditions should be as similar as possible. In the case of GPS, 8 satellites can be seen by the GPS receiver in the open sky environment at any time. The higher the visibility of the satellites over the receiver, the better the accuracy of the position. In scenario 9, there is a visibility of 6,7, and 8 satellites for a period of approximately 9 to 11 minutes.

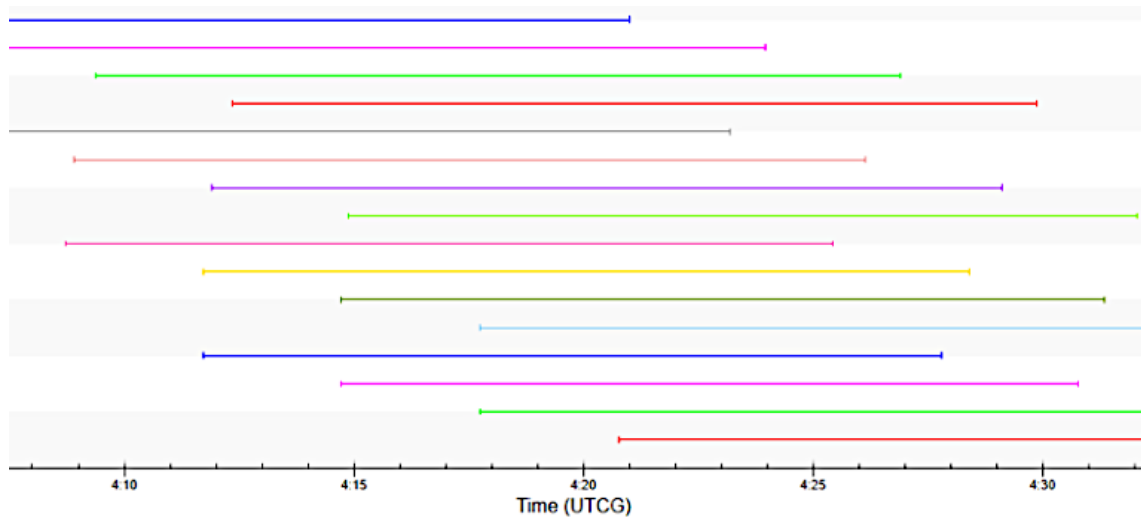


Figure 50: Access times (scenario 9)

Among the 9 scenarios simulated in STK, scenario 9 configuration design showed the best outcome regarding the highest visibility amount of the satellites for adequate contact time with the receiver. Therefore, the orbital parameters of this design were imported and tested in Skydel. Table 14 summarizes the configurations and outcomes of the 9 tested scenarios in STK.

Table 14: Summary of the 9 scenarios

Scenario	Configurations			Results		
	Planes	Satellites inter-plane	In-track spacing between the satellites in adjacent planes	Satellite visibility	Contact time (minutes)	Meeting the requirements
1	90° apart	90° apart	22.5°	3	8 minutes	X
2	90° apart	45° apart	22.5°	4	100 milliseconds	X
3	30° apart	90° apart	22.5°	4	1.5 minutes	X
4	30° apart	45° apart	22.5°	4	2.5 minutes	X
5	30° apart	30° apart	0°	4	7 minutes	✓
6	30° apart	20° apart	0°	4	10 minutes	✓
7	20° apart	20° apart	0°	4, 5	12 minutes, 10 minutes	✓
8	10° apart	20° apart	0°	5	7-11 minutes	✓
9	10° apart	10° apart	0°	6,7,8	9-11 minutes	✓

3.2 Importing the Orbital Parameters from STK to Skydel

The orbital parameters of Scenario 9 presented in Tables 15 & 16, were imported from STK to Skydel, and the results are shown in Figures 36 & 37.

Table 15: Orbital parameters of scenario 9 in Skydel

Start Time	2022-09-27 08:00:00
Reference Time	2022-09-27 08:00:00
Root Semimajor Axis	2677.87 m ^{1/2}
Eccentricity	0° = 0 semicircle
Argument of Perigee	0° = 0 semicircle
Inclination	40° = 0.2222 semicircle

Table 16: RAAN & true anomaly for each satellite in scenario 9

Output Signal Type	SV ID	Planes	RAAN	True Anomaly
Galileo E1	1	Plane 1	60° = 0.3333 semicircle	0° = 0 semicircle
	2		60° = 0.3333 semicircle	10° = 0.0556 semicircle
	3		60° = 0.3333 semicircle	20° = 0.1111 semicircle
	4		60° = 0.3333 semicircle	30° = 0.1667 semicircle
	5	Plane 2	70° = 0.3889 semicircle	0° = 0 semicircle
	7		70° = 0.3889 semicircle	10° = 0.0556 semicircle
	8		70° = 0.3889 semicircle	20° = 0.1111 semicircle
	9		70° = 0.3889 semicircle	30° = 0.1667 semicircle
	11	Plane 3	80° = 0.4444 semicircle	0° = 0 semicircle
	12		80° = 0.4444 semicircle	10° = 0.0556 semicircle
	13		80° = 0.4444 semicircle	20° = 0.1111 semicircle
	15		80° = 0.4444 semicircle	30° = 0.1667 semicircle
	19	Plane 4	90° = 0.5 semicircle	0° = 0 semicircle
	21		90° = 0.5 semicircle	10° = 0.0556 semicircle
	24		90° = 0.5 semicircle	20° = 0.1111 semicircle
	25		90° = 0.5 semicircle	30° = 0.1667 semicircle

At around 08:25 am, most of the satellites were crowded in the Northeast side of the Sky View diagram as presented in Figure 36. This was expected because the planes in this scenario are 10° apart only and the satellites are close to each other in each plane. It was also observed that the satellites are condensed at lower elevation angles, a feature of the spatial density in LEO (Al-Ruwais, 2008). In addition, the Position Dilution of Precision value (PDOP) calculated by Skydel was 4.12 and thus considered acceptable to give a 3D position fix (Mapasyst, 2019).

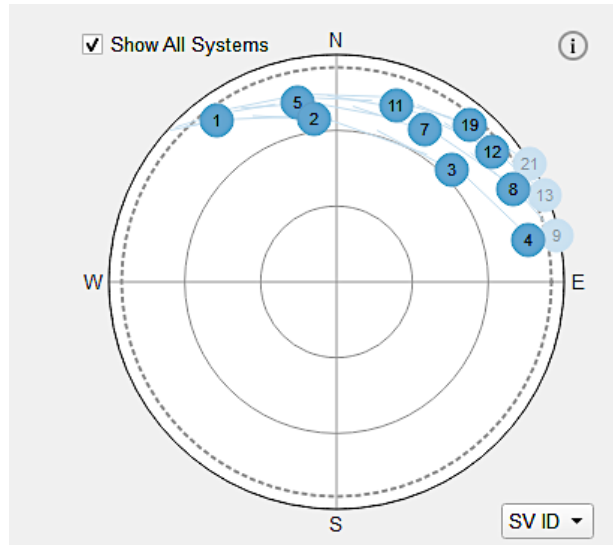


Figure 51: Scenario 9 at 08:25 am in Skydel

As seen in Figure 37, the satellites at 10:15 am are still condensed at lower elevation angles, but they became more uniformly distributed around the receiver than at 08:25 am. As a result, decreasing the spatial density of the satellites has improved the PDOP value calculated by Skydel from 1.524 to 4.12.

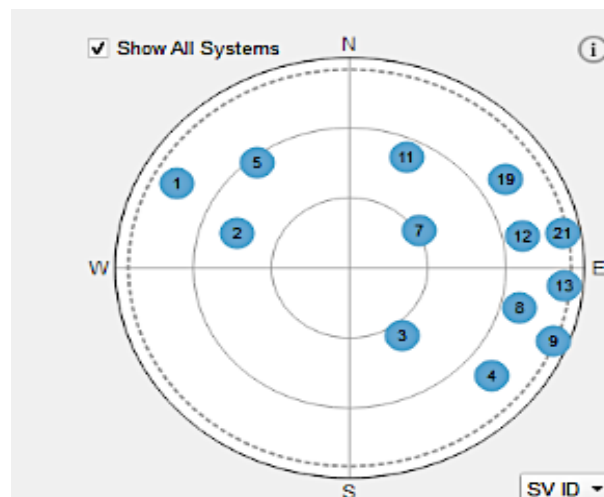


Figure 52: Scenario 9 at 10:15 in Skydel

The next section presents the outcomes of the positioning accuracy assessment for this LEO configuration design and some other LEO designs as well.

3.3 Assessing the Performance of a LEO-based GNSS using Skydel

All the scenarios (a-d) have the following properties:

- I. Vehicle body (simulator): Fixed on a bridge in Abu Dhabi as shown in Figure 38.
 - Latitude: 24.24872242°
 - Longitude: 54.46941196°
 - Altitude: 2 m
- II. Elevation Mask: 5°



Figure 53: Simulator position in Skydel

- a. Scenario 9: a constellation of 16 satellites transmitting Galileo E1 signal (refer to Tables 15 & 16 for orbital parameters).

The first observation from the start of the simulation is that, even though the PDOP values provided in Skydel were considered suitable to give a 3D position fix, it took time for the receiver to lock, more than 7 minutes, and sometimes it doesn't lock at all, for the same configuration and conditions. Secondly, once the GNSS receiver locks, it maintains the lock for a short period only, maximum 3 minutes, and then it loses connection (refer to Figure 39). Thirdly, the simulation has been running for 18 hours, yet the receiver did not lock during any revisit time of the satellites. Finally, the best 3D

positioning accuracy for this configuration, computed from u-centre software, was 45.81 m, despite the good PDOP values provided by Skydel for this scenario.

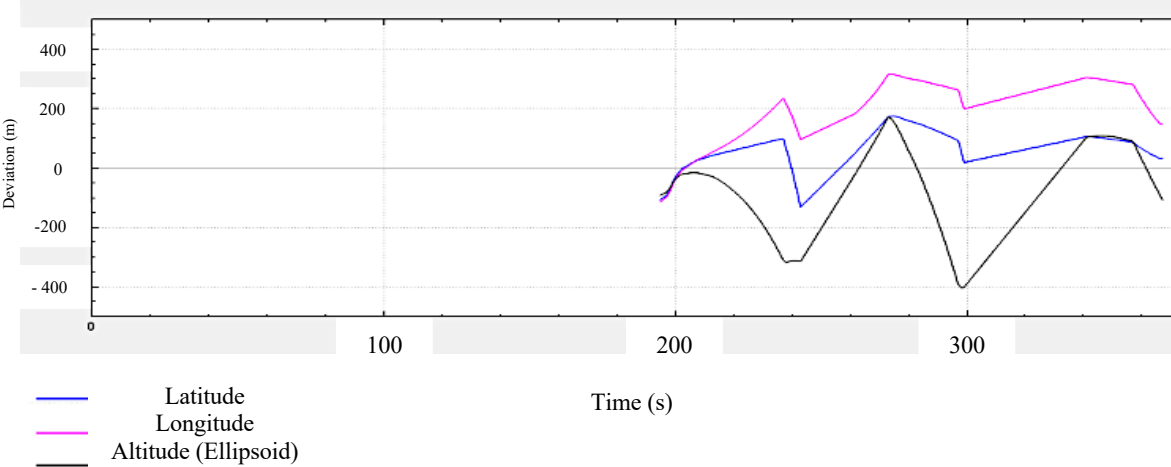


Figure 54: The deviation graph of scenario 9 in Skydel

To verify whether the PDOP values provided by Skydel is computed for the tracked satellites only or for all the satellites in the Sky View, u-center software has been used. After enabling the logging of the PDOP values in u-center, the simulation was repeated. The results of the PDOP values in u-center showed different results than Skydel, with a minimum PDOP value of 9.5 and a maximum PDOP value of 16.7 for this scenario. After that, the untracked satellites by the receiver were removed from the simulation before repeating it; only then were the same PDOP values provided by both Skydel and u-center. As a result, only the PDOP values provided by u-center would be considered in this research. Table 17 summarizes the outcomes of testing Scenario9 both in Skydel and U-centre.

Table 17: Figures of merit of scenario 9

PDOP Values	9.5 – 16.7
Time to Lock	7 minutes
Locking Period	3 minutes
Continuity	No
Positioning Accuracy (PACC 3D)	45.81

- b. Scenario 10: a bigger constellation has been built using all the 22 Galileo SV IDs. The planes have been spaced 10° more than Scenario 9, to make the satellites more uniformly distributed around the receiver. 22 satellites transmitting Galileo E1 signal consisting of 4 planes, with 5 satellites assigned to the first and fourth planes, and 6 satellites assigned to the second and third planes. The planes are 20° apart, the satellites are 10° apart inter-plane, and the in-track spacing between the satellites in adjacent planes is 0° (refer to Tables 18 & 19 for orbital parameters).

Table 18: Orbital parameters of scenario 10 in Skydel

Start Time	2022-09-27 08:00:00
Reference Time	2022-09-27 08:00:00
Root Semimajor Axis	2677.87 m $\frac{1}{2}$
Eccentricity	$0^\circ = 0$ semicircle
Argument of Perigee	$0^\circ = 0$ semicircle
Inclination	$40^\circ = 0.2222$ semicircle

Table 19: RAAN & true anomaly for each satellite in scenario 10

Signal Output Type	SV ID	Plane	RAAN	True Anomaly
Galileo E1	1	Plane 1	$50^\circ = 0.2778$ semicircle	$0^\circ = 0$ semicircle
	2		$50^\circ = 0.2778$ semicircle	$10^\circ = 0.0556$ semicircle
	3		$50^\circ = 0.2778$ semicircle	$20^\circ = 0.1111$ semicircle
	4		$50^\circ = 0.2778$ semicircle	$30^\circ = 0.1667$ semicircle
	5		$50^\circ = 0.2778$ semicircle	$40^\circ = 0.2222$ semicircle
	7	Plane 2	$70^\circ = 0.3889$ semicircle	$0^\circ = 0$ semicircle
	8		$70^\circ = 0.3889$ semicircle	$10^\circ = 0.0556$ semicircle
	9		$70^\circ = 0.3889$ semicircle	$20^\circ = 0.1111$ semicircle
	11		$70^\circ = 0.3889$ semicircle	$30^\circ = 0.1667$ semicircle
	12		$70^\circ = 0.3889$ semicircle	$40^\circ = 0.2222$ semicircle
	13		$70^\circ = 0.3889$ semicircle	$50^\circ = 0.2778$ semicircle
	15	Plane 3	$90^\circ = 0.5$ semicircle	$0^\circ = 0$ semicircle
	19		$90^\circ = 0.5$ semicircle	$10^\circ = 0.0556$ semicircle
	21		$90^\circ = 0.5$ semicircle	$20^\circ = 0.1111$ semicircle
	24		$90^\circ = 0.5$ semicircle	$30^\circ = 0.1667$ semicircle
	25		$90^\circ = 0.5$ semicircle	$40^\circ = 0.2222$ semicircle
	26		$90^\circ = 0.5$ semicircle	$50^\circ = 0.2778$ semicircle
	27	Plane 4	$110^\circ = 0.6111$ semicircle	$0^\circ = 0$ semicircle
	30		$110^\circ = 0.6111$ semicircle	$10^\circ = 0.0556$ semicircle
	31		$110^\circ = 0.6111$ semicircle	$20^\circ = 0.1111$ semicircle
	33		$110^\circ = 0.6111$ semicircle	$30^\circ = 0.1667$ semicircle
	36		$110^\circ = 0.6111$ semicircle	$40^\circ = 0.2222$ semicircle

Designing the planes to be 20° apart rather than 10° apart has reduced the satellite’s spatial density (refer to Figure 40).

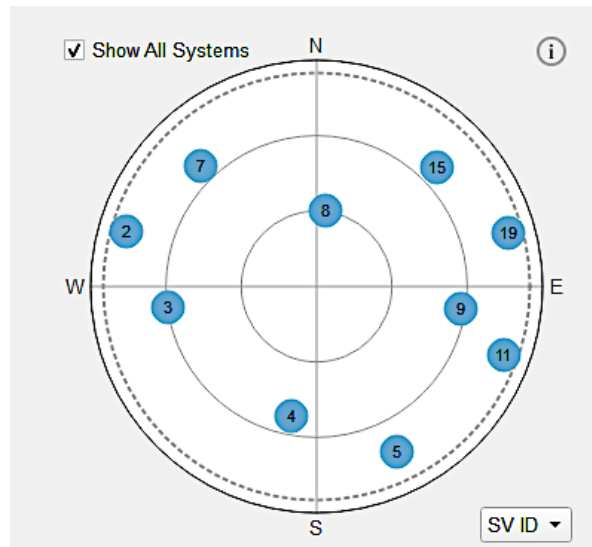


Figure 55: Satellite spatial density in scenario 10

There was no improvement compared to the previous scenario regarding the time the receiver took to lock. The time ranged between 6 to 10 minutes, different on each try, and sometimes the receiver did not lock at all. Furthermore, the locking time of the receiver in this scenario was also insufficient, ranging between 2 to 4 minutes. In addition, the receiver did not lock during the revisit time of the satellites. However, the PDOP values have been improved in this scenario, with a minimum PDOP value of 4.1 and a maximum PDOP value of 15. Also, the best 3D positioning accuracy obtained for this scenario was 18.19 m, better than the one in Scenario 9 but still not as expected. Table 20 summarizes the outcomes of testing Scenario 10 in Skydel and U-centre.

Table 20: Figures of merit of scenario 10

PDOP Values	4.1 – 15
Time to Lock	6-10 minutes
Locking Period	2-4 minutes
Continuity	No
Positioning Accuracy (PACC 3D)	18.19 m

- c. Scenario 11: In an attempt to verify if the short locking period of the receiver is due to the insufficient number of satellites, 37 BeiDou satellites were added to the constellation of Scenario 10 to satisfy the constellation with roughly 60 satellites. However, an error occurred in the software when modifying the orbital parameters of BeiDou SV IDs, and the issue is described in Appendix B.
- d. Scenario 12: A constellation of 54 satellites using 22 Galileo satellites transmitting Galileo E1 signal (1575.42 MHz), and 32 GPS satellites transmitting GPS L1C/A signal (1575.42 MHz). The constellation has been distributed into 4 planes; the first and last planes had 13 satellites per plane, and the third and fourth planes had 14 satellites per plane. The orbital spacing of Scenario 10 was used in this scenario (refer to Tables 21 & 22 for orbital parameters).

Table 21: Orbital parameters of scenario 12 in Skydel

Start Time	2022-10-17 08:00:00
Reference Time	2022-10-17 08:00:00
Root Semimajor Axis	2677.87 m ^{1/2}
Eccentricity	0° = 0 semicircle
Argument of Perigee	0° = 0 semicircle
Inclination	40° = 0.2222 semicircle

Table 22: RAAN & true anomaly for each satellite in scenario 12

Output Signal Type	SV ID	Plane	Satellite number per plane	RAAN	True Anomaly
Galileo E1	1	Plane 1	1	50° = 0.2778 semicircle	0° = 0 semicircle
	2		2	50° = 0.2778 semicircle	10° = 0.0556 semicircle
	3		3	50° = 0.2778 semicircle	20° = 0.1111 semicircle
	4		4	50° = 0.2778 semicircle	30° = 0.1667 semicircle
	5		5	50° = 0.2778 semicircle	40° = 0.2222 semicircle
	7		6	50° = 0.2778 semicircle	50° = 0.2778 semicircle
	8		7	50° = 0.2778 semicircle	60° = 0.3333 semicircle
	9		8	50° = 0.2778 semicircle	70° = 0.3889 semicircle
	11		9	50° = 0.2778 semicircle	80° = 0.4444 semicircle
	12		10	50° = 0.2778 semicircle	90° = 0.5 semicircle
	13	11	50° = 0.2778 semicircle	100° = 0.5556 semicircle	
	15	12	50° = 0.2778 semicircle	110° = 0.6111 semicircle	
	19	13	50° = 0.2778 semicircle	120° = 0.6667 semicircle	
	21	Plane 2	1	70° = 0.3889 semicircle	0° = 0 semicircle
	24		2	70° = 0.3889 semicircle	10° = 0.0556 semicircle
	25		3	70° = 0.3889 semicircle	20° = 0.1111 semicircle
	26		4	70° = 0.3889 semicircle	30° = 0.1667 semicircle
	27		5	70° = 0.3889 semicircle	40° = 0.2222 semicircle
30	6		70° = 0.3889 semicircle	50° = 0.2778 semicircle	
31	7		70° = 0.3889 semicircle	60° = 0.3333 semicircle	
33	8		70° = 0.3889 semicircle	70° = 0.3889 semicircle	
36	9	70° = 0.3889 semicircle	80° = 0.4444 semicircle		
GPS L1CA	1	Plane 3	10	70° = 0.3889 semicircle	90° = 0.5 semicircle
	2		11	70° = 0.3889 semicircle	100° = 0.5556 semicircle
	3		12	70° = 0.3889 semicircle	110° = 0.6111 semicircle
	4		13	70° = 0.3889 semicircle	120° = 0.6667 semicircle
	5		14	70° = 0.3889 semicircle	130° = 0.7222 semicircle
	6		1	90° = 0.5 semicircle	0° = 0 semicircle
	7		2	90° = 0.5 semicircle	10° = 0.0556 semicircle
	8		3	90° = 0.5 semicircle	20° = 0.1111 semicircle
	9		4	90° = 0.5 semicircle	30° = 0.1667 semicircle
	10		5	90° = 0.5 semicircle	40° = 0.2222 semicircle
	11	6	90° = 0.5 semicircle	50° = 0.2778 semicircle	
	12	7	90° = 0.5 semicircle	60° = 0.3333 semicircle	
	13	8	90° = 0.5 semicircle	70° = 0.3889 semicircle	
	14	9	90° = 0.5 semicircle	80° = 0.4444 semicircle	
	15	10	90° = 0.5 semicircle	90° = 0.5 semicircle	

Table 23: RAAN & true anomaly for each satellite in scenario 12 (continued)

Output Signal Type	SV ID	Plane	Satellite number per plane	RAAN	True Anomaly
GPS L1CA	16	Plane 3	11	90° = 0.5 semicircle	100° = 0.5556 semicircle
	17		12	90° = 0.5 semicircle	110° = 0.6111 semicircle
	18		13	90° = 0.5 semicircle	120° = 0.6667 semicircle
	19		14	90° = 0.5 semicircle	130° = 0.7222 semicircle
	20	Plane 4	1	110° = 0.6111 semicircle	0° = 0 semicircle
	21		2	110° = 0.6111 semicircle	10° = 0.0556 semicircle
	22		3	110° = 0.6111 semicircle	20° = 0.1111 semicircle
	23		4	110° = 0.6111 semicircle	30° = 0.1667 semicircle
	24		5	110° = 0.6111 semicircle	40° = 0.2222 semicircle
	25		6	110° = 0.6111 semicircle	50° = 0.2778 semicircle
	26		7	110° = 0.6111 semicircle	60° = 0.3333 semicircle
	27		8	110° = 0.6111 semicircle	70° = 0.3889 semicircle
	28		9	110° = 0.6111 semicircle	80° = 0.4444 semicircle
	29		10	110° = 0.6111 semicircle	90° = 0.5 semicircle
	30		11	110° = 0.6111 semicircle	100° = 0.5556 semicircle
	31		12	110° = 0.6111 semicircle	110° = 0.6111 semicircle
	32		13	110° = 0.6111 semicircle	120° = 0.6667 semicircle

In this scenario, it was observed that the receiver could give a 3D position fix after 30 seconds to 3 minutes only (refer to Figure 41). This is the shortest locking period of the receiver among all the tested scenarios.

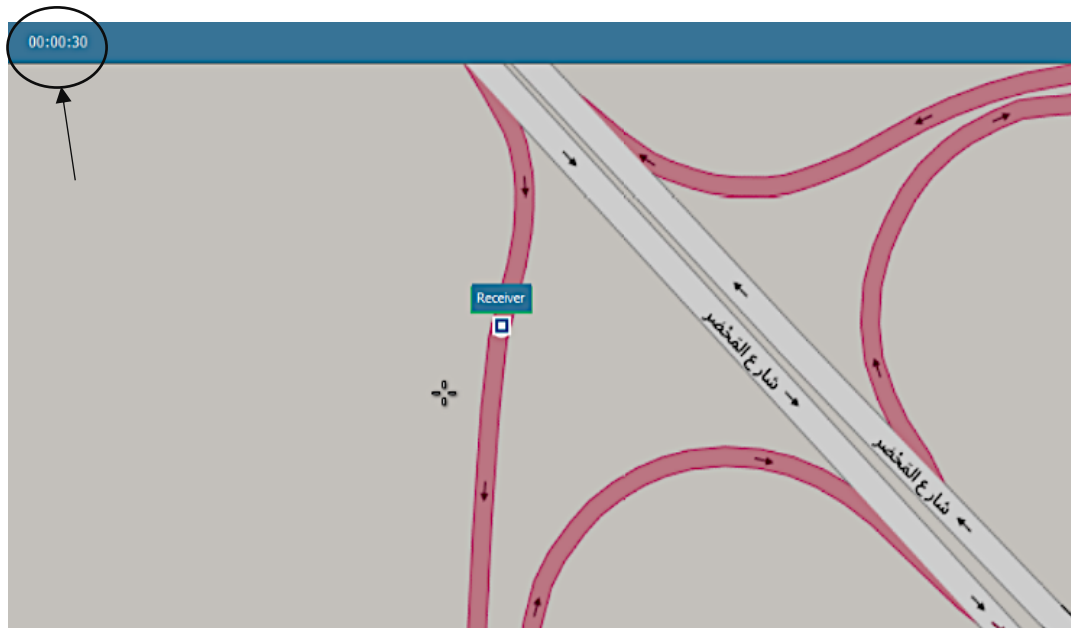


Figure 56: Receiver's locking period for scenario 12

The second observation was that the receiver has locked with at least 4 satellites for 7 to 12 minutes, which is a longer period than both Scenario 9 and Scenario 10 (refer to Figure 42). The connection with the receiver was intermittent, as there was connection loss a few times, for roughly 30 seconds, during the locking period. In addition to that, the receiver locked during the revisit time of the satellites, however, this was not consistent. Thirdly, it was observed that the receiver could always lock with more than 4 satellites, mostly 6 to 8.

Although the receiver could lock with more than 4 satellites and for an adequate contact time with the receiver (longer period as compared to Scenario 10), the 3D positioning accuracy did not improve. The best 3D positioning accuracy for this scenario was 20.29 m with a minimum PDOP value of 6.6 and a maximum PDOP value of 10.6. Table 23 summarizes the outcomes of testing Scenario12 both in Skydel and U-centre.

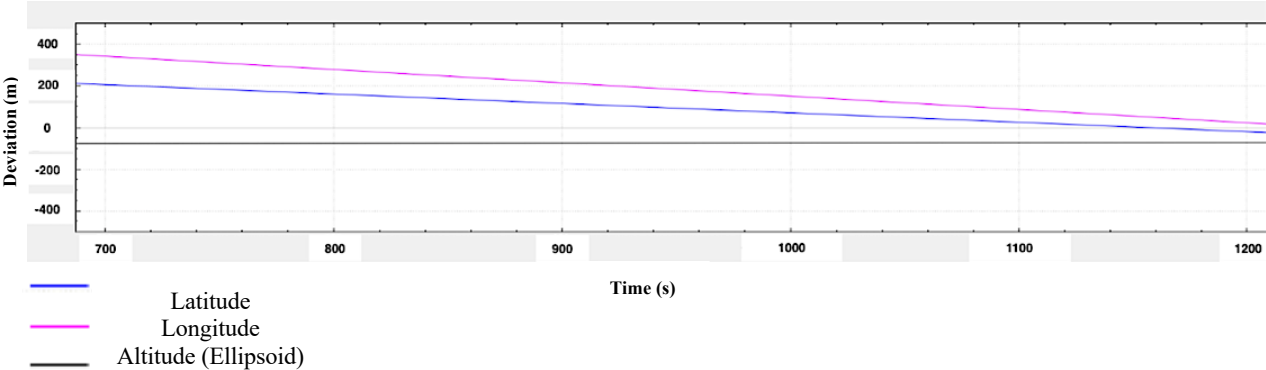


Figure 57: Deviation graph of scenario 12

Table 24: Figures of merit of scenario 12

PDOP Values	6.6 – 10.6
Time to Lock	30 sec -1 min
Locking Period	7-12 minutes
Continuity	Yes
Positioning Accuracy (PACC 3D)	20.29 m

- e. Scenario 13: to verify if the high positioning error received in the previous scenarios is due to the high PDOP values obtained for the simulated constellations, an

additional spacing between the planes and the satellites was used to make the signals more evenly spread from each other. A constellation of 35 satellites using 32 GPS satellites transmitting GPS L1C/A signal (1575.42 MHz), and 3 Galileo satellites transmitting Galileo E1 signal (1575.42 MHz). The constellation has been distributed into 5 planes, with 7 satellites in each plane. The spacing used in this scenario is close to one of the proposed constellations of GNSSaS. The planes are 45° apart, the satellites are 30° apart inter-plane, and the in-track spacing between the satellites in adjacent planes is 0° (refer to Tables 24 & 25 for orbital parameters).

Table 25: Orbital parameters of scenario 13 in Skydel

Start Time	2022-12-06 08:00:00
Reference Time	2022-12-06 08:00:00
Root Semimajor Axis	2677.87 m ^{1/2}
Eccentricity	$0^\circ = 0$ semicircle
Argument of Perigee	$0^\circ = 0$ semicircle
Inclination	$40^\circ = 0.2222$ semicircle

Table 26: RAAN & true anomaly for each satellite in scenario 13

Output Signal Type	SV ID	Plane	Satellite number per plane	Satellite Name	SV ID	RAAN	True Anomaly	
GPS L1/CA	1	Plane 1	1	Sat11	1	0° = 0 semicircle	0° = 0 semicircle	
	2		2	Sat12	2	0° = 0 semicircle	30° = 0.1667 semicircle	
	3		3	Sat13	3	0° = 0 semicircle	60° = 0.3333 semicircle	
	4		4	Sat14	4	0° = 0 semicircle	90° = 0.5 semicircle	
	5		5	Sat15	5	0° = 0 semicircle	120° = 0.6667 semicircle	
	6		6	Sat16	6	0° = 0 semicircle	150° = 0.8333 semicircle	
	7		7	Sat17	7	0° = 0 semicircle	180° = 1 semicircle	
	8	Plane 2	1	Sat21	8	45° = 0.25 semicircle	0° = 0 semicircle	
	9		2	Sat22	9	45° = 0.25 semicircle	30° = 0.1667 semicircle	
	10		3	Sat23	10	45° = 0.25 semicircle	60° = 0.3333 semicircle	
	11		4	Sat24	11	45° = 0.25 semicircle	90° = 0.5 semicircle	
	12		5	Sat25	12	45° = 0.25 semicircle	120° = 0.6667 semicircle	
	13		6	Sat26	13	45° = 0.25 semicircle	150° = 0.8333 semicircle	
	14		7	Sat27	14	45° = 0.25 semicircle	180° = 1 semicircle	
	15	Plane 3	1	Sat31	15	90° = 0.5 semicircle	0° = 0 semicircle	
	16		2	Sat32	16	90° = 0.5 semicircle	30° = 0.1667 semicircle	
	17		3	Sat33	17	90° = 0.5 semicircle	60° = 0.3333 semicircle	
	18		4	Sat34	18	90° = 0.5 semicircle	90° = 0.5 semicircle	
	19		5	Sat35	19	90° = 0.5 semicircle	120° = 0.6667 semicircle	
	20		6	Sat36	20	90° = 0.5 semicircle	150° = 0.8333 semicircle	
	21		7	Sat37	21	90° = 0.5 semicircle	180° = 1 semicircle	
	22	Plane 4	1	Sat41	22	135° = 0.75 semicircle	0° = 0 semicircle	
	23		2	Sat42	23	135° = 0.75 semicircle	30° = 0.1667 semicircle	
	24		3	Sat43	24	135° = 0.75 semicircle	60° = 0.3333 semicircle	
	25		4	Sat44	25	135° = 0.75 semicircle	90° = 0.5 semicircle	
	26		5	Sat45	26	135° = 0.75 semicircle	120° = 0.6667 semicircle	
	27		6	Sat46	27	135° = 0.75 semicircle	150° = 0.8333 semicircle	
	28		7	Sat47	28	135° = 0.75 semicircle	180° = 1 semicircle	
	29	Plane 5	1	Sat51	29	180° = 1 semicircle	0° = 0 semicircle	
	30		2	Sat52	30	180° = 1 semicircle	30° = 0.1667 semicircle	
	31		3	Sat53	31	180° = 1 semicircle	60° = 0.3333 semicircle	
	32		4	Sat54	32	180° = 1 semicircle	90° = 0.5 semicircle	
Galileo E1	1			5	Sat55	1	180° = 1 semicircle	120° = 0.6667 semicircle
	2			6	Sat56	2	180° = 1 semicircle	150° = 0.8333 semicircle
	3			7	Sat57	3	180° = 1 semicircle	180° = 1 semicircle

Compared to Scenario 12, increasing the space between the planes in the constellation by 25° degrees and between the satellites in each plane by 20° has reduced the number of the satellites in visibility from 8 to 4 only (refer to Figure 43). In addition,

the time it took the receiver to lock has increased from an average of 45 seconds in Scenario 12 to 1 minute in this scenario. Furthermore, the locking period got reduced from an average of 10 minutes in Scenario 12 to an average of 3 minutes, which is expected because of the reduced number in the visibility of the satellites in this scenario. Also, the receiver did not lock during the satellites' revisit time, as there were rarely 4 satellites visible by the receiver in this scenario.

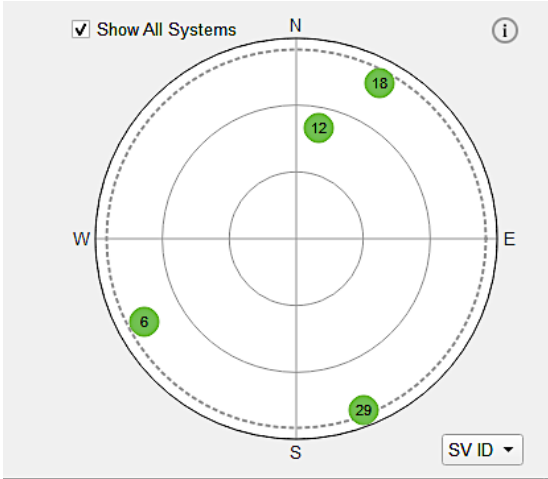


Figure 58: Sky view of scenario 13 in Skydel

However, the PDOP values improved considerably in this scenario with a minimum PDOP value of 2.1 and a maximum PDOP value of 3.3. As a result, the best 3D positioning accuracy obtained has improved from 20.29 m to 5.86 m as compared to Scenario 12. This is considered the most accurate PACC 3D obtained among all the tested scenarios, but still not in the cm-level expected for LEO GNSS (Long, 2019). Table 26 summarizes the outcomes of testing Scenario 13 in Skydel and U-centre.

Table 27: Figures of merit of scenario 13

PDOP Values	2.1 – 3.3
Time to Lock	1 minute
Locking Period	3 minutes
Continuity	N/A
Positioning Accuracy (PACC 3D)	5.86 m

3.4 A Comparison Assessment between the Performance of LEO and MEO-based GNSS using Skydel

The same figures of merit obtained for assessing the performance of a LEO-based GNSS have been obtained for the current MEO GNSS constellations in Skydel. The MEO constellations evaluated were GPS at 20,189 km altitude and Galileo at 23,229 km altitude. The signal output type for the tested GPS and Galileo constellations were GPS L1/CA (1575.42 MHz) and Galileo E1 (1575.42 MHz) signals, respectively. Table 27 summarizes the outcomes of assessing the performance of MEO and LEO GNSS constellations in Skydel and U-centre.

Table 28: Performance comparison between LEO and MEO constellations

Figures of Merit	LEO Scenario 12	LEO Scenario 13	MEO GPS	MEO Galileo
Time to Lock	20 sec - 1 min	1 min	37 sec	37 sec
Locking Period	7-12 min	3 min	Continuous	Continuous
Continuity	Not consistent	N/A	Continuous	Continuous
PDOP Values	6.6 – 10.6	2.1 – 3.3	2	2
Positioning Accuracy (PACC 3D)	20.29 m	5.86 m	3.1 m	3.1 m

Compared with the best results obtained for testing a LEO-based GNSS in Skydel, the simulated LEO constellations showed no better results regarding the positioning accuracy and the PDOP values, with the best PACC 3D of 5.86 m compared to 3.1 m for MEO based GNSS. In addition, the simulated LEO constellations did not have a consistent continuity, unlike the two MEO constellations which had continuous locking periods with the receiver. Finally, the time the receiver took to lock in the simulated LEO constellation had an average of 60 seconds, while in MEO it had an average of 30 seconds. The next chapter justifies of the obtained results.

Chapter 4: Discussions

As observed in the performance assessment comparison between the simulated LEO and MEO constellations, the results in terms of the receiver's time to lock, continuity, and the best 3D positioning accuracy (PACC 3D) obtained in LEO were no better than the obtained results in MEO. This chapter discusses the possible reasons behind the results obtained in Chapter 3, and the link budget of the proposed LEO constellation at 800 km altitude.

4.1 Discussion of the Performance of the Simulated LEO Constellation

A satellite placed in LEO would travel faster than if it was placed in MEO. For example, a satellite at an altitude of 800 km above the Earth's surface would approximately have an orbital speed of 27,000 km/h (7.5 km/s), instead of 14,000 km/h (3.89 km/s) for a MEO satellite at 20,000 km altitude. Thus, a LEO satellite would have twice the orbital speed and hence a higher doppler frequency than a MEO satellite.

In order to explain the results of Chapter 3, the following parameters for the simulated LEO constellation were analyzed:

- a. Doppler frequency rates and Doppler slopes.
- b. Radial velocity and radial acceleration rates.
- c. The ratio of the carrier power to the noise power density (C/N_0).

To compute the above parameters for Galileo E1 signal at an altitude of 800 km, some measured data, including the doppler frequency of the satellites, have been obtained from Skydel software for a period of 6 hours. Figure 44 presents the doppler frequency rates (f_d) versus elapsed time of Galileo SV ID 12 E1 signal (1575.42 MHz) simulated in LEO at 800 km altitude. As shown in Figure 44, the maximum measured doppler frequency (f_d) is about $\pm 33,000$ Hz.

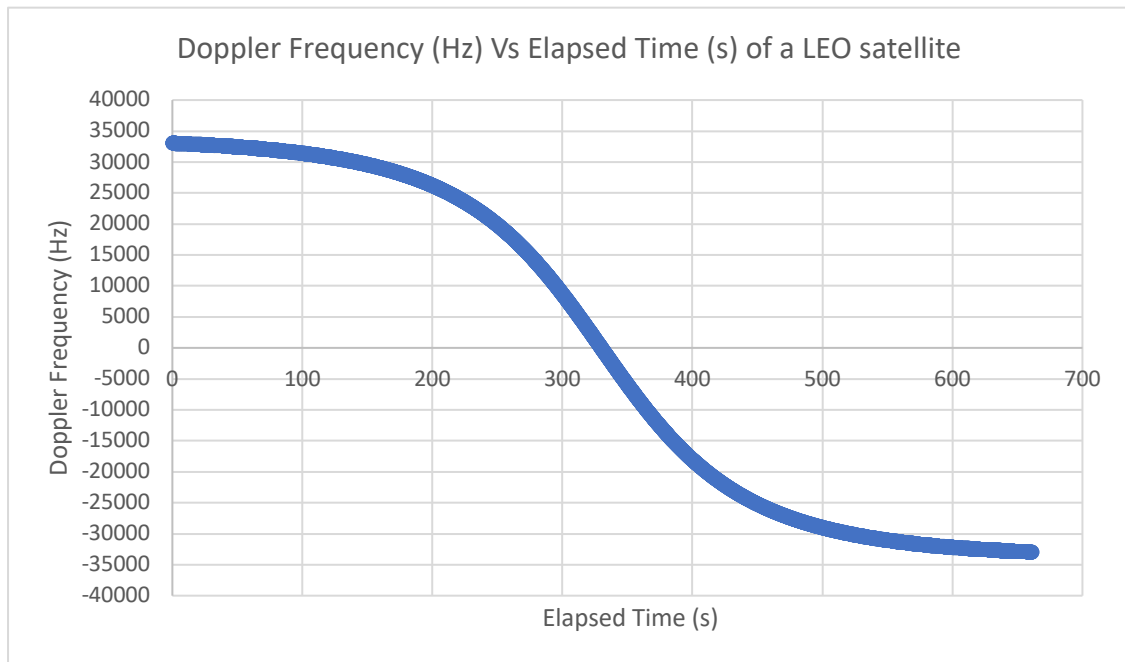


Figure 59: Doppler frequency vs. elapsed time of a LEO satellite at 800 km

The same doppler frequency rate plot was repeated for Galileo SV ID 12 E1 signal (1575.42 MHz) in MEO at an altitude of 23,229 km as shown in Figure 45. Compared with the maximum doppler frequency (f_d) observed at LEO, the maximum doppler frequency (f_d) recorded at MEO was about 3,300 Hz. Thus, modifying the altitude of a satellite from MEO to LEO means a 10 times increase in the doppler frequency rates of the satellite as seen by the receiver.

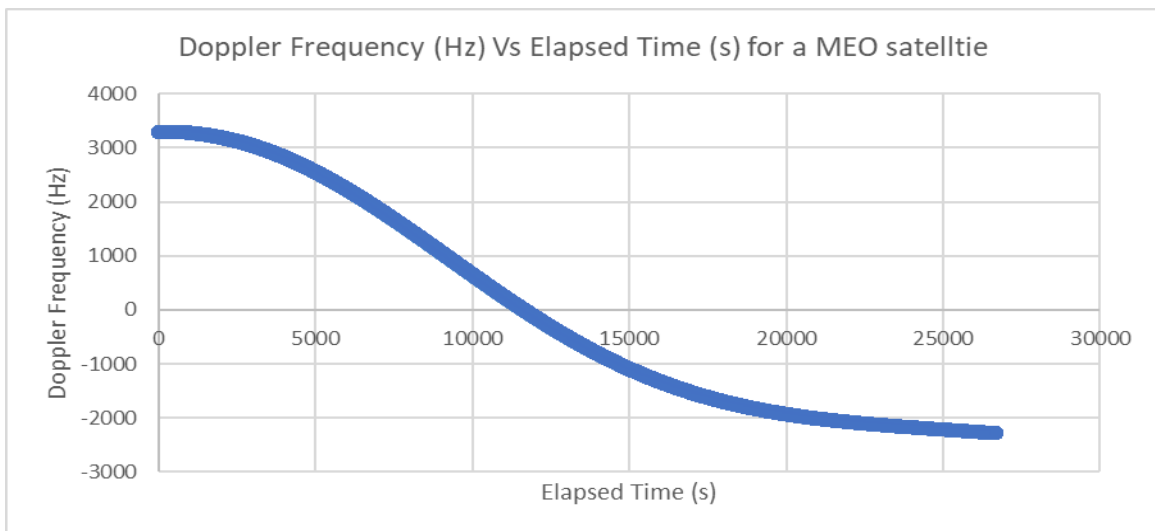


Figure 60: Doppler frequency vs. elapsed time of a MEO Galileo satellite at 23,229 km

The doppler frequency slopes for both LEO and MEO Galileo SV ID 12 have been produced and presented in Figures 46 & 47, respectively. It can be seen that a LEO spacecraft have a much stronger doppler slope and doppler shifts compared to a MEO spacecraft.

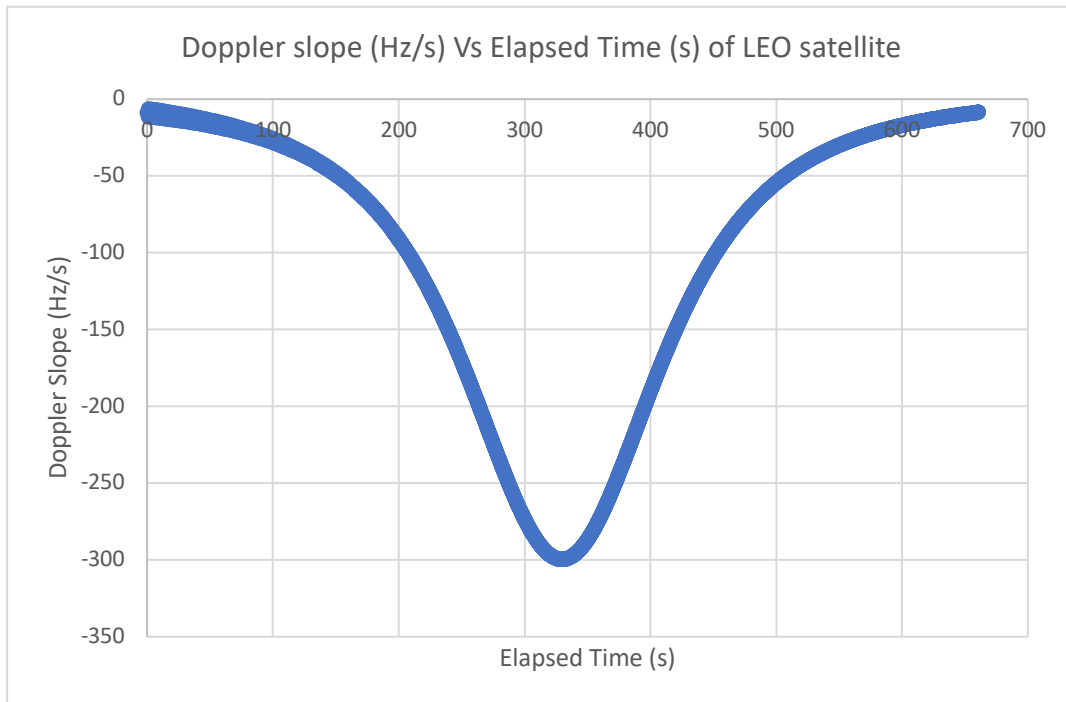


Figure 61: Doppler slope vs. elapsed time of a LEO satellite at 800 km

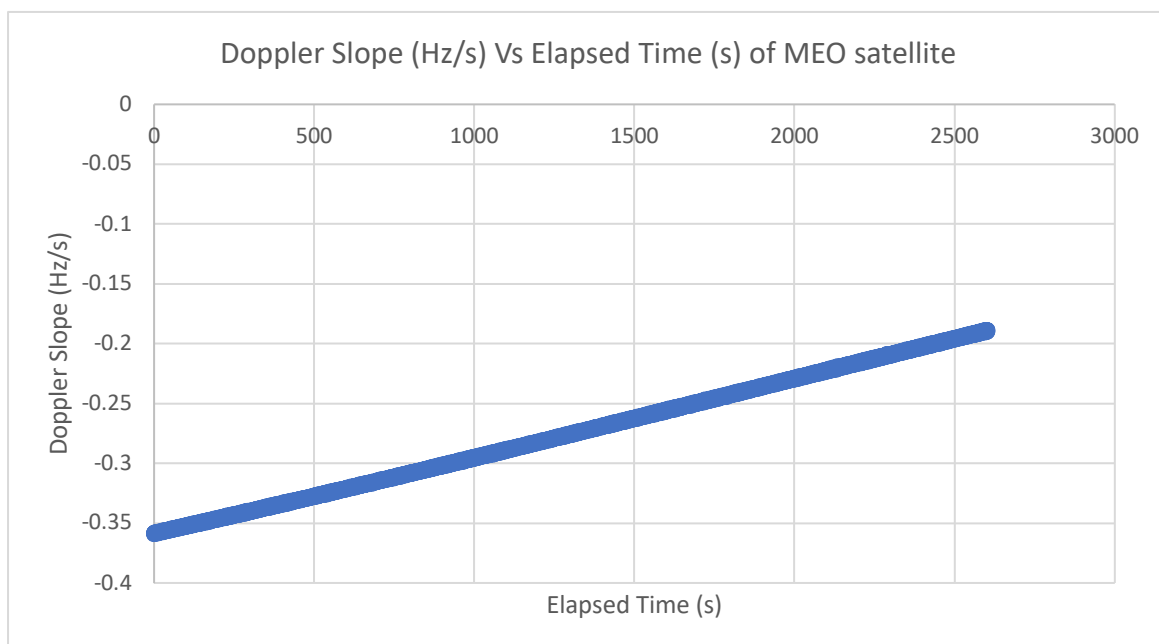


Figure 62: Doppler slope vs. elapsed time of a MEO Galileo satellite at 23,229 km

Figure 48 presents the radial velocity of Galileo SV ID 12 in LEO with respect to time. The radial velocity rates (v_r) have been calculated using Equation (1):

$$v_r = \frac{c \cdot f_d}{f_c} \quad (1)$$

where c is the speed of light, f_d is the doppler frequency, and f_c is the Carrier frequency (E1= 1575.42 MHz).

As shown in Figure 48, the maximum radial velocity at 800 km altitude was about $\pm 6,284.80$ m/s (± 6.28 km/s).

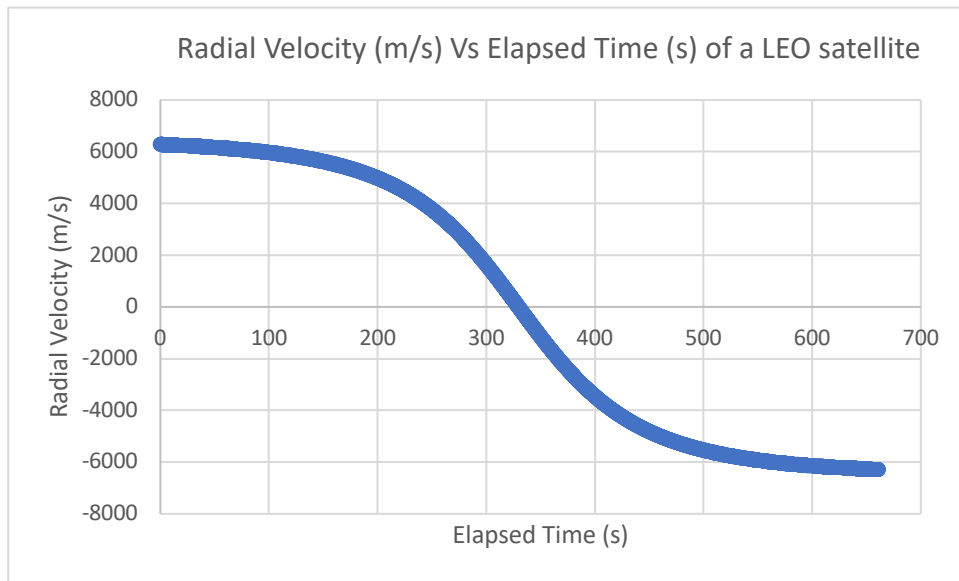


Figure 63: Radial velocity vs. elapsed time of a LEO satellite at 800 km

In addition, the radial acceleration rates have been obtained using Equation (2) and plotted in a chart illustrated in Figure 49.

$$a_r = \frac{v^2}{r} \quad (2)$$

where v is the radial velocity, and r is the distance between the satellite and the receiver. The maximum radial acceleration at 800 km is about 49.37 m/s² (0.05 km/ s²).

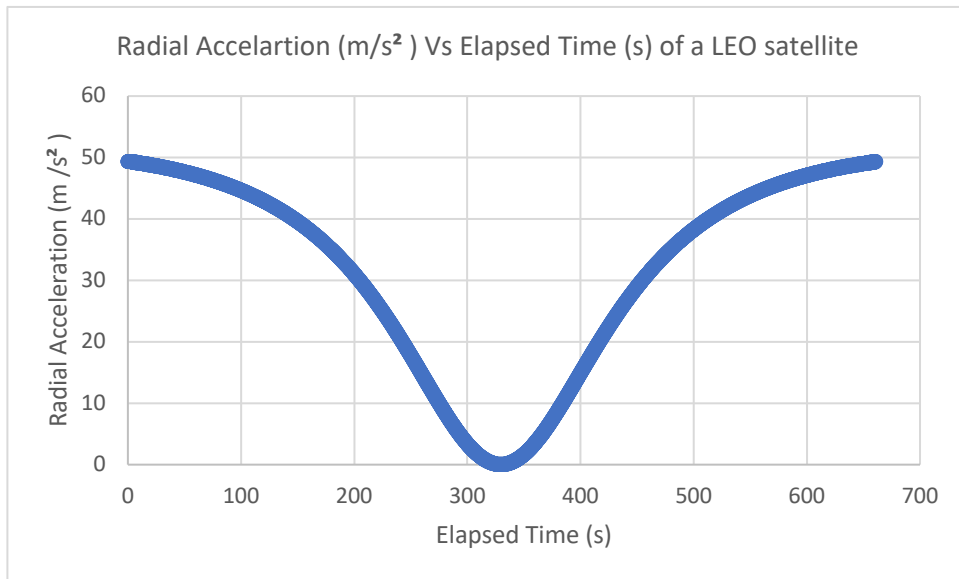


Figure 64: Radial acceleration vs. elapsed time of a LEO satellite at 800 km

Compared with the radial velocity rates (V_r) of a MEO GNSS satellite, the radial velocity and radial acceleration rates of Galileo SV ID 12 in MEO have been computed and plotted in a scatter diagram presented in Figures 50 & 51. The maximum radial velocity obtained was 630 m/s, and the maximum radial acceleration obtained was 0.017 m/s². This means that the radial velocity of a LEO satellite is approximately 10 times greater than that of a MEO satellite, and the radial acceleration of a LEO satellite is approximately 2900 times greater than that of a MEO satellite.

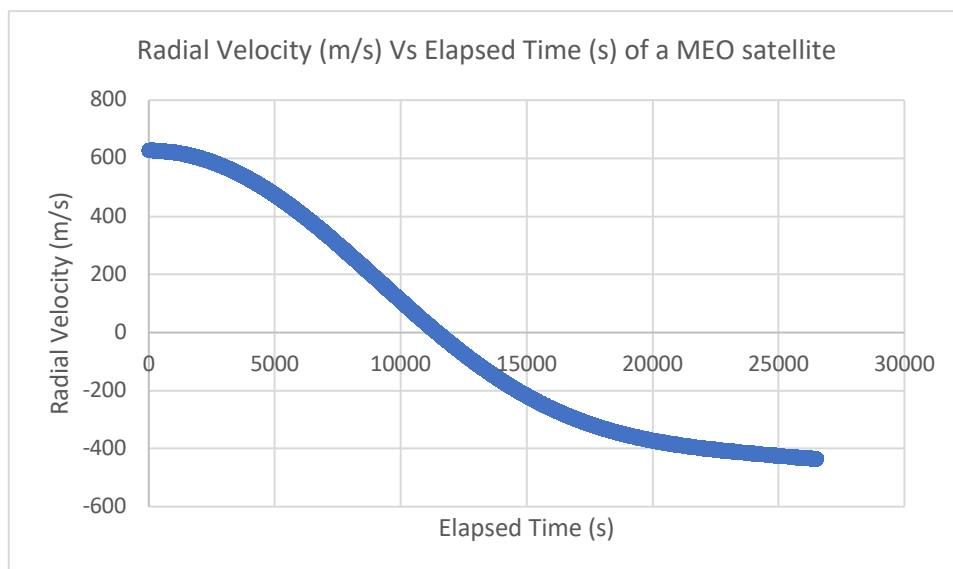


Figure 65: Radial velocity vs. elapsed time of a MEO satellite at 23,229 km

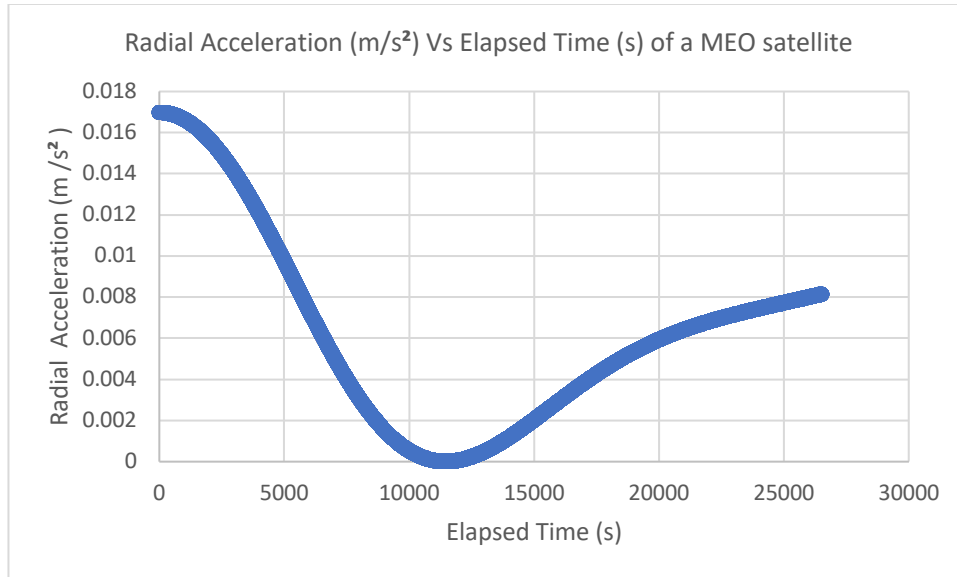


Figure 66: Radial acceleration vs. elapsed time of a MEO satellite at 23,229 km

The carrier-to-noise ratio (C/N0) of Galileo E1 signal (1575.42 MHz) at 800 km altitude was calculated using the equations below.

Firstly, according to (Steigenberger, Thoenert, & Montenbruck, 2018), the Equivalent Intrinsic Radiated Power (EIRP) of Galileo E1 signal is 37 dBW, given by Equation (3):

$$EIRP = P_t \cdot G_t \quad (3)$$

in which, P_t is the transmitted power, and G_t is the gain of the transmitter.

Secondly, the received power (P_r) on the ground at the input of the antenna with 0 dBi gain, which is also called the received carrier power (C), has been calculated using Equation (4):

$$P_r = C = \frac{P_t \cdot G_t \cdot G_r}{L_p} \quad (4)$$

in which G_r is the gain of the omnidirectional receiving antenna with a 0 dBi gain and L_p is the total propagation losses. The total propagation losses L_p has been calculated using Equation (5):

$$L_p = L_a \cdot L_{fs} \quad (5)$$

in which L_a is the atmospheric losses with an assumption of 1.5 dB for a LEO spacecraft and L_{fs} is the free space losses at 800 km altitude. The free space losses are obtained using Equation (6):

$$L_{fs} = \frac{(4\pi \cdot D \cdot f)^2}{c^2} \quad (6)$$

in which D is the distance between the satellite and the receiver, f is the carrier frequency for Galileo E1 signal, and c is the speed of light.

From Equation (5), the total propagation losses of Galileo E1 signal obtained at 800 km altitude is 155.95 dB. As a result, the received power (P_r) or the received carrier strength (C) would be -118.95 dBW. Therefore, the noise spectral density (N_0) in the reception system or the receiver is -202.067 dB (refer to Chapter 4.2 for calculations).

Using the EIRP of Galileo E1 signal at 23,229 km, the carrier-to-noise power ratio on the ground (C/N_0) would be 83.117 dBHz. However, the transmitted power depends on the satellite's altitude because the closer the satellite is to the receiver, the less the free space losses would be. To calculate the C/N_0 of Galileo E1 signal from a satellite at 800 km, the free space path losses at 800 km ($L_{fs} = 154.45$ dB) was subtracted from the free space losses at 23,229 km ($L_{fs} = 183.71$ dB), resulting to a value of a 29.26 dB. Considering this, the carrier-to-noise power ratio for Galileo E1 signal at 800 km altitude becomes 53.857 dBHz. Figure 52 shows an example of the C/N_0 measured by the ublox receiver for the tracked satellites. Both the computed and the measured C/N_0 of Galileo E1 signal transmitted from 800 km are shown to be consistent with the C/N_0 ranges of Galileo E1 signal recoded from COTS GNSS receiver with a range of 40 to 55 dBHz (Zaminpardaz & Teunissen, 2017).

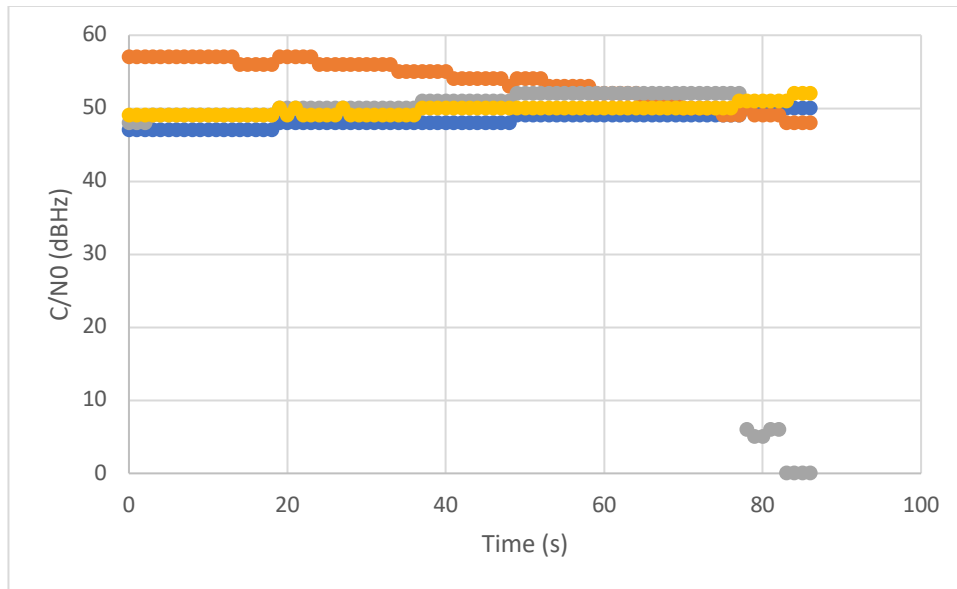


Figure 67: Example of the measured C/N0 of the tracked satellites by ublox receiver

Figures 44 to 51 show that the doppler frequency, doppler slope, radial velocity and radial acceleration of LEO satellites are significantly higher than MEO. This would explain the longer time the receiver takes to lock, the shorter locking period, and the inconsistent continuity in the previously tested LEO scenarios compared to MEO GPS and Galileo, despite having good C/N0 as shown in Figure 52.

In terms of the intermittent locking in the satellites' first pass, which affected the time to lock and the locking period, the reason would be due to the limitations of the ublox receiver used in this research, which has not been designed to acquire and track LEO PNT GNSS signals considering their much stronger dynamics compared to MEO.

In addition, the shorter locking period in the simulated LEO scenarios (3 to 12 minutes) compared to the continuous locking in MEO could most likely be due to the number of the LEO satellites visible to the receiver. In case of MEO constellations, there are always at least 8 satellites in the visibility of the receiver, hence the locking period is continuous. In the simulated LEO scenarios, the number of satellites in the constellation was limited to a maximum of 54 satellites, which does not provide full coverage at 800 km altitude. The optimum amount at this altitude would be 96 satellites (internal dissuasion with the GNSS augmentation System (GNSSaS) team). Hence, the number of satellites visible to the receiver in the simulated LEO scenarios was less and sometimes

there were no satellites visible to the receiver at all, which could explain the non-continuous and/or the shorter locking period of LEO compared to MEO.

The inconsistent time to lock and the non-continuous locking observed in the simulated LEO scenarios could be explained by the higher dynamics of a LEO satellite and the almanac management that currently does not exist in the simulated LEO satellites. The existing Galileo constellation has its almanac, a set of Keplerian parameters with long validity period that allows the receiver to reconstruct the approximate satellites' position coordinates, thus helps in reducing the acquisition and tracking time of the receiver. As the current simulated LEO constellation scenarios lack the almanac information and rely on the ephemerides only, the receiver's acquisition time and the locking time were observed to be longer than that of MEO Galileo and GPS.

The worst PACC 3D of the simulated LEO constellation compared to MEO Galileo and GPS could be explained by the limitations of the ublox receiver not being designed to be compatible with LEO PNT signals. Ublox receiver (EVK-M8T) used in this research is a single-frequency L1/E1 receiver. Also, the PACC 3D is based on code-pseudorange measurements, which could only provide at most 2.5 m accuracy (NEO/LEA-M8T Product Summary, 2018). The cm-level accuracy for LEO PNT constellations is expected when using a dual frequency receiver, which helps eliminate the ionospheric errors, and carrier phase measurements with ambiguity resolution algorithms (Tian et al, 2014).

Considering the previously mentioned justifications to the results obtained in Chapter 3, it has been concluded that the current COTS ground-based GNSS receivers are not designed to acquire LEO PNT signals, as they cannot cope with the higher dynamics of LEO satellites. Therefore, methods to improve the performance of the GNSS receivers' compatibility with the simulated LEO scenarios will be provided in Chapter 5.3.

The following section demonstrates the link budget of the proposed NSSTC's GNSSaS LEO satellite network. The objective of the link budget is to set the requirements for designing a GNSS receiver compatible with GNSSaS LEO satellite.

4.2 Link Budget Analysis of GNSSaS

GNSSaS is a LEO PNT satellite augmentation system, a long-term satellite development program at NSSTC in the UAE. The mission objective of the program is to assess the performance of LEO PNT signals in terms of positioning accuracy by transmitting L5 and S-bands GNSS signals.

Table 28 presents a detailed link budget for GNSSaS L5 (1176.42 MHz) and S-bands (2491.75 MHz) for one of the altitudes considered in the feasibility study for the GNSSaS constellation, which is 800 km. The link budget analysis is presented for the best-case scenario (when the satellite is at zenith), and the worst-case scenario (when the satellite is at 5 degrees elevation angle).

Table 29: Link budget of a LEO GNSS spacecraft

Item	Symbol	Units	Downlink				Comments
			L5		S-band		
			5°	90°	5°	90°	
Equiv. Isotropic Radiated Power	EIRP	dBW	9.70	2.40	17.30	6.50	Equation 7
Receiver Antenna Gain	(G_r)	dBi	0.00	0.00	0.00	0.00	
Propagation Path Length	D	km	2782.68	800.00	2782.68	800.00	Equation 8
Free Space Path Loss	(L_{fs})	dB	162.70	151.90	169.26	158.43	Equation 9
Ionospheric Losses	(L_{ion})	dB	1.00	1.00	1.00	1.00	
Tropospheric Losses	(L_{trop})	dB	0.50	0.50	0.50	0.50	
Total Atmospheric Losses	(L_{atmo})	dB	1.50	1.50	1.50	1.50	Equation 10
Total Propagation Losses	(L_p)	dBi	164.2	153.4	170.76	159.93	Equation 11
Boltzmann Constant	(K)	$m^2 kg s^{-2} K^{-1}$	$1.38 \cdot 10^{-23}$				
Speed of Light	(c)	m/s	$3 \cdot 10^8$				
Antenna Noise Temperature	(T_{ant})	K	150	150	150	150	
Receiver Noise Temperature	(T_r)	K	300	300	300	300	
Total System Noise Temperature	(T_s)	K	450	450	450	450	Equation 12
Noise Density	($N0$)	dB	-202.06	-202.06	-202.06	-202.06	Equation 13
Received Carrier Strength (Received Power)	(C) (P_r)	dBW	-154.4	-151.0	-153.46	-153.43	Equation 14
Carrier-to-Noise Ratio	($C/N0$)	dBW	47.667	51.067	48.607	48.637	

Note:

- $EIRP = P_t + G_t$ (7)

where P_t is the transmitted power in dBW, and G_t is the gain of the transmitter in dBi.

- $D = \frac{\sqrt{(R_e+h)^2 \cdot (1+\tan^2(\theta_{el})) - R_e^2} - R_e \cdot \tan \theta_{el}}{\sqrt{1+\tan^2(\theta_{el})}}$ (8)

where D is the distance between the transmitter and the receiver, R_e is the Earth radius, h is the height of the satellite above Earth surface, and θ_{el} is the elevation angle in rad.

- $L_{fs} = \frac{(4\pi \cdot D \cdot f)^2}{c^2}$ (9)

where f is the carrier frequency, and c is the speed of light.

- $L_{atmo} = L_{ion} + L_{trop}$ (10)

- $L_p = L_{fs} + L_{atmo}$ (11)

- $T_s = T_{ant} + T_r$ (12)

- $N0 = k * T_s$ (13)

- $C = P_r = \frac{P_t \cdot G_t \cdot G_r}{L_p}$ (14)

Chapter 5: Conclusion

This chapter refocuses on the purpose of this research, outlines the findings, and includes the study's limitations and some future research recommendations.

5.1 Conclusions

In the near future, there will be a resurgent demand for more accurate GNSS PNT services. This research highlights the advantages of the LEO-based GNSS compared to the current MEO-based GNSS. It is very important to design an orbit configuration for a LEO augmentation system and/or a stand-alone LEO navigation system and assess its operation and performance to set the standards for a prototype LEO GNSS constellation. In this research, a mini-LEO GNSS constellation was designed and simulated using STK software, followed by simulation and assessment using Skydel GNSS simulator tool. Furthermore, the performance of simulated orbits was assessed using a GNSS receiver in terms of the time to lock, locking period, continuity, PDOP, and the PACC 3D. Finally, the performance of the simulated mini-LEO GNSS constellation was compared with the existing MEO GPS and Galileo. The following section presents the significant findings and limitations of this research.

5.2 Research Findings and Limitations

From all the simulated LEO GNSS constellations, the best PACC 3D obtained was not in the cm-level expected from the LEO GNSS, and the receiver's performance in the case of LEO GNSS was no better than it was for MEO GNSS. One of the contributing factors behind the obtained results was that current COTS GNSS receivers could not cope with the higher dynamics of LEO satellites in terms of doppler frequency, radial velocity, and radial acceleration. Furthermore, the lack of almanac management in the simulated LEO constellations has also contributed to the obtained results. Therefore, the GNSS receiver's performance compatible with LEO GNSS was assessed in this research, and some recommendations for improvements were suggested.

The major limitations of this research are both software and hardware based. Regarding the number of satellites in the constellation that could be simulated in Skydel software, the number was limited to 54 only, which does not provide global coverage in

LEO and limits the satellite's visibility by the receiver. Regarding the hardware, ublox EVK-M8T COTS GNSS receiver was mainly designed to acquire existing MEO PNT signals. As a result, it could not cope with the higher dynamics of LEO satellites. In addition to that, ublox EVK-M8T is a single frequency L1/E1 receiver, and the position computed by the receiver is based on MEO GNSS algorithms and not LEO GNSS algorithms. Furthermore, it works on code-pseudorange measurements, which could only provide a maximum accuracy of 2.5 m.

5.3 Recommendations and Way Forward

To reasonably perform the comparative assessment between MEO and LEO GNSS, the conditions between both constellations should be as similar as possible regarding satellite visibility. Skydel version 22.7.1 used in this research, might have future updates which would enable more than 54 satellites to be placed in LEO. Once a new version supporting additional satellites to be placed in LEO is released, a new configuration design and assessment could be performed. This orbit configuration enhancement could enable better PDOP values, a continuity of the lock between the receiver with at least four satellites. Furthermore, the scenarios assessed in this research could be repeated using a different COTS GNSS receiver or a prototype receiver, which is specially designed to include algorithms to improve acquisition sensitivity and tracking accuracy of highly dynamic navigation signals. In addition, a dual frequency GNSS receiver could be used to eliminate the ionospheric errors and to use carrier phase measurements with ambiguity resolution algorithms to obtain a cm-level positioning accuracy. On the space segment side, including the robust navigation message that would include the almanacs of the proposed constellation and the isoflux radiation pattern of the centered phase dual-frequency antenna is suggested for the improvement of the constellation's performance.

References

- AGI, ANSYS Gove, Inc (2023). Retrieved January 16, 2023, from <https://www.agi.com>
- Al-Ruwais, A.S., & Ahmed, A.S. (2008), Elevation-Angle Variation of LEO Satellite over the Kingdom of Saudi Arabia, Arab Gulf Journal of Scientific Research, 26 (3):145-151.
- BasuMalick, C. (2022, June 10). *What is GNSS (Global Navigation Satellite System)? Meaning, Working, and Applications in 2022*. Spice Works. Retrieved September 6, 2022, from <https://www.spiceworks.com/tech/iot/articles/what-is-gnss/>
- Bury, G., Sośnica, K., Zajdel, R., Strugarek D., & Hugentobler, U. (2021). *Determination of precise Galileo orbits using combined GNSS and SLR observations*, GPS Solutions, 25 (11), doi: 10.1007/s10291-020-01045-3
- Chen, M. (2022, September 25). *What is the PPP?* Tersus GNSS. Retrieved October 11, 2022, from https://www.tersus-gnss.com/tech_blog/what-is-the-ppp
- FAA. (n.d.). *Satellite navigation - GPS - how it works*. Federal Aviation Administration. Retrieved September 29, 2022, from https://www.faa.gov/about/office_org/headquarters_offices/ato/service_units/tech_ops/navservices/gnss/gps/howitworks#:~:text=The%20basic%20GPS%20service%20provides,the%20surface%20of%20the%20earth.
- GISGeography. (2022, May 30). *GPS accuracy: HDOP, PDOP, GDOP, multipath & the atmosphere*. GISGeography.com. Retrieved October 24, 2022, from <https://gisgeography.com/gps-accuracy-hdop-pdop-gdop-multipath/>
- Guan, M., Xu, T., Gao, F., Nie, W., & Yang, H.(2020), *Optimal Walker Constellation Design of LEO Based Global Navigation and Augmentation System*, Remote Sensing 12(11), doi:10.3390/rs12111845.
- ISRO-IRNSS-ICD-SPS-1.1 (August, 2017). Retrieved January 4, 2023, from https://www.isro.gov.in/media_isro/pdf/Publications/Vispdf/Pdf2017/irnss_sps_icd_version1.1-2017.pdf

- Lawrence, D., Cobb, S., Gutt, G., O'Connor, M., Reid, T., Walter, T., & Whelan, D. (2017, July). *Navigation From LEO*. GPSWorld.com. Retrieved December 8, 2022, from https://web.stanford.edu/group/scpnt/gpslab/pubs/papers/Lawrence_GPSWorld_July2017.pdf
- Liu, G. & Wang, L. (2022), *Joint Tracking GPS and LEO signals with adaptive vector tracking loop in challenging environments*, 7th Intl. Conference on Ubiquitous Positioning, Indoor Navigation and Location-Based Services (UPINLBS 2022), 18–19 March 2022, Wuhan, China.
- Long, Y. (2019, December 10). *The Centispace-1*. 14th Meeting of the International Committee on Global Navigation Satellite Systems. Unoosa.org. Retrieved February 1, 2023 from https://www.unoosa.org/documents/pdf/icg/2019/icg14/WGB/icg14_wgb_S5_4.pdf
- Mapasyst. (2019, August 21). *Position Dilution of Precision (PDOP)*. Extension.org. Retrieved January 26, 2023, from <https://mapasyst.extension.org/position-dilution-of-precision-pdop/>
- Matt. (2017, March 15). *What is PDOP? And why it's obsolete*. ANATUM GeoMobile Solutions. Retrieved January 26, 2023, from https://www.agsgis.com/What-is-PDOP-And-Why-its-Obsolete_b_43.html
- Mcduffie, J. (2017, June 19). *Why the Military Released GPS to the Public*. Popular Mechanics. Retrieved October 13, 2022, from <https://www.popularmechanics.com/technology/gadgets/a26980/why-the-military-released-gps-to-the-public/>
- Meg. (2022, November 11). *Why is GPS data sometimes inaccurate?* Strava Support. Retrieved December 13, 2022, from <https://support.strava.com/hc/en-us/articles/216917917-Why-is-GPS-data-sometimes-inaccurate->
- Misra, P., & Enge, P. (2011). *Global Positioning System: Chapter 1: Signals, Measurements, and Performance* (Revised Second Edition). ISBN 0-9709544-1-7. Ganga-Jamuna Press.
- NEO/LEA-M8T Series, Product Summary, UBX-16000801 - R06, 2018. Retrieved September 28, 2022, from https://content.u-blox.com/sites/default/files/products/documents/NEO-LEA-M8T_ProductSummary_%28UBX-16000801%29.pdf

NSSTC (2019), *GNSSaS Program Overview and System Approach*, GNSSaS Mission Concept Review (MCR), Internal Document.

Ong, S. (2016, May 2). *How does your GPS know where you are?* Scienceline.org. Retrieved September 21, 2022, from <https://scienceline.org/2016/05/how-does-your-gps-know-where-you-are/>

Orolia Skydel User Manual, Revision 22.12.0, 24 Jan 2020. Retrieved October 13, 2022, from <https://www.rolia.com/manuals/skydel/>

Puzzo, L. (2021, July 2). *GPS Accuracy and GPS Drift – Should you rely on it anymore?* Mosaic51. Retrieved September 14, 2022, from <https://www.mosaic51.com/community/gps-accuracy-and-gps-drift-should-you-rely-on-it-anymore/>. <https://www.mosaic51.com/community/gps-accuracy-and-gps-drift-should-you-rely-on-it-anymore/>

Reid, T., Neish, A., Walter, T., & Enge, P. (2016). *Leveraging Commercial Broadband LEO Constellations for Navigation*. 10.33012/2016.14729.

Roberts, T. (2022, June 14). *Popular Orbits 101*. Aerospace 101. Retrieved October 5, 2022, from <https://aerospace.csis.org/aerospace101/earth-orbit-101/#:~:text=Satellites%20in%20LEO%20typically%20take,incl%20Earth%20observation%20and%20reconnaissance.>

Steigenberger, P., Thoenert, S., & Montenbruck, O. (2018), *GNSS satellite transmit power and its impact on orbit determination*. *J Geod* 92, 609–624. Retrieved November 10, 2022, from <https://doi.org/10.1007/s00190-017-1082-2>.

Su M., Su X., Zhao Q., & Liu J. (2019), *BeiDou Augmented Navigation from Low Earth Orbit Satellites*, *Sensors*, 198, doi:10.3390/s19010198

Tian S., Dai W., Liu R., Chang J., & Li G. (2014), *System Using Hybrid LEO-GPS Satellites for Rapid Resolution of Integer Cycle Ambiguities*, *IEEE Transactions on Aerospace and Electronic Systems*.

Diggelen F., & Enge P. *The World's first GPS MOOC and Worldwide Laboratory using Smartphones*, *Proceedings of the 28th International Technical Meeting of the Satellite Division of The Institute of Navigation (ION Please GNSS+ 2015)*, Tampa, Florida, September 2015, pp. 361-369.

Wang, L., Xu, B., Chen, R., & Li, T. (2019, May). *The challenges of LEO based navigation augmentation system – lessons learned from Luojia-1A satellite*. ResearchGate, doi: 10.1007/978-981-13-7759-4_27

What are Global Navigation Satellite Systems? (n.d.). NovAtel. Retrieved September 8, 2022, from <https://novatel.com/tech-talk/an-introduction-to-gnss/what-are-global-navigation-satellite-systems-gnss>

Zahradnik, F. (2021, August 28). *What is trilateration?* Lifewire.com. Retrieved September 12, 2022, from <https://www.lifewire.com/trilateration-in-gps-1683341>

Zaminpardaz, S., & Teunissen, P. J. G. (2017, October). *Analysis of Galileo IOV + FOC signals and E5 RTK performance*, GPS Solutions 21(4), doi: 10.1007/s10291-017-0659-9

List of Publications

Alrais, M. (2023). Design and Assessment of a LEO GNSS Mini-Constellation for Positioning, Navigation, and Timing (PNT). ION GNSS+ 2023 Conference, Denver, CO, USA.

Appendices

Appendix A: Hardware and Software Specifications

- i. Minimal Computer Requirements to run a basic simulation in Skydel software (Orolia Skydel User Manual, 2020):

Component	Minimal Requirement
CPU	Intel Core i5, 3rd generation Minimal PassMark score of 7000 www.cpubenchmark.net/
RAM	8 GB DDR3
Storage	4 GB free space. We strongly recommend having at least 10% of free space on the O/S drive.
GPU	Nvidia GeForce, Quadro or Tesla Minimum of 384 CUDA Cores CUDA compute capability of 5.0
Network Card 1 GbE	Intel PRO/1000 CT Desktop Gigabit Typically, any onboard Intel, Realtek, or Broadcom card will be sufficient. Other brands are not recommended.
Network Card 10 GbE	Intel X550-T2 Intel X520-DA2 (E10G42BTDA)

- ii. Ublox EVK-M8T specifications (ublox EVK-M8T User Guide, 2018):



EVK-M8T User Guide

2 Specifications

Parameter	Specification
Serial Interfaces	1 USB V2.0
	1 RS232, max. baud rate 921,6 kBd
	DB9 +/- 12 V level
	14 pin – 3.3 V logic
	1 DDC (I2C compatible) max. 400 kHz
Timing Interfaces	1 SPI – clock signal max. 5,5 MHz – SPI DATA max. 1 Mbit/s
	2 Time-pulse outputs
Dimensions	105 x 64 x 26 mm
Power Supply	5V via USB or external powered via extra power supply pin 14 (V5_IN) 13 (GND)
Normal Operating temperature	-40°C to +65°C

Table 2: EVK-M8T specifications

Appendix B: Scenario 11

i. Error of Scenario 11 in Skydel:

In this scenario, 37 BeiDou satellites were added to the 22 Galileo satellites simulated in Scenario 10 in Skydel. A constellation of a total of 59 satellites with 22 satellites transmitting Galileo E1 signal (1575.42 MHz) and 37 satellites transmitting BeiDou B1 signal (1561.098 MHz). The constellation has been distributed into 4 planes, the first plane had 14 satellites, and the rest had 15 satellites per plane. The orbital spacing of Scenario 10 was used in this scenario (refer to Tables A & B for orbital parameters).

Table A: Orbital parameters of scenario 11 in Skydel

Start Time	2022-09-27 08:00:00
Reference Time	2022-09-27 08:00:00
Root Semimajor Axis	2677.87 m ^{1/2}
Eccentricity	0° = 0 semicircle
Argument of Perigee	0° = 0 semicircle
Inclination	40° = 0.2222 semicircle

Table B: RAAN & true anomaly for each satellite in scenario 11

Signal Output Type	SV ID	Plane	Satellite number per plane	RAAN	True Anomaly
Galileo E1	1	Plane 1	1	50° = 0.2778 semicircle	0° = 0 semicircle
	2		2	50° = 0.2778 semicircle	10° = 0.0556 semicircle
	3		3	50° = 0.2778 semicircle	20° = 0.1111 semicircle
	4		4	50° = 0.2778 semicircle	30° = 0.1667 semicircle
	5		5	50° = 0.2778 semicircle	40° = 0.2222 semicircle
	7		6	50° = 0.2778 semicircle	50° = 0.2778 semicircle
	8		7	50° = 0.2778 semicircle	60° = 0.3333 semicircle
	9		8	50° = 0.2778 semicircle	70° = 0.3889 semicircle
	11		9	50° = 0.2778 semicircle	80° = 0.4444 semicircle
	12		10	50° = 0.2778 semicircle	90° = 0.5 semicircle
	13		11	50° = 0.2778 semicircle	100° = 0.5556 semicircle
	15		12	50° = 0.2778 semicircle	110° = 0.6111 semicircle
	19		13	50° = 0.2778 semicircle	120° = 0.6667 semicircle
	21		14	50° = 0.2778 semicircle	130° = 0.7222 semicircle
	24	Plane 2	1	70° = 0.3889 semicircle	0° = 0 semicircle
	25		2	70° = 0.3889 semicircle	10° = 0.0556 semicircle
	26		3	70° = 0.3889 semicircle	20° = 0.1111 semicircle
	27		4	70° = 0.3889 semicircle	30° = 0.1667 semicircle
	30		5	70° = 0.3889 semicircle	40° = 0.2222 semicircle
	31		6	70° = 0.3889 semicircle	50° = 0.2778 semicircle
	33		7	70° = 0.3889 semicircle	60° = 0.3333 semicircle
	36		8	70° = 0.3889 semicircle	70° = 0.3889 semicircle
	6		9	70° = 0.3889 semicircle	80° = 0.4444 semicircle
	7		10	70° = 0.3889 semicircle	90° = 0.5 semicircle
8	11	70° = 0.3889 semicircle	100° = 0.5556 semicircle		
9	12	70° = 0.3889 semicircle	110° = 0.6111 semicircle		
10	13	70° = 0.3889 semicircle	120° = 0.6667 semicircle		
11	14	70° = 0.3889 semicircle	130° = 0.7222 semicircle		
12	15	70° = 0.3889 semicircle	140° = 0.7778 semicircle		
BeiDou B1	13	Plane 3	1	90° = 0.5 semicircle	0° = 0 semicircle
	14		2	90° = 0.5 semicircle	10° = 0.0556 semicircle
	16		3	90° = 0.5 semicircle	20° = 0.1111 semicircle
	19		4	90° = 0.5 semicircle	30° = 0.1667 semicircle
	20		5	90° = 0.5 semicircle	40° = 0.2222 semicircle
	21		6	90° = 0.5 semicircle	50° = 0.2778 semicircle
	22		7	90° = 0.5 semicircle	60° = 0.3333 semicircle
	23		8	90° = 0.5 semicircle	70° = 0.3889 semicircle
	24		9	90° = 0.5 semicircle	80° = 0.4444 semicircle
	25		10	90° = 0.5 semicircle	90° = 0.5 semicircle
	26		11	90° = 0.5 semicircle	100° = 0.5556 semicircle
	27		12	90° = 0.5 semicircle	110° = 0.6111 semicircle
	28		13	90° = 0.5 semicircle	120° = 0.6667 semicircle
	29		14	90° = 0.5 semicircle	130° = 0.7222 semicircle
	30		15	90° = 0.5 semicircle	140° = 0.7778 semicircle

Table B: RAAN & true anomaly for each satellite in scenario 11 (continued)

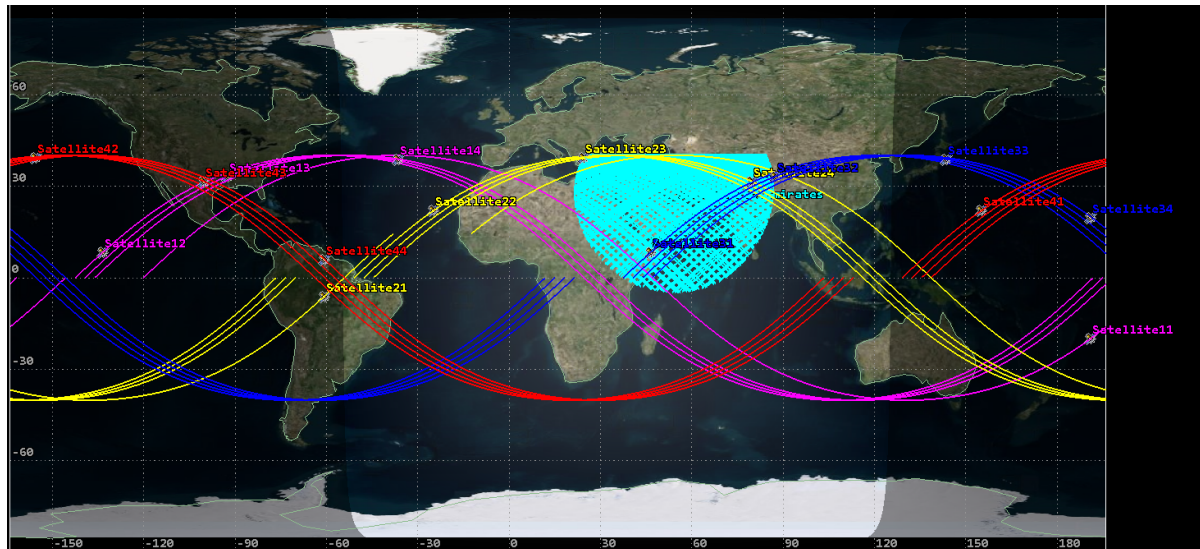
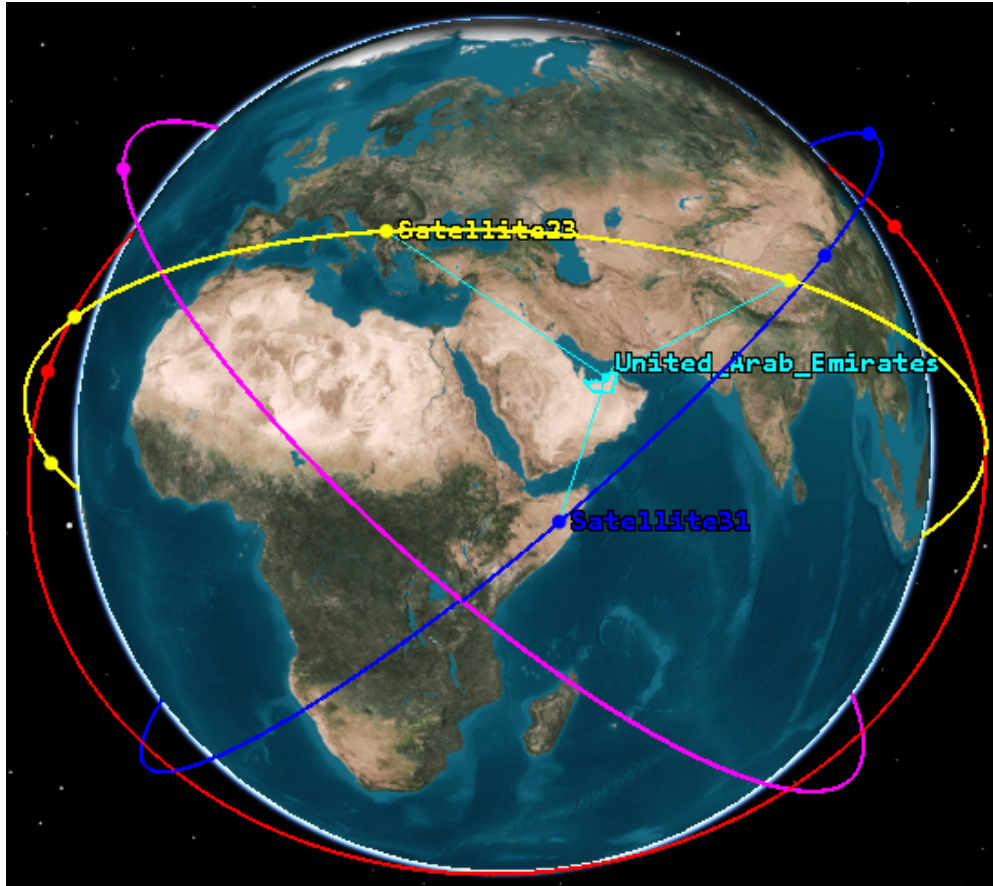
Signal Output Type	SV ID	Plane	Satellite number per plane	RAAN	True Anomaly
BeiDou B1	32	Plane 4	1	110° = 0.6111 semicircle	0° = 0 semicircle
	33		2	110° = 0.6111 semicircle	10° = 0.0556 semicircle
	34		3	110° = 0.6111 semicircle	20° = 0.1111 semicircle
	35		4	110° = 0.6111 semicircle	30° = 0.1667 semicircle
	36		5	110° = 0.6111 semicircle	40° = 0.2222 semicircle
	37		6	110° = 0.6111 semicircle	50° = 0.2778 semicircle
	38		7	110° = 0.6111 semicircle	60° = 0.3333 semicircle
	39		8	110° = 0.6111 semicircle	70° = 0.3889 semicircle
	40		9	110° = 0.6111 semicircle	80° = 0.4444 semicircle
	41		10	110° = 0.6111 semicircle	90° = 0.5 semicircle
	42		11	110° = 0.6111 semicircle	100° = 0.5556 semicircle
	43		12	110° = 0.6111 semicircle	110° = 0.6111 semicircle
	44		13	110° = 0.6111 semicircle	120° = 0.6667 semicircle
	45		14	110° = 0.6111 semicircle	130° = 0.7222 semicircle
	46		15	110° = 0.6111 semicircle	140° = 0.7778 semicircle

As expected, the satellites spatial density and the PDOP values were similar to Scenario 10, since the spacing between the satellites and the planes in both scenarios are the same.

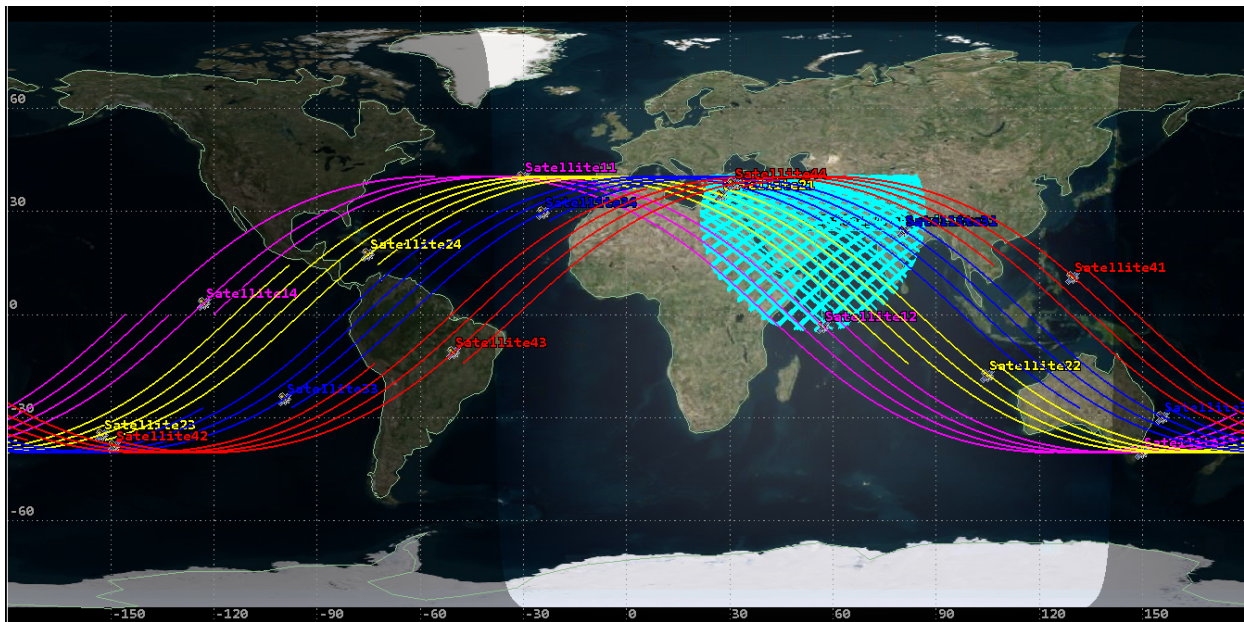
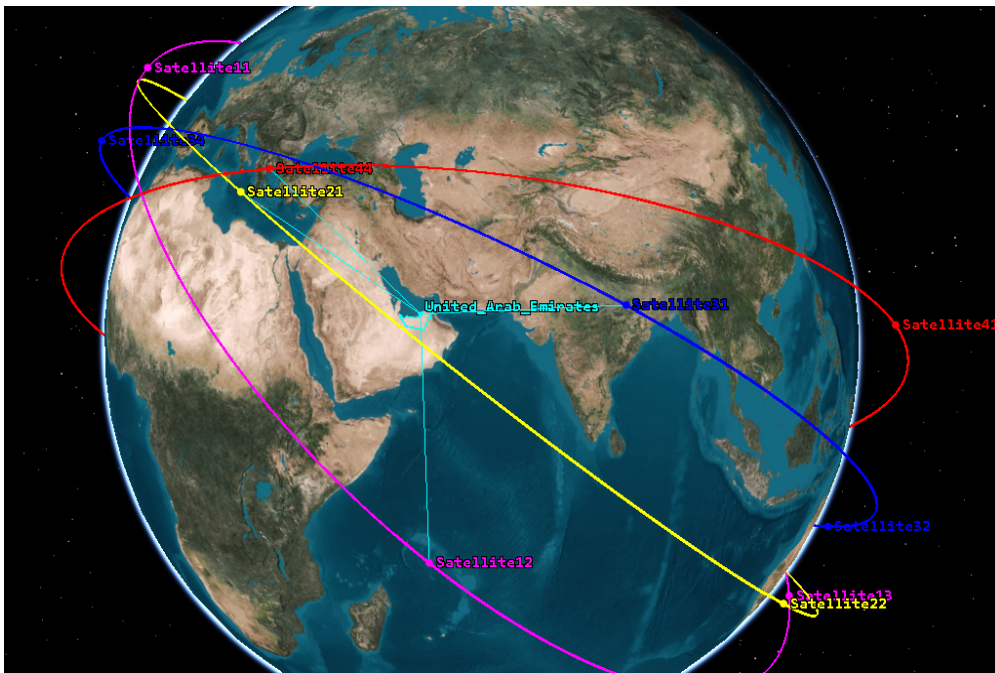
However, an error appears once the test is started in this scenario. Error: No i0 value for BeiDou Reserved Satellite type. The constellation has been tested alone, and a portion of the constellation has been tested, but the same error occurred. It has been concluded that BeiDou constellation would not work, when modified to LEO, in the current Skydel version 22.7.1, and thus has not been used in this thesis research for assessing the performance of a LEO based GNSS.

Appendix C: 3D & 2D Graphics for the Tested Scenarios in STK

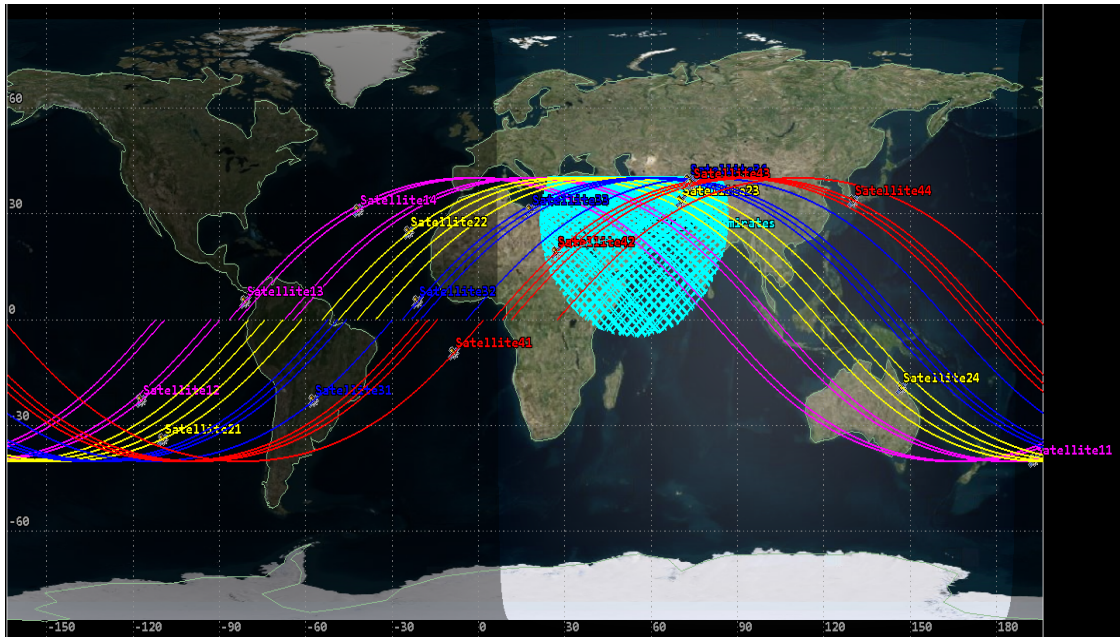
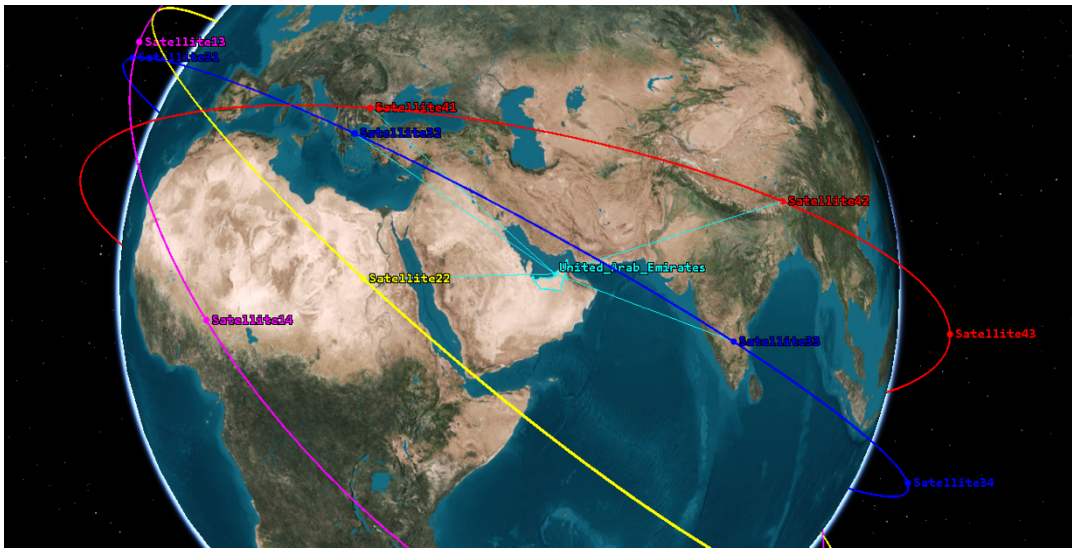
i. Scenario 2



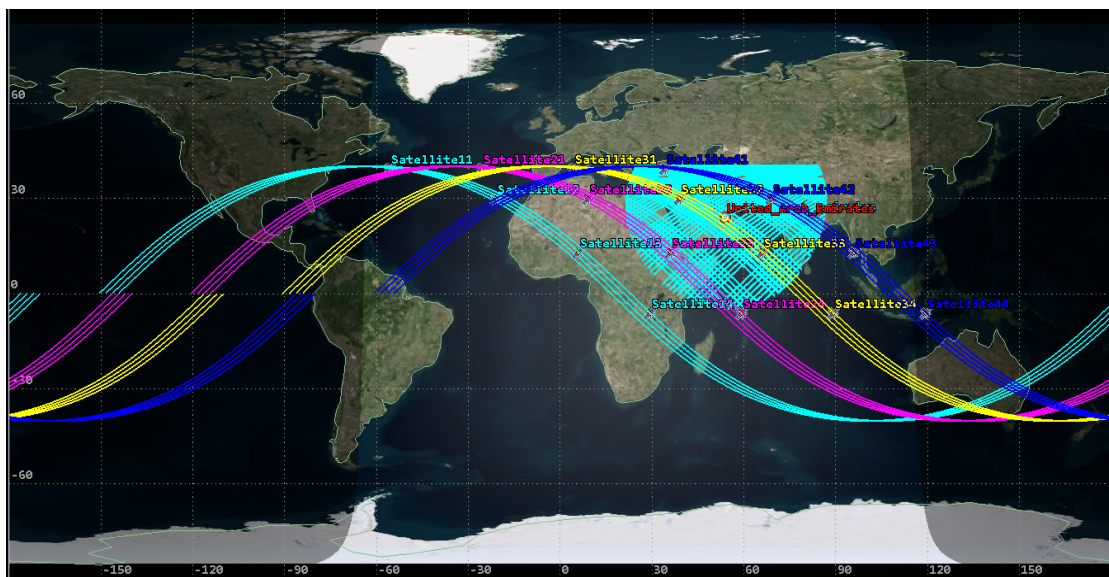
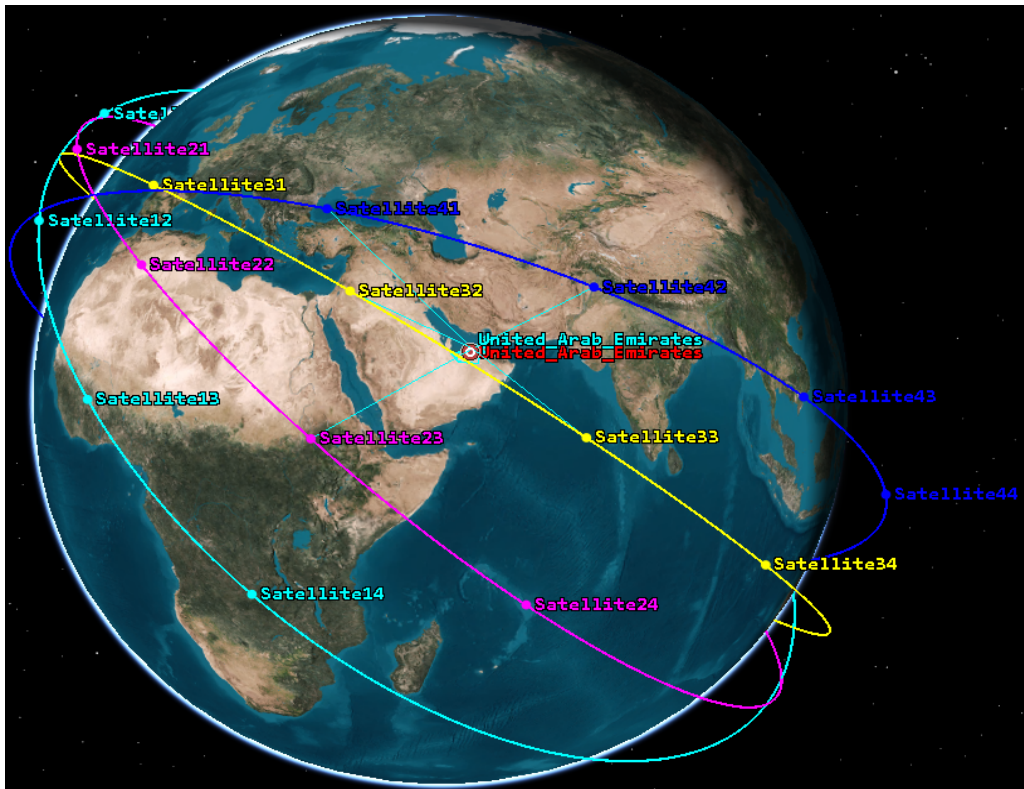
ii. Scenario 3



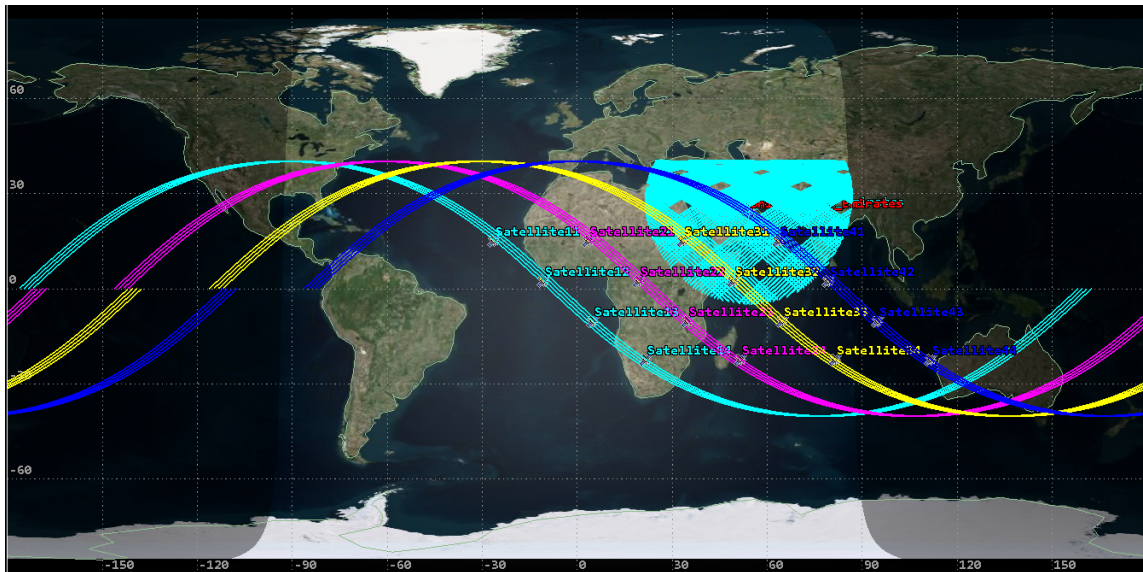
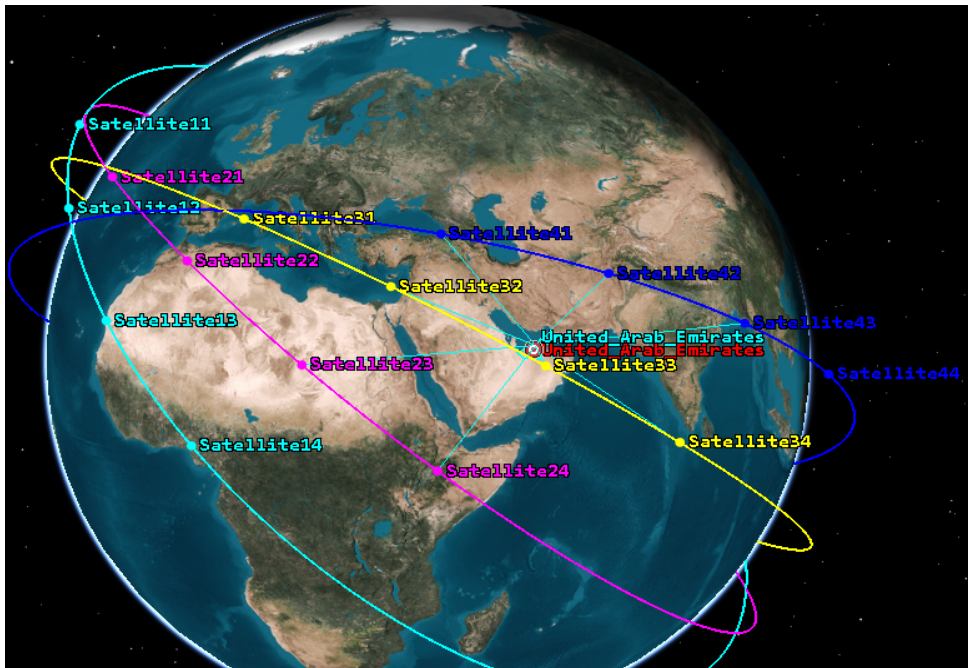
iii. Scenario 4



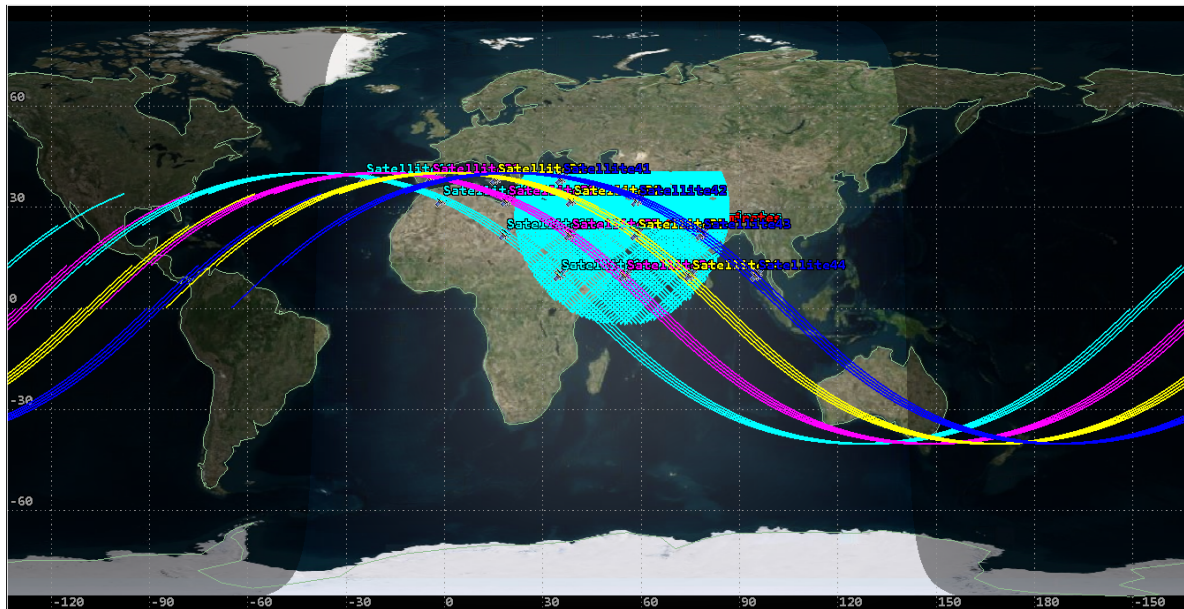
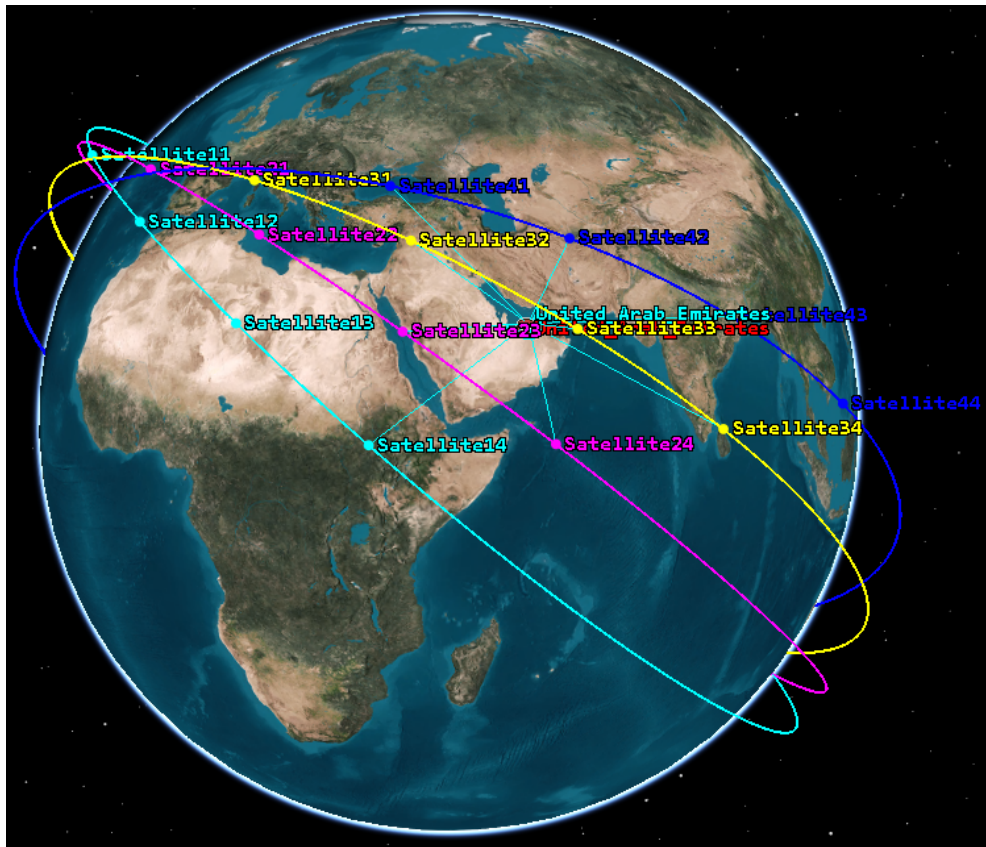
iv. Scenario 5



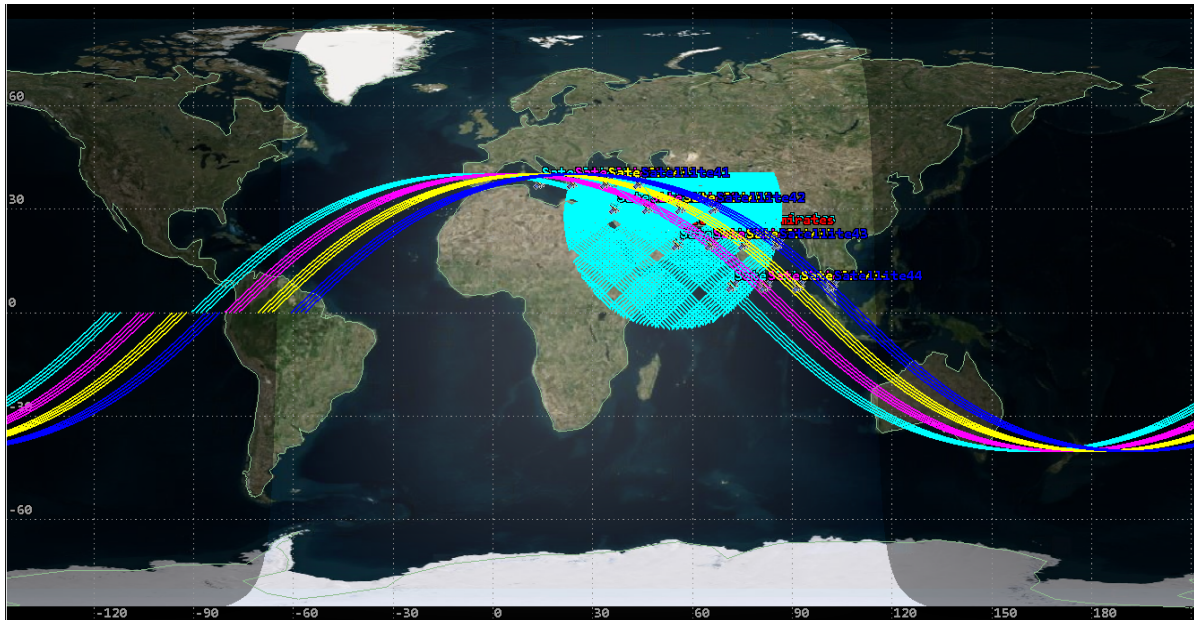
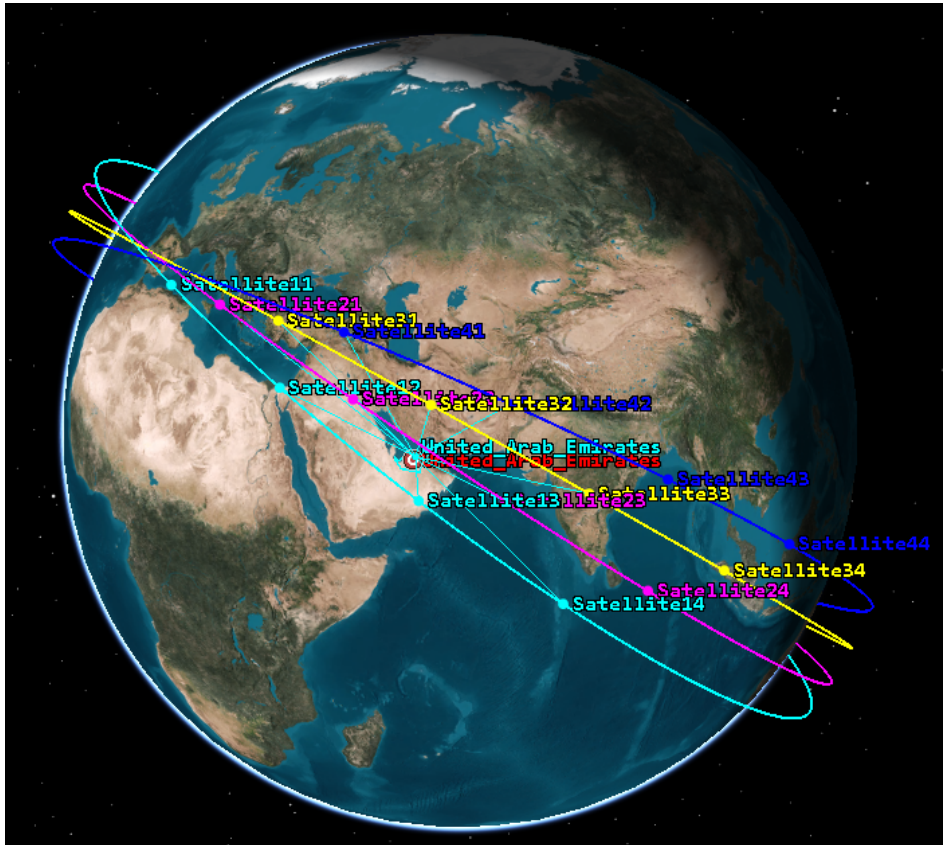
v. Scenario 6



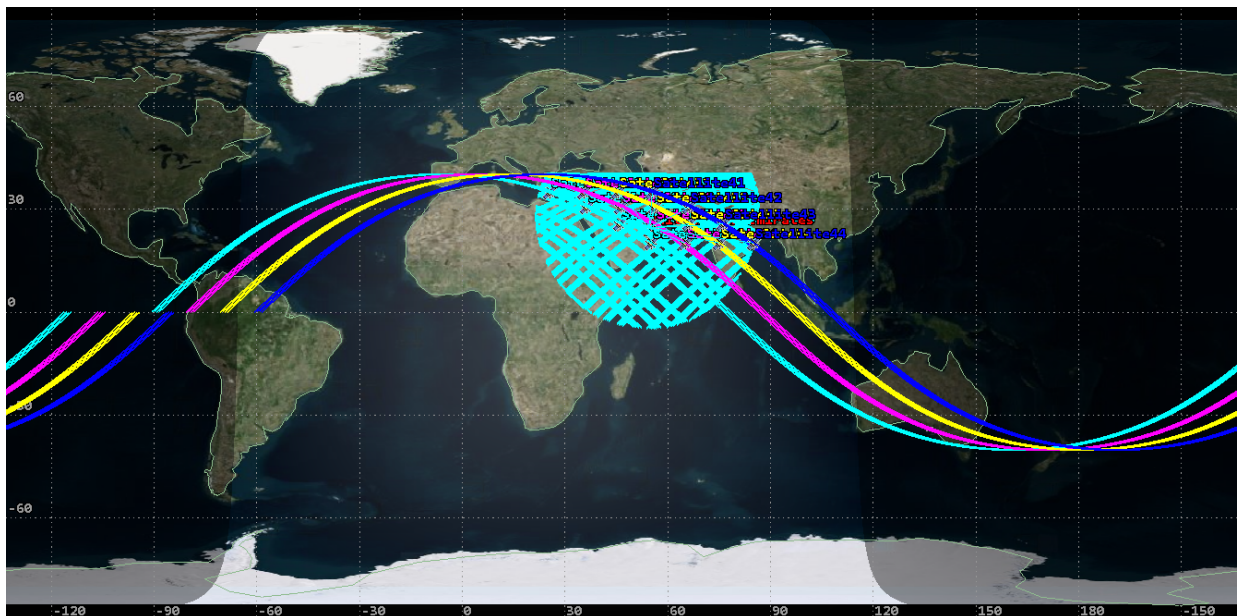
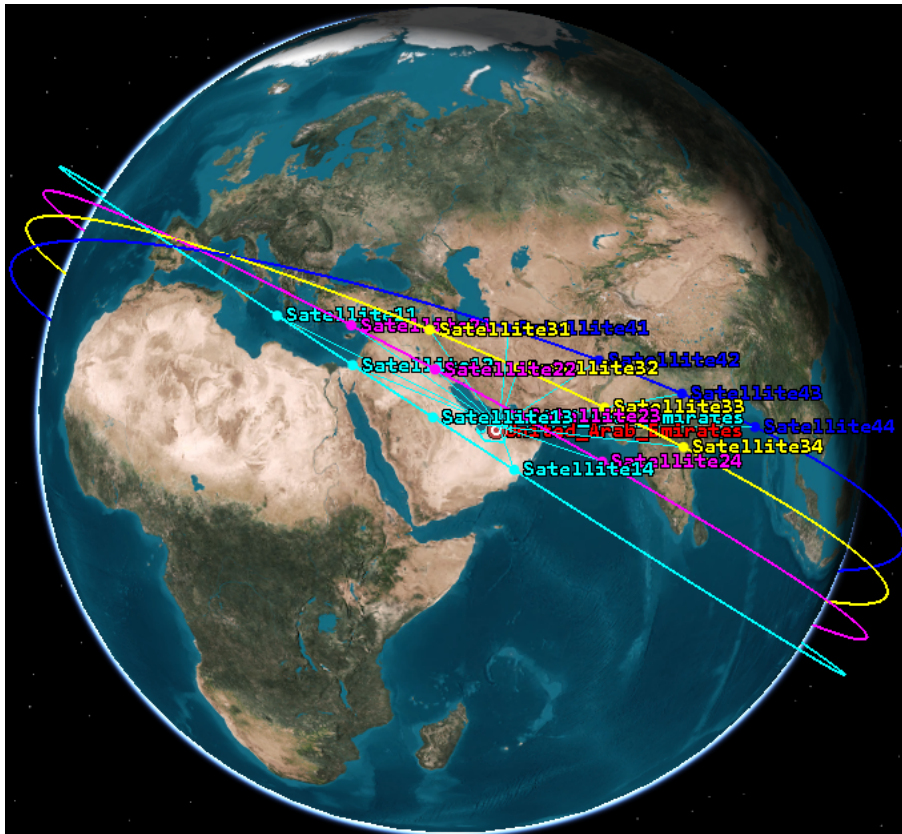
vi. Scenario 7



vii. Scenario 8



viii. Scenario 9





جامعة الإمارات العربية المتحدة
United Arab Emirates University



UAE UNIVERSITY MASTER THESIS NO. 2023: 44

This research highlights the advantages of the LEO-based GNSS compared to the current MEO-based GNSS. In this research, a mini-LEO GNSS constellation was designed and simulated using STK software, followed by simulation and assessment using Skydel GNSS simulator tool. Furthermore, the performance of the simulated orbits was assessed using a GNSS receiver. Finally, the performance of the simulated mini-LEO GNSS constellation was compared with the existing MEO GPS and Galileo.

Mariya Abdulkhaleq Abdullah Mohamad received her Master of Science in Space Science from the Department of Physics, College of Science at UAEU University, UAE. She received her Bachelor of Applied Science in Aviation Maintenance Engineering from the Higher Colleges of Technology, Dubai, UAE.

www.uaeu.ac.ae

Online publication of thesis:
<https://scholarworks.uaeu.ac.ae/etds/>

UAEU عمادة المكتبات
Libraries Deanship

جامعة الإمارات العربية المتحدة
United Arab Emirates University

قسم الخدمات المكتبية الرقمية - Digital Library Services Section